DETERMINING ANCHORING SYSTEMS FOR MARINE RENEWABLE ENERGY DEVICES MOORED IN A WESTERN BOUNDARY CURRENT

by

Michael Grant Seibert

A Thesis Submitted to the Faculty of

The College of Engineering and Computer Science

in Partial Fulfillment of the Requirements for the Degree of

Master of Science

Florida Atlantic University

Boca Raton, Florida

May 2011

Copyright © 2011 by Michael Seibert

DETERMINING ANCHORING SYSTEMS FOR MARINE RENEWABLE ENERGY DEVICES MOORED IN A WESTERN BOUNDARY CURRENT

by

Michael Grant Seibert

This thesis was prepared under the direction of the candidate's thesis advisors, Dr. Karl von Ellenrieder and Dr. James VanZwieten, Department of Ocean and Mechanical Engineering, and has been approved by the members of his supervisory committee. It was submitted to the faculty of the College of Engineering and Computer Science and was accepted in partial fulfillment of the requirements for the degree of Master of Science.

SUPERVISORY COMMITTEE:

Karl von Ellenrieder, Ph.D.
Thesis Co-Advisor

James VanZwieten, Ph.D.
Thesis Co-Advisor

Edgar An, Ph.D.

Palaniswamy Ananthkrishnan, Ph.D.

Mohammad Ilyas, Ph.D.
Chair, Department of Ocean and Mechanical Engineering

William Venezia, Ph.D.

Karl K. Stevens, Ph.D., P.E.
Dean, College of Engineering and Computer Science

Barry T. Rosson, Ph.D.
Dean, Graduate College

April 15, 2011
Date

ACKNOWLEDGMENTS

I would like to thank my advisors, Dr. Karl von Ellenrieder and Dr. Jim VanZweiten, for their support. Dr. VanZweiten's drive to seek research and exposure opportunities for his student's is a true asset of an advisor and it has greatly benefited my development as an engineer.

I am grateful to SNMREC for all the opportunities they have presented me with and to all the employees who have held a large part in my education outside of the classroom.

Finally, I would like to thank Bill Venezia of the Navy's South Florida Ocean Measurement Facility and Bob Taylor of Sound and Sea Technology for passing on their technical knowledge and practical experience.

ABSTRACT

Author: Michael Seibert

Title: Determining Anchoring Systems for Marine Renewable Energy Devices Moored in a Western Boundary Current

Institution: Florida Atlantic University

Title: Karl Von Ellenrieder, Ph.D.
James VanZweiten, Ph.D.

Degree: Master of Science

Year: 2011

In this thesis anchoring systems for marine renewable energy devices are examined for an area of interest off the coast of Southeast Florida that contains both ocean current and thermal resources for future energy extraction. Bottom types observed during previous regional benthic surveys are compiled and anchor performance of each potential anchor type for the observed bottom types is compared. A baseline range of environmental conditions is created by combining local current measurements and offshore industry standards. Numerical simulations of single point moored marine hydrokinetic devices are created and used to extract anchor loading for two potential deployment locations, multiple mooring scopes, and turbine rotor diameters up to 50 m. This anchor loading data is used for preliminary anchor sizing of deadweight and driven

plate anchors on both cohesionless and cohesive soils. Finally, the capabilities of drag embedment and pile anchors relevant to marine renewable energy devices are discussed.

DETERMINING ANCHORING SYSTEMS FOR MARINE RENEWABLE ENERGY DEVICES MOORED IN A WESTERN BOUNDARY CURRENT

LIST OF FIGURES x

LIST OF TABLES xvii

NOMENCLATURE xviii

ACRONYMS xx

1. Introduction 1

1.1 Need for Anchoring Investigation 1

1.2 Southeast Florida's Ocean Energy Resources 3

1.3 Marine Renewable Energy Systems 5

1.4 Anchor Study Area of Interest 9

1.5 History of Mooring Systems in the Florida Current 10

1.6 Thesis Outline 11

1.7 Contributions 13

2. Suitable Anchor Types for Use within the Area of Interest 14

2.1 Potential Anchor Types for Use within the Area of Interest 14

2.2 Regional Bottom Types and Anchor Performance 19

3. Anchor Loading Extraction 27

3.1 Metocean Conditions 27

3.1.1 Waves 31

3.1.2 Wind 33

3.1.3 Current 33

3.1.4 Recommendations for Floating OTEC System Analysis 38

3.2 Marine Hydrokinetic Turbine Anchor Loading 39

3.3 Marine Hydrokinetic Turbine Simulation Results 43

3.3.1 Anchor Loads 44

3.3.2 Required Lift Force 48

3.3.3 Estimated Power Outputs 50

3.4 Floating OTEC System Anchor Loading 53

4. Preliminary Anchor Sizing for Single Point Moored MHK Devices 56

4.1 Deadweight (Gravity) Anchor Sizing 56

4.1.1 Deadweight Anchor with no Shear Keys on Cohesionless Soil 58

4.1.2 Deadweight Anchor with no Shear Keys on Cohesive Soil 65

4.1.3 Deadweight Anchor with Shear Keys on Cohesionless Soil 72

4.1.4 Deadweight Anchor with Shear Keys on Cohesive Soil 74

4.2 Driven Plate Anchors 76

4.2.1 Driven Plate Anchors in Cohesionless Soil 76

4.2.2 Driven Plate Anchors in Cohesive Soil 81

4.3 Traditional Drag Embedment Anchors 83

4.4 Pile Anchors 88

5. CONCLUDING REMARKS 93

5.1 Summary and Conclusions 93

5.2 Gaps in Current Knowledge of the Area of Interest and Related Future Work 97

REFERENCES 99

LIST OF FIGURES

Figure 1: “Temperature cross section along 26° 05’N on July 22, 2008” (Leland, 2009) 4

Figure 2: “Maximum, mean, and minimum velocity magnitude, plotted by depth” at 26.11 North Latitude, 79.50 West Longitude (Raye, 2002) 5

Figure 3: NIOT OTEC Plant mooring configuration (Ravindran, 2000) 7

Figure 4: "Neutrally-buoyant turbine on a tensioned cable" (Clarke et al., 2008) 8

Figure 5: "Bottom-moored, buoyant turbine" (Clarke et al., 2008) 8

Figure 6: “Diagrammatic representation of the C-plane under normal operating conditions" (VanZwieten et al., 2006) 9

Figure 7: FAU’s initial proposed limited lease area for alternative energy resource assessment and technology development – Proposed Lease Area (1). Courtesy US Dept. of Interior MMS (SNMREC, 2010) 10

Figure 8: "Generic anchor types" (Sound and Sea Technology, 2009) 15

Figure 9: Anchor behavioral criteria (Sound and Sea Technology, 2009) 16

Figure 10: Benthic habitat map of Calypso port survey (Messing et al., 2006) 20

Figure 11: Path of Calyspo pipeline benthic survey denoted as red line (Messing et al., 2006) 21

Figure 12: "Representative unconsolidated sediment substrates. A. Obsolete rippled sediment, B. Flat textured bioturbated sediment" (Messing et al., 2006)..... 22

Figure 13: "Representative low-cover (A, C, E) and high-cover (B, D, F) hard-bottom substrates" (Messing et al., 2006) 22

Figure 14: "Sediment substrates. A. Smooth weakly bioturbated, textured (with small tubes); B. Border between lineated (above) and obsolete rippled sediment (below); C. Smooth weakly bioturbated, with unidentified tufts" (Messing et al., 2006)..... 24

Figure 15: "A-B. Low-cover hardbottom. A. Scattered black and white rubble; B. partly buried low-relief outcrop. C-D. High-cover hardbottom. C. Crowded rubble. D. Low-relief eroded outcrop" (Messing et al., 2006) 24

Figure 16: "A. Low-relief jointed pavement on escarpment between high-relief ledges. B. Side of high-relief ledge with projecting lace corals (Stylasteridae). C. Moderate-relief outcrops and boulders. D. Steep sediment an boulder-strewn slope just below figure 16B (projecting lace corals visible at top)" (Messing et al., 2006)..... 25

Figure 17: Wind speed, wave height, and bubble layer depth measurements of Hurricane Frances (Black et al., 2007) 32

Figure 18: Map of bathymetry transect along 26° 05' N represented by yellow line. Yellow pushpins denote 80.1° W and 79.6° W corresponding to Figure 19. Orange circles denote location of ADCP buoy deployed for 18 months (top circle) in 330 m and SNMREC's buoy deployed for 13 months (bottom circle) in 340 m 34

Figure 19: Bathymetry along 26° 05'N (Leland, 2009). Estimated position of Miami Terrace and Terrace Escarpment at this latitude 35

Figure 20: Maximum Current Profile for 325 m depth (FAU ADCP data)..... 36

Figure 21: Maximum current Profile for 700 m depth (HYCOM data) 37

Figure 22: CAD Drawing of FAU's First Generation Experimental Hydrokinetic Turbine 41

Figure 23: SI to English unit conversion scale 45

Figure 24: Turbine anchor loading for 325 m depth..... 45

Figure 25: Turbine anchor vertical loading for 325 m depth..... 46

Figure 26: Turbine anchor horizontal loading for 325 m depth..... 46

Figure 27: Turbine anchor loading for 700 m depth..... 47

Figure 28: Turbine anchor vertical loading for 700 m depth..... 47

Figure 29: Turbine anchor horizontal loading for 700 m depth..... 48

Figure 30: Net buoyant force for turbine at 50 m depth in 325 m location 49

Figure 31: Net buoyant force for turbine at 50 m depth in 700 m location 50

Figure 32: Maximum theoretical power production vs. rotor diameter for 0 to 10 m diameters 52

Figure 33: Maximum theoretical power production vs. rotor diameter for 10 to 50 m diameters 52

Figure 34: Deadweight anchor types (Taylor, 1982) 58

Figure 35: Anchor dimensions for concrete deadweight anchor with no shear keys at 325 m depth location and 1.25 mooring scope for loose sand 62

Figure 36: Anchor dimensions for concrete deadweight anchor with no shear keys at 325 m depth location and 1.50 mooring scope for loose sand 63

Figure 37: Anchor dimensions for concrete deadweight anchor with no shear keys at 325 m depth location and 2.00 mooring scope for loose sand 63

Figure 38: Anchor dimensions for concrete deadweight anchor with no shear keys at 700 m depth location and 1.25 mooring scope for loose sand 64

Figure 39: Anchor dimensions for concrete deadweight anchor with no shear keys at 700 m depth location and 1.50 mooring scope for loose sand 64

Figure 40: Anchor dimensions for concrete deadweight anchor with no shear keys at 325 m depth location and 1.25 mooring scope for cohesive soil solved for using plan area from Figure 35 67

Figure 41: Anchor dimensions for concrete deadweight anchor with no shear keys at 325 m depth location and 1.50 mooring scope for cohesive soil solved for using plan area from Figure 36 68

Figure 42: Anchor dimensions for concrete deadweight anchor with no shear keys at 325 m depth location and 2.00 mooring scope for cohesive soil solved for using plan area from Figure 37 68

Figure 43: Anchor dimensions for concrete deadweight anchor with no shear keys at 700 m depth location and 1.25 mooring scope for cohesive soil solved for using plan area from Figure 38 69

Figure 44: Anchor dimensions for concrete deadweight anchor with no shear keys at 700 m depth location and 1.50 mooring scope for cohesive soil solved for using plan area from Figure 39 69

Figure 45: Anchor dimensions for concrete deadweight anchor with no shear keys at 325 m depth location and 1.25 mooring scope for cohesive soil solved for using weight from Figure 35 70

Figure 46: Anchor dimensions for concrete deadweight anchor with no shear keys at 325 m depth location and 1.50 mooring scope for cohesive soil solved for using weight from Figure 36 70

Figure 47: Anchor dimensions for concrete deadweight anchor with no shear keys at 325 m depth location and 2.00 mooring scope for cohesive soil solved for using weight from Figure 37 71

Figure 48: Anchor dimensions for concrete deadweight anchor with no shear keys at 700 m depth location and 1.25 mooring scope for cohesive soil solved for using weight from Figure 38 71

Figure 49: Anchor dimensions for concrete deadweight anchor with no shear keys at 700 m depth location and 1.50 mooring scope for cohesive soil solved for using weight from Figure 39 72

Figure 50: Necessary anchor weight of concrete deadweight with full keying skirts on cohesionless soil at each location 74

Figure 51: Necessary weight of deadweight anchor with shear keys to resist overturning in cohesive soil 75

Figure 52: "Holding capacity factors for cohesionless soils" (Forrest et al., 1995) 78

Figure 53: Necessary keyed depth for seven plate areas presented as a function of rotor diameter at 325 m depth location and 1.25 mooring scope for loose sand 79

Figure 54: Necessary keyed depth for seven plate areas presented as a function of rotor diameter at 325 m depth location and 1.50 mooring scope for loose sand 79

Figure 55: Necessary keyed depth for seven plate areas presented as a function of rotor diameter at 325 m depth location and 2.00 mooring scope for loose sand 80

Figure 56: Necessary keyed depth for seven plate areas presented as a function of rotor diameter at 700 m depth location and 1.25 mooring scope for loose sand 80

Figure 57: Necessary keyed depth for seven plate areas presented as a function of rotor diameter at 700 m depth location and 1.50 mooring scope for loose sand 81

Figure 58: "Holding capacity factors for cohesive soils" (Forrest et al., 1995) 82

Figure 59: Necessary plate area with increasing soil shear strength for eight rotor diameters at 325 m depth location and 1.25 mooring scope in cohesive soil 82

Figure 60: Anchor holding capacity in sand (API, 2005) 84

Figure 61: Anchor holding capacity in soft clay or mud (API, 2005) 85

Figure 62: Percent holding capacity versus drag distance in soft clay (API, 2005) 86

Figure 63: Estimated maximum fluke tip penetration (API, 2005) 87

Figure 64: Pile Anchor Types (Sound and Sea Technology, 2009) 90

Figure 65: Turbine Anchor Loading for 325 m Depth with Approximate Maximum Capacities of Pile Anchors 91

Figure 66: Turbine Anchor Loading for 700 m Depth with Approximate Maximum Capacities of Pile Anchors 92

LIST OF TABLES

Table 1: "Anchor Characteristics Summary" (Sound and Sea Technology, 2009) 17

Table 2: "Mooring Configuration Options" (Sound and Sea Technology, 2009) 18

Table 3: Metocean Conditions 30

Table 4: Independent Extreme Values for Hurricane Winds in The Central Gulf of Mexico (89.5˚W To 86.5˚W) (API, 2007) 33

Table 5: Estimated Power Outputs for 325m and 700m depths at Maximum Current Velocity 51

Table 6: Soil type classified by grain size distribution (Vryhof Anchors, 2005) 59

Table 7: Relation between shear strength and test values (Vryhof Anchors, 2005) 60

Table 8: "Approximate correlation between the angle of internal friction φ and the relative density of fine to medium sand" (Vryhof Anchors, 2005) 60

Table 9: "Friction Coefficients for Anchor Materials on Granular Soils (tan φ)" (Sound and Sea Technology, 2009) 60

Table 10: American (ASTM) and British (BS) standards for consistency of clays (Vryhof Anchors, 2005) 67

NOMENCLATURE

A	drag area (rotor swept area) (Section 3.2)
A	plan area of deadweight anchor (Section 4.1)
A	area of plate anchor (Section 4.2)
B	minimum anchor width of gravity anchor without shear keys
c	cohesive soil shear strength
C_d	drag coefficient
D	drag (Section 3.2)
D	embedded depth of the keyed plate anchor (Section 4.2)
F_h	horizontal anchor loading
F_u	ultimate anchor holding capacity
F_v	vertical anchor loading
g	acceleration due to gravity
g_b	effective (buoyant) weight of the soil
G_{su}	rate of increase of shear strength
H	maximum height of the mooring line connection point above the base of the anchor with or without shear keys
K_p	passive earth pressure coefficient
L	length of deadweight anchor

N_c	bearing capacity factor for cohesive soil
N_q	bearing capacity factor for cohesionless soil
P	expected power output
r	rotor radius
S_{ua}	average undrained shear strength from seabed surface to depth z
S_{uz}	undrained shear strength at the bottom of the anchor
U	current speed
W	anchor weight in water
z	depth to bottom of anchor
z_s	depth to bottom of shear keys
γ_b	buoyant unit weight of soil
γ_s	buoyant unit weight of the deadweight
η	efficiency (Betz maximum efficiency)
π	pi
ρ	density of seawater
ρ_c	density of concrete
ρ_{sw}	density of seawater
ϕ	angle of internal friction

ACRONYMS

ADCP	acoustic doppler current profiler
BOEMRE	Bureau of Ocean Energy Management, Regulation, and Enforcement (formerly the Minerals Management Service)
CTD	conductivity temperature depth
ESRU	Energy Systems Research Unit
FAU	Florida Atlantic University
HBOI	Harbor Branch Oceanographic Institute
MHK	marine hydrokinetic
MRE	marine renewable energy
NDBC	National Data Buoy Center
NIOT	National Institute of Ocean Technology
OTEC	ocean thermal energy conversion
OWET	Oregon Wave Energy Trust
SNMREC	Southeast National Marine Renewable Energy Center
WEC	wave energy conversion

1. INTRODUCTION

Identifying and understanding anchoring systems required to hold marine renewable energy (MRE) devices stationary in energy dense locations off South Florida's coast is a crucial element in future commercial deployments. The Southeast National Marine Renewable Energy Center (SNMREC) at Florida Atlantic University (FAU) was established to assist industry with understanding deployment siting and providing scaled testing capability for commercial installation of MRE systems in South Florida's ocean energy resources. The SNMREC leverages an academic setting to improve and advance the knowledge base for MRE technology. The SNMREC's ongoing resource assessment has verified available ocean thermal and current resources off Florida's coast that can mitigate Florida's increasing energy demand if research and development progresses in areas critical for deployment and testing of MRE systems, including moorings and anchors for these generators and platforms.

1.1 Need for Anchoring Investigation

Anchor selection and design, as in any design process should be treated as an iterative investigation balancing complexity of technology with economics, while fulfilling requirements and maintaining safety. The inherent complexity of developing and deploying anchoring systems for large scale devices or unusual anchoring scenarios directly increases the cost of design and installation of the system in order to obtain cost

competitive energy production. The MRE sector identifies the deployment of scaled prototypes, which demonstrate cost competitive energy production, as a necessity to meet the industry's expected potential. As novel designs for MRE devices are being investigated and developed, anchoring and mooring of MRE devices can sometimes become an afterthought. Conceptualizing the deployment of commercial MRE devices off the coast of South Florida will give insight to device developers and researchers about the anchor types and sizes available for the given environment, as well as identify gaps in knowledge of the specific deployment region which challenge advancement.

An anchor study within the region requires a thorough investigation of environmental parameters such as regional metocean conditions for design and surveys of the benthic environment. However, eventually, detailed site specific surveys will be necessary for final designs. The benthic environment directly influences the type of anchor, size of anchor, and deployment location that can be used because of performance limitations of different anchor types as well as potential ecological concerns. A comprehensive range of anchoring scenarios for the region is created to address multiple MRE device types at different locations. The anchoring scenarios must be simulated with environmental characteristics of the region to extract the most accurate anchor loading predictions. Anchor loading predictions can then be used to size the applicable anchor types. A custom basis for environmental conditions to be used in simulation of the deployed devices was created because site specific metocean surveys have not been completed and survivability standards have not been finalized for full scale devices. Relevant safety factors used in offshore industry must be compared and integrated into simulation for realistic design parameters.

While designing an economical anchoring system that will successfully hold an MRE system at the desired location is important, the environmental impact must also be assessed as proper anchor selection and sizing can reduce potential benthic impacts. Benthic impact is not only based on the size of anchor to be used, but also the methods of deployment, ability to recovery, and characteristics of the anchor mooring line attachment for each type of anchor. Conclusions of the potential benthic impact can be formulated from the anchor sizing presented in this thesis and is left to the reader. While this work defines and quantifies anchor requirements for MRE devices as a quick reference in graphical representation, it also serves as a reference for the process of anchor selection and design in the investigated region.

1.2 Southeast Florida's Ocean Energy Resources

The Florida Straits located between South Florida's eastern coast and the western coasts of the Bahamian Islands is currently being studied with great interest because of its energy dense ocean current and an available ocean thermal energy potential. An ongoing ocean thermal resource assessment of the Florida Straits along latitude 26° 05'N, as presented by Leland in 2009, shows that 5.5 to 28 km (3 to 15 nautical miles) from shore, in depths from 250 to 300 m, there exists the potential for cold seawater based air conditioning, or possibly seasonal OTEC power production. This study shows that in the Summer, these nearshore cold and warm water resources meet or exceed the average 20°C temperature difference (Figure 1) traditionally recommended as the temperature difference required to make OTEC economically feasible. It was also shown that further

offshore along this latitude, east of 79.8°W, exists the required temperature difference for year round OTEC power production where depths reach 700 m. Measurements that confirm the offshore OTEC potential were taken at three CTD cast sites between 33 and 44 km (18 and 24 nautical miles) from shore in depths ranging from 580 m to 680 m and show an annual average temperature difference between 21°C and 22°C at each of the three sites.

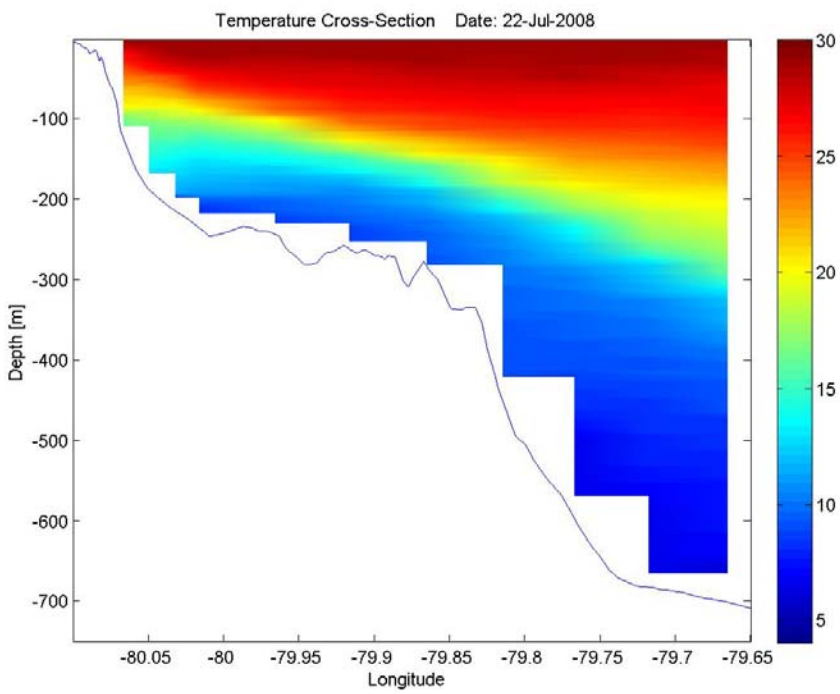

Figure 1: "Temperature cross section along 26° 05'N on July 22, 2008" (Leland, 2009).

Ocean current resource assessment over a 19 month period, May 18, 2000 through November 27, 2001, "shows current maximums to exceed 2.0 m/s in the upper 100 meters and can exceed 1.8 m/s at 200 meters" (Figure 2) occurring in the Summer months (Raye, 2002). The mean current speeds for the 19 month deployment of a subsurface ADCP buoy, placed 3 miles to west of the mean axis of the Florida Current, exceed 1 m/s to a depth of 150 meters (Figure 2) (Driscoll et al., 2008). Maximum current velocities

occur near the surface (Figure 2) and decrease with depth, revealing that approximately 50% of the Florida Current's power is located in the upper 100 m (Duerr and Dhanak, 2010). This current is a significant energy source that can potentially be harvested by MHK turbines. The mean current velocity at 50 meters, a target depth for an Aquantis, LLC's hydrokinetic turbine, is 1.54 m/s with a standard deviation of 0.24 m/s (Raye, 2002). Both maximum sustained current velocities and temperature differences occur during summer months, matching Florida's peak energy consumption (Leland, 2009).

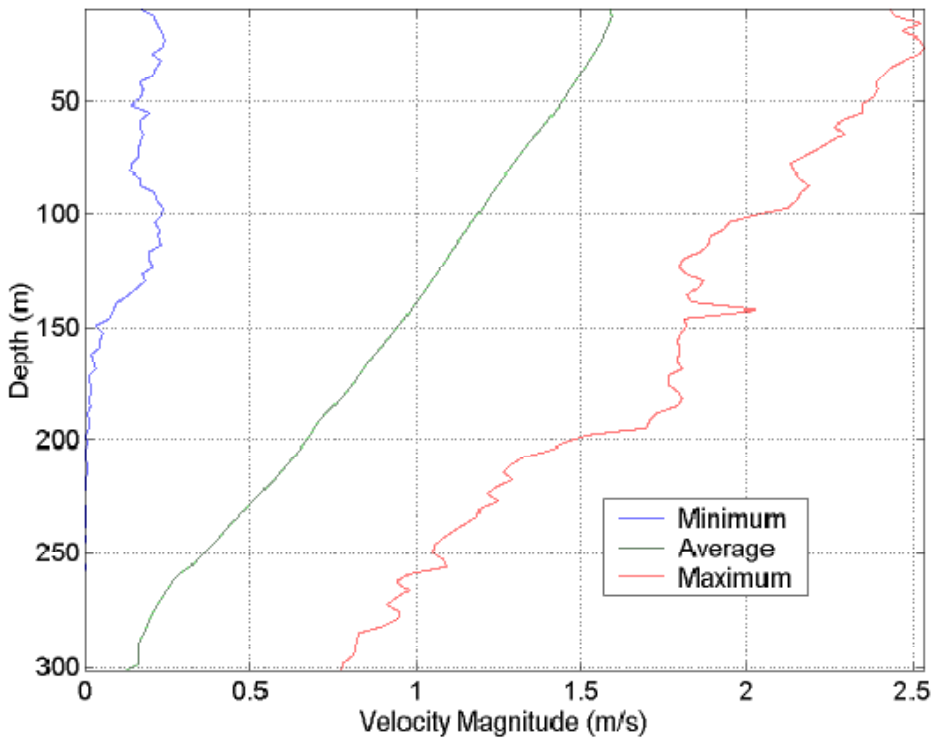

Figure 2: "Maximum, mean, and minimum velocity magnitude, plotted by depth" at 26.11 North Latitude, 79.50 West Longitude (Raye, 2002).

1.3 Marine Renewable Energy Systems

Applicable MRE systems (OTEC and hydrokinetic turbines) require anchor systems to hold position in these energy dense locations, while surviving extreme

metocean conditions. Not included in this study is the application of computerized station keeping systems that do not use a mooring system, which could be a feasible solution for some OTEC plants. Such a system is beyond the scope of this work and will most likely not be an economical solution off of Southeast Florida because of large drag loads generated by the Florida Current.

Three types of platforms deemed most feasible for housing OTEC plants are semi-submersible, spar, and ship shaped (monohull) structures (Coastal Response Research Center, 2010). Past floating OTEC plants and prototypes, such as: Mini OTEC deployed in Hawaii in 1979, OTEC-1 deployed in Hawaii in 1980, and National Institute of Ocean Technologies (NIOT) attempts to deploy a system in India in 2000, have been housed on barges or tankers to accommodate the spatial needs of the system (Ravindran, 2000). Most recently India's NIOT has made attempts to moor their 1 MW OTEC barge (68.5 m x 16 m x 4 m) using a single point mooring (Figure 3) that utilizes its intake pipe as a structural component of the mooring system (Ravindran, 2000).

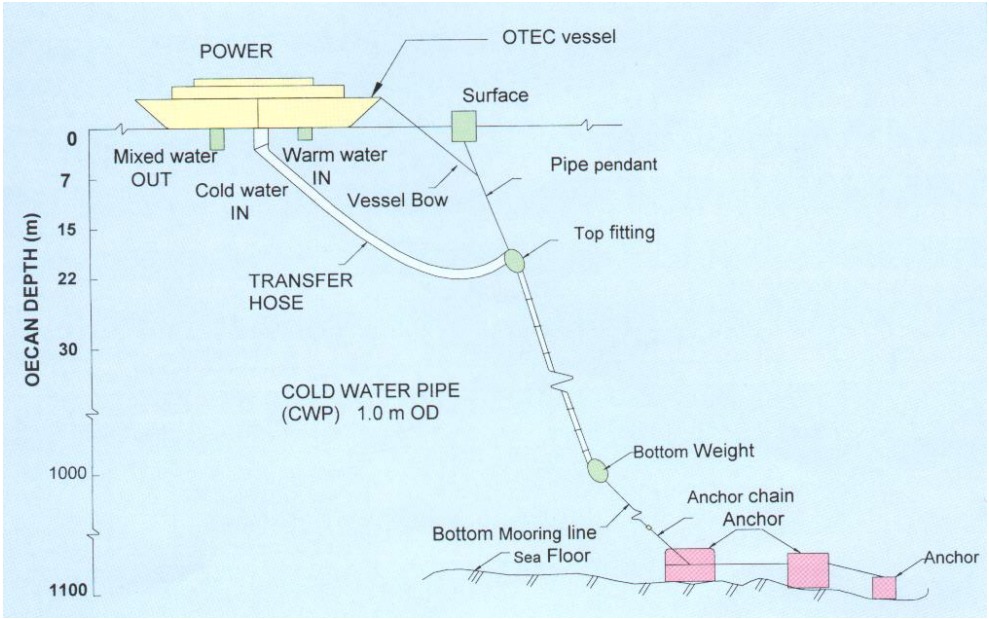

Figure 3: NIOT OTEC Plant mooring configuration (Ravindran, 2000).

Multiple hydrokinetic turbine development efforts are also underway, with the goal of deploying commercially viable devices using single or multi-point moored systems. Two such systems, other than SNMREC's first generation experimental hydrokinetic turbine (Driscoll et al., 2008), are the development of Aquantis LLC's C-plane (VanZwieten et al., 2006) and the 2nd generation single point mooring supported contra-rotating marine current turbine developed by the Energy Systems Research Unit (ESRU) at the University of Strathclyde (Clarke et al., 2009). It is acknowledged by Clarke that "if full benefits from the resource are to be gained and larger scale commercial deployment is to be undertaken, it will be necessary at some stage to deploy larger machines in deeper water using lower cost flexible, single riser, tensioned moorings" (2009). This type of mooring was demonstrated in ESRU's 2nd generation prototype system that "can be tuned to extract energy over a wide range of water depths by "flying" a neutrally-buoyant device from a flexible, tensioned mooring" (Figure 4) (Clarke et al.,

2009). An additional design discussed by ESRU is utilizing the nacelle of the turbine for buoyancy to create a taut mooring (Figure 5). Aquantis's C-plane design is tethered to the seafloor and utilizes control surfaces for variable depth operation (Figure 6) (VanZwieten et al., 2006).

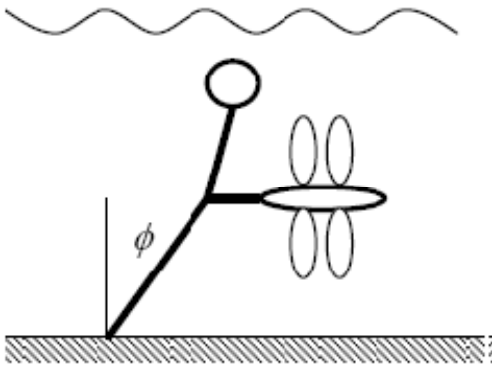

Figure 4: "Neutrally-buoyant turbine on a tensioned cable" (Clarke et al., 2008).

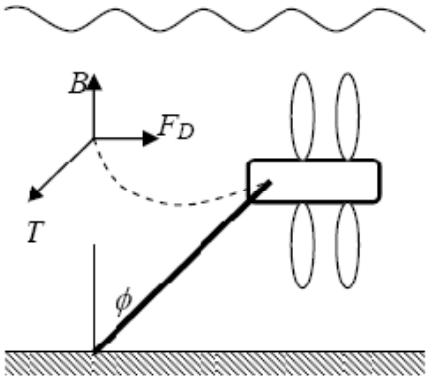

Figure 5: "Bottom-moored, buoyant turbine" (Clarke et al., 2008).

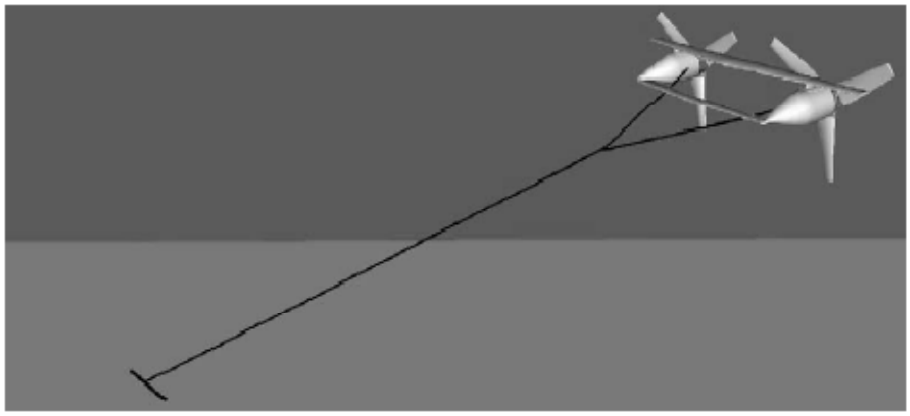

Figure 6: "Diagrammatic representation of the C-plane under normal operating conditions" (VanZwieten et al., 2006).

1.4 Anchor Study Area of Interest

SNMREC, formerly FAU's Center for Ocean Energy Technology, is leading a multi phase effort to create an offshore energy testing capability that "will involve permanent infrastructure offshore of South Florida, in the Florida current, to serve as an integrated, standardized testing and research range for advanced marine, hydrokinetic, and ocean thermal devices" (Driscoll et al., 2008). This infrastructure will "provide capability to government agencies, technology developers, and universities for testing and evaluation of ocean energy systems" (Driscoll et al., 2008). While SNMREC is assessing ocean energy resources throughout the state, nationally, and in some studies even globally, its initial primary area of interest is off of Southeast Florida. Referred to for the remainder of this work as the "area of interest" is Florida Atlantic University's initial proposed Limited Lease Area for Alternative Energy Resource Assessment and Technology (a reserved area with pending activity authorization from the former US Minerals Management Service, BOEMRE) denoted by light yellow "lease blocks" extending perpendicular from the coast of Ft. Lauderdale in Figure 7. The activity area

has been refined since it was initially proposed, but still remains the study area for this thesis because of the resources available throughout the full area. Operations thus far performed within the area of interest include, but have not been limited to, mooring of subsurface instrumentation buoys and manned submersible benthic surveys. Using a documented overview of the physical features of the area of interest along with regularly measured ocean energy resources and environmental conditions will provide companies with valuable information when they use the laboratory for testing of MRE systems. Performing an anchor study for the area will benefit both FAU's testing and evaluation operations and device developers who are considering the area off of Southeast Florida as a potential location for commercial deployment.

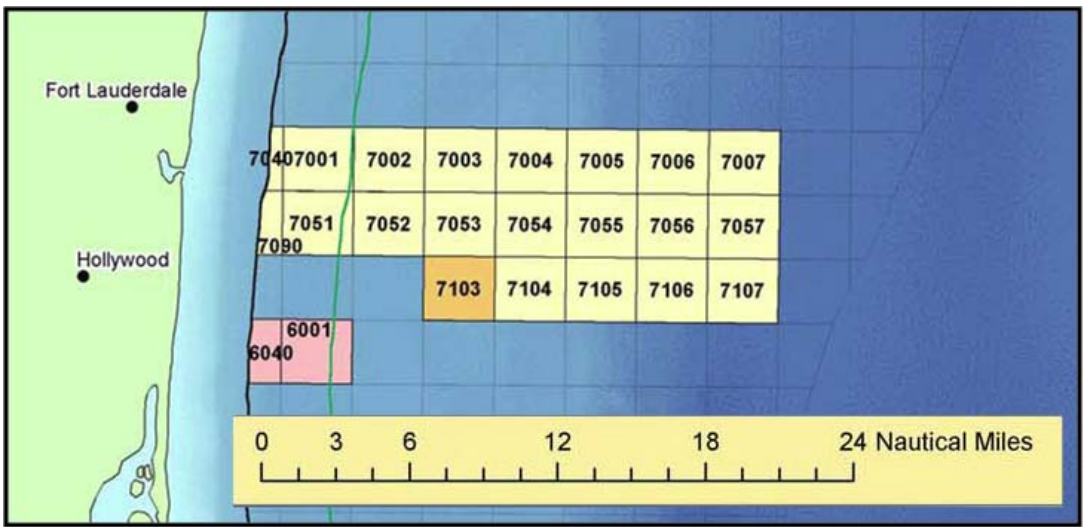

Figure 7: FAU's initial proposed limited lease area for alternative energy resource assessment and technology development – Proposed Lease Area (1). Courtesy US Dept. of Interior MMS (SNMREC, 2010).

1.5 History of Mooring Systems in the Florida Current

A literature review has exposed few attempts to moor offshore in the Florida Current for multiple months. Systems that have been moored within or near the current

for multiple months have primarily been weather and instrumentation buoys. NOAA's 6-meter long Nomad weather buoys are used for metocean data collection near the Gulf Stream off the Coast of Cape Canaveral and are designed for long-term survivability in severe seas (NDBC - Moored Buoy Program). These weather buoys and SNMREC's approximately 1.2 m diameter spherical subsurface ADCP buoys are only a fraction of the size and therefore create only a small fraction of the drag force expected from full scale MRE systems. No attempts to moor energy production facilities for extended periods of time have been made in the Florida Current. The only example of an MRE device being deployed in the Florida Current occurred in April of 1985 when Nova Energy Limited deployed a Vertical Axis Hydro Turbine from a moored ship that extracted energy from the current for less than a day (Davis et al., 1986). Difficulties during testing proved to engineers that a "design feature that had significant effect on both cost and viability was the mooring system" (Davis et al., 1986). The fact that "the major cost item was the construction and setting in place, [at 300 m in a 2m/s current], of very large gravity anchors required" for this project suggests that during the costly development and deployment of prototype MRE devices, the design of the anchoring and mooring system must be given adequate attention such that it does not hinder device feasibility (Davis et al., 1986).

1.6 Thesis Outline

The focus of this work is to determine applicable anchors for use off the coast of southeast Florida applying existing knowledge of the benthic habitat and to examine preliminary sizing methods for each anchor. A basis for extreme metocean conditions for

the region is developed for use in simulation of MRE systems and extracted anchor loading estimates from MRE simulations are used to quantify the range of anchor requirements of MRE systems suitable for use off Florida's coast.

Chapter 2 provides a regional survey of bottom types observed in past studies. Anchor types are compared for their applicability and performance on the known bottom types of the region.

Chapter 3 explains a basis for selecting environmental conditions which have not yet been standardized in the MRE field or for this location. The environmental conditions are applied dynamically to single point moored hydrokinetic turbine simulations until steady state operation is reached. Anchor loading is then extracted from the simulations to be used for preliminary anchor sizing. Past studies on anchor loading and preliminary anchor sizing for single point moored OTEC power production plants in the Gulf Stream are also discussed.

Chapter 4 uses the anchor loading results of chapter 3 to perform preliminary anchor sizing for single point moored marine hydrokinetic (MHK) devices. Anchor sizing is addressed for each anchor loading scenario created in chapter 3 for both cohesionless and cohesive soils. Anchor sizing plots for increasing rotor diameters are presented along with the methods of attaining each.

Chapter 5 discusses the results of this anchor study including the regional environmental study and results of preliminary anchor sizing for MRE devices in the area of interest. Current gaps in knowledge pertaining to the design and development of anchoring and mooring systems are identified and future related work to close current knowledge gaps is recommended.

1.7 Contributions

The five primary contributions of this thesis are:

1) Completing a regional study of seafloor characteristics of the benthic environment for use in selecting anchors.
2) Comparing suitability and performance of multiple anchor types for the bottom types discussed in contribution one.
3) Establishing a baseline range of maximum environmental conditions for the region to be used in the simulation of MRE devices.
4) Developing generic simulations of moored marine hydrokinetic devices in the Florida current in order to extract the magnitude of forces at the seabed mooring line connection point for a comprehensive range of mooring scenarios.
5) Performing preliminary anchor sizing for marine hydrokinetic devices for mooring scenarios created in contribution four.

2. SUITABLE ANCHOR TYPES FOR USE WITHIN THE AREA OF INTEREST

A regional study of the benthic environment began with a review of existing benthic survey information for Southeast Florida. Bottom types observed during the surveys are summarized and applicable anchor types are discussed. General descriptions along with notable features of the anchors applicable to each bottom type are provided as a basis for future anchor selection within the region.

2.1 Potential Anchor Types for Use within the Area of Interest

The four general anchor types examined for their applicability within the area of interest are deadweight (gravity), drag-embedment, pile, and plate (direct embedment) (Figure 8). Each of the four anchor types has multiple design variations and deployment methods depending on the characteristics of the seabed and direction of loading.

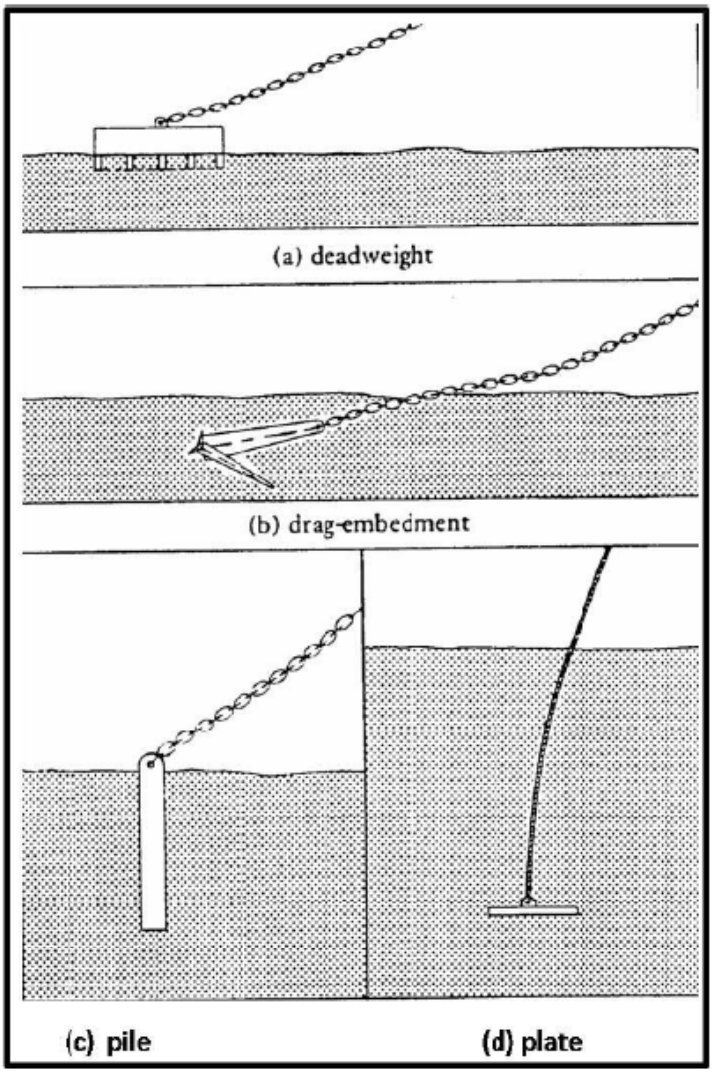

Figure 8: "Generic anchor types" (Sound and Sea Technology, 2009).

Figure 9 summarizes the behavioral criteria of the four examined anchor types in different anchoring scenarios. A comprehensive anchoring and mooring study was completed in 2009 by Sound and Sea Technology for the Oregon Wave Energy Trust (OWET) applying "industry knowledge for existing anchoring and mooring techniques as applied to wave energy conversion (WEC) devices in and around Oregon" (Sound and Sea Technology, 2009). Table 1, created in the aforementioned study, lists advantageous and disadvantageous characteristics of each anchor type. Also created during this study

is Table 2, which rates the applicability of each of the four anchor types depending on the type of mooring configuration selected. Mooring configuration selection is specific to each type of MRE device depending on the method in which it extracts energy from the ocean. Mooring system configuration can be optimized to achieve the desired behavior of the device. Environmental parameters also play a role in selecting mooring system configuration. Bottom types occurring in area of interest for use with Figure 9 and Tables 1 and 2 are presented in Section 2.2

Seafloor Material	Deadweight	Pile	Plate	Drag
Soft clay, mud	++	+	++	++
Soft clay layer (0-20 ft) over hard layer	++	++	o	+
Stiff clay	++	++	++	++
Sand	++	++	++	++
Hard glacial till	++	++	++	+
Boulders	++	o	o	o
Soft rock or coral	++	++	++	+
Hard, massive rock	++	+	+	o
Seafloor Topography				
Slope < 10 deg	++	++	++	++
Slope > 10 deg	o	++	++	o
Loading Direction				
Omnidirectional	++	++	++	o
Unidirectional	++	++	++	++
Large uplift	++	++	++	o
Lateral Load Range				
To 100,000 lb	++	+	++	++
100,000 to 1,000,000 lb	+	++	+	++
Over 1,000,000 lb	o	++	o	o

++ Functions well
+ Functions, but not normally the best choice
o Does not function well

Figure 9: Anchor behavioral criteria (Sound and Sea Technology, 2009).

Table 1: "Anchor Characteristics Summary" (Sound and Sea Technology, 2009).

Drag	Deadweight	Pile	Plate
Advantages	**Advantages**	**Advantages**	**Advantages**
High capacity (> 100,000 lbs) possible. Broad range of types and sizes available. Standard, off-the-shelf equipment. Broad use experience. Continuous resistance can be provided even if maximum capacity is exceeded. Anchor is recoverable.	Resists uplift, allowing short mooring line scope. No setting distance is required. Anchor is reliable because most holding force is due to anchor mass. Simple, on-site construction is feasible. Size is limited only by load-handling equipment. Economical if material is readily available. Reliable on thin sediment cover over rock. Mooring line connection is easy to inspect and service.	High capacity (>100,000 lbs) possible. Resists uplift, allowing short mooring line scopes. Anchor setting is not required. Dragging is eliminated. Drilled and grouted piles are especially suited for hard coral or rock seafloors. Simple, on-site construction is feasible. Anchor does not protrude above seafloor. Driven piles are cost-competitive with other high-capacity anchors when driving equipment is available. Comes in a wide range of sizes and shapes, such as pipe and structural shapes. Field modifications permit piles to be tailored to suit particular requirements. Accurate anchor placement is possible. Can be driven into layered seafloor.	High capacity (> 100,000 lbs) is possible. Resists uplift, allowing short mooring line scopes. Dragging is eliminated. Has higher holding capacity-to-weight ratio than any other type. Easier handling due to relatively light weigh Can function on moderate slopes and hard seafloors.[1] Easier installation due to possible instant embedment on seafloor contact.[1] Accurate placement is possible. Anchor does not protrude above seafloor. Can accommodate layered seafloors or seafloors with variable resistance.
Disadvantages	**Disadvantages**	**Disadvantages**	**Disadvantages**
Anchor cannot resist uplift; large line scopes are needed to cause near horizontal loading at seafloor. Does not function in hard seafloors. Behavior is erratic in layered seafloors. Penetrating/dragging anchor can damage pipelines, cables, etc.	Lateral load resistance is low compared to other anchor types. Usable water depth is reduced; deadweight can be an undesirable obstruction. Requires large-capacity load-handling equipment for placement.	Taut moorings may aggravate ship response to waves (low resilience).[1] Drilled and grouted installation is expensive and requires special skills and equipment. Costs increase rapidly in deep water or exposed locations where special installation vessels are required. Special equipment (pile extractor) is required to retrieve or refurbish the mooring. More extensive site data are required than for other anchor types. Pile-driving equipment must maintain position during installation. [1] True for any taut mooring	Susceptible to cyclic load-strength reduction when used in taut moorings in loose sand coarse silt seafloors. For critical moorings, knowledge of soil engineering properties is required. Anchor typically is not recoverable. Special consideration is needed for ordnance.[1] Anchor cable is susceptible to abrasion and fatigue.[1] Gun system is not generally recoverable in deep water (> 1,000 ft) Surface vessel must maintain position durin installation.

Table 2: "Mooring Configuration Options" (Sound and Sea Technology, 2009).

Mooring Configuration	Anchor Type	Comments
Catenary	Deadweight	Skirted deadweight or enhanced deadweight (PHA) for limited sediment or rock.
	Drag	Primary choice for sediment seafloors. Broad use experience.
	Pile	Applicable but may be high cost unless equipment and expertise is readily available
	Plate	Applicable but requires more specialized installation equipment.
Multi-catenary	Deadweight	Skirted deadweight or enhanced deadweight (PHA) with sinkers to reduce line angle at PHA. May be a practical option for limited sediment or rock seafloors. Handling weight will drive cost.
	Drag	Must be used with sinkers to reduce line angle to near horizontal angle at the seabed. While this increases handling difficulty it may be a cost effective option because there is boad use experience with this type of system.
	Pile	Applicable for single WEC installations but may be high cost unless equipment and expertise is readily available. Suction piles may be the preferred pile option for sediment seafloors. May be cost effective for energy farms.
	Plate	Plates can be a cost effective option for single WECs but this depends upon the availability of installation equipment and expertise. Plates are not recommended when load sharing may be required for energy farm applications.
Taut	Deadweight	Applicable but large line loads require high weight to resist vertical and horizontal loads. On seafloors with rock or thin sediment this option should be considered.
	Drag	Cannot handle uplift loads.
	Pile	Broad use experience for soil and rock seafloors. Local expertise and equipment are important to the selection of the least cost pile type and installation method.
	Plate	May be the least cost option for sediment seafloors but not appropriate for rock.

Applicability
High
Medium
Low
Not Applicable

2.2 Regional Bottom Types and Anchor Performance

The most useful sources of information available on the bottom types in the region of interest are the Final Report of the *Calypso LNG Deepwater Port Project, Florida Marine Benthic Video Survey* (Messing et al., 2006.a), the Final Report of the *Calypso U.S. Pipeline, LLC, Mile Post (MP) 31- MP0 Deep-water Marine Benthic Video Survey* (Messing et al., 2006.b), and a set of submersible dives performed by Harbor Branch Oceanographic Institution (HBOI) on behalf of the SNMREC. Both the Calypso port survey and the Calypso pipeline survey occurred north of the area of interest, but the submersible dives on behalf of the SNMREC occurred within the area of interest. Two additional sources, Ballard and Uchupi (1971) and Neumann and Ball (1970) are geological studies on the Miami Terrace completed in the 1970s that support the findings of the more recent surveys, (SNMREC, 2010).

The Calypso surveys were completed using the Television Observed Nautical Grappling System (TONGS) which is a deep water heavy-lift underwater vehicle outfitted with video and still cameras (Messing et al., 2006.a). The Calypso port survey took place along the transect lines in Figure 10 approximately 10 miles northeast of Port Everglades (Messing et. al., 2006.a). The Calypso pipeline survey took place along the red line extending from the Calypso port survey and running northeast towards Grand Bahama Island, Bahamas (Figure 11).

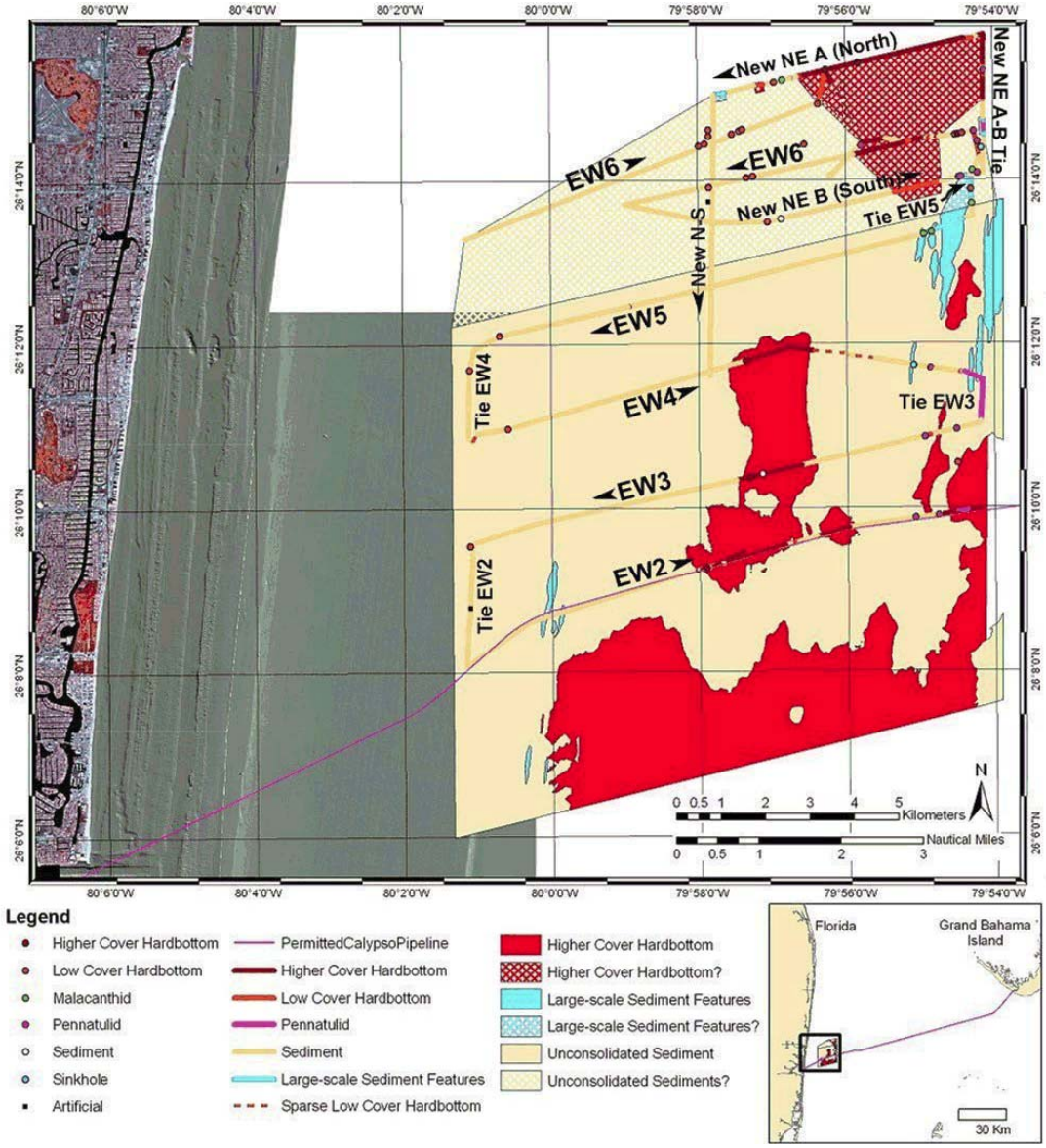

Figure 10: Benthic habitat map of Calypso port survey (Messing et al., 2006.a).

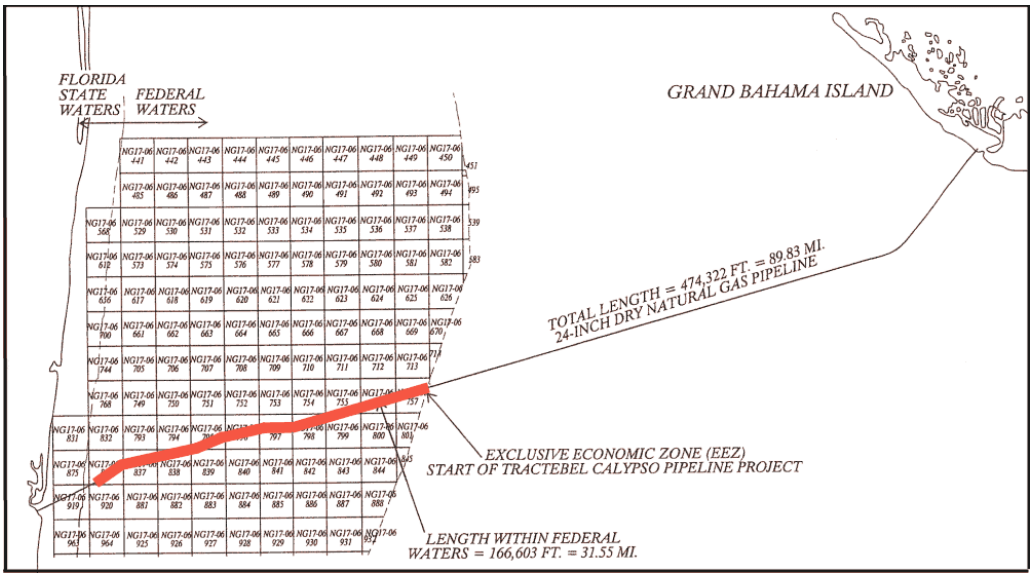

Figure 11: Path of Calyspo pipeline benthic survey denoted as red line (Messing et al., 2006.b).

The report generated from these surveys lists benthic habitat descriptions with accompanying longitude and latitude. Bottom types described within the habitat categories of the Calypso port survey include sediment substrates, unconsolidated mud or sand substrates (Figure 12). As displayed in Figure 9, all four anchor types function in sand, clay or mud where adequate sediment depths exists, but only deadweight and pile anchors function well on low to high cover hardbottom (Figure 13). As stated in Table 1, piles can be driven in to layered seafloors and drilled and grouted piles are suitable for rock seafloors but have increased installation costs due to special equipment needed.

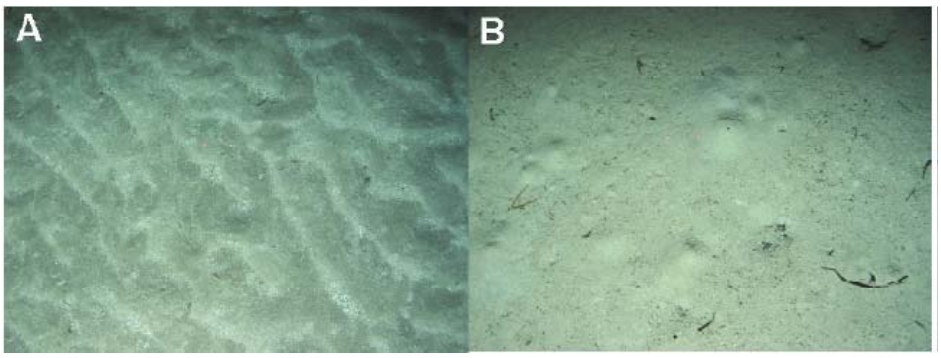

Figure 12: "Representative unconsolidated sediment substrates. A. Obsolete rippled sediment, B. Flat textured bioturbated sediment" (Messing et al., 2006.a).

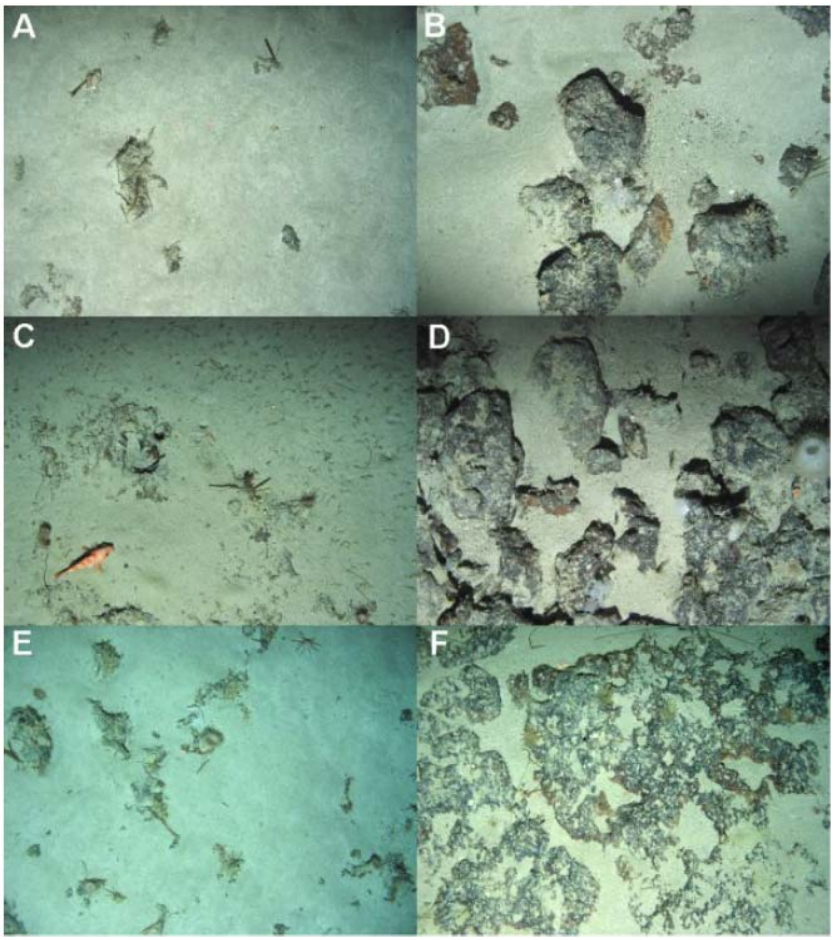

Figure 13: "Representative low-cover (A, C, E) and high-cover (B, D, F) hard-bottom substrates" (Messing et al., 2006.a).

Bottom types described within the habitat categories of the Calypso pipeline survey include sediment substrates (Figure 14) and varying cover hard bottoms (Figure 15) like those seen in the Calypso port survey in addition to moderate to high relief bottoms (Figure 16) (Messing et al., 2006.b). The changes in bottom type moving from west to east can be observed along the Calypso pipeline survey. The reported observations on the portion of the transect occurring on top of the Miami terrace is mostly a hard bottom described by limestone slabs and pavements with different combinations of gravel, rubble and sediment overlay. The low relief hard bottom with some overlay changes to a moderate relief to high relief hard bottom as the survey moves eastward down the Terrace Escarpment into the Straits of Florida (Figure 16). Associated depths are 200 to 300 m atop the Miami Terrace dropping to 600 to 800 meters in the Florida Straits.

A significant drop is observed over the Terrace Escarpment characterized by high-relief hard bottom consisting of ledges, steep slopes, and escarpments with up to 20 m relief (Messing et al., 2006.b). The combination of high relief with steep slopes that occur on the Terrace Escarpment may want to be avoided for anchoring purposes. A deadweight anchor may work in the high relief areas but would not function well on steep slopes (Figure 9). Anchoring methods such as pile or plate could be looked at for steeper slopes (Figure 9) but come with increased design and deployment costs (Table 1). In the 600 to 800 meter depths, there exist regions described as alternating obsolete rippled and smooth sediment with regions of coral rubble (Messing et al., 2006.b). Again all anchor types will function in sediment as long as the required sediment depth for each type exists. For drag embedment it must be assured that there is enough drag distance in the sediment to embed to the desired depth.

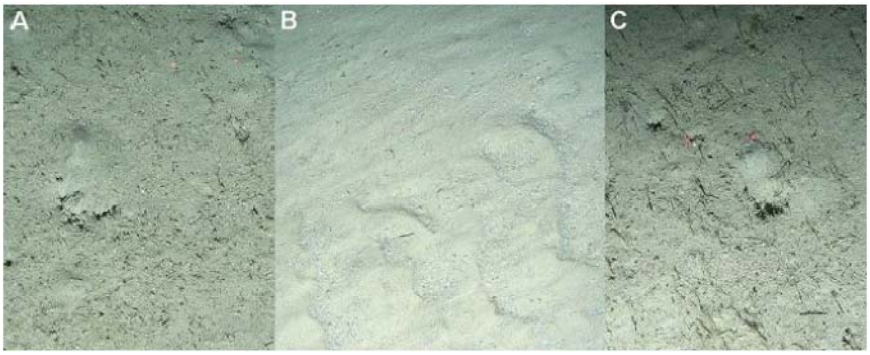

Figure 14: "Sediment substrates. A. Smooth weakly bioturbated, textured (with small tubes); B. Border between lineated (above) and obsolete rippled sediment (below); C. Smooth weakly bioturbated, with unidentified tufts" (Messing et al., 2006.b).

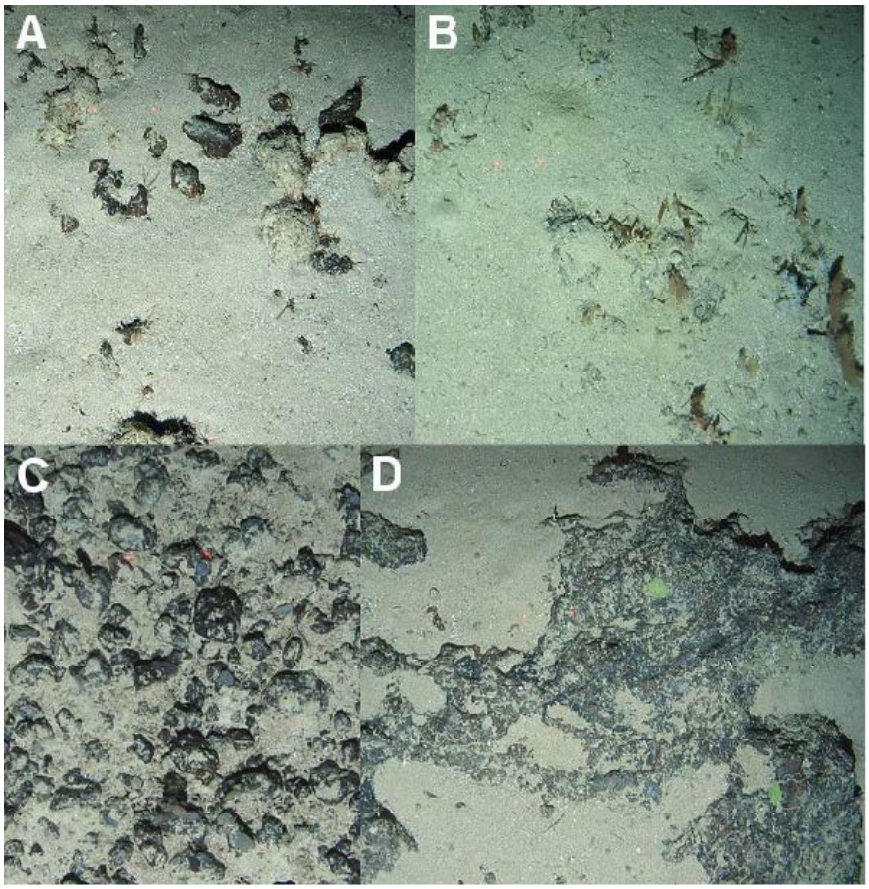

Figure 15: "A-B. Low-cover hardbottom. A. Scattered black and white rubble; B. partly buried low-relief outcrop. C-D. High-cover hardbottom. C. Crowded rubble. D. Low-relief eroded outcrop" (Messing et al., 2006.b).

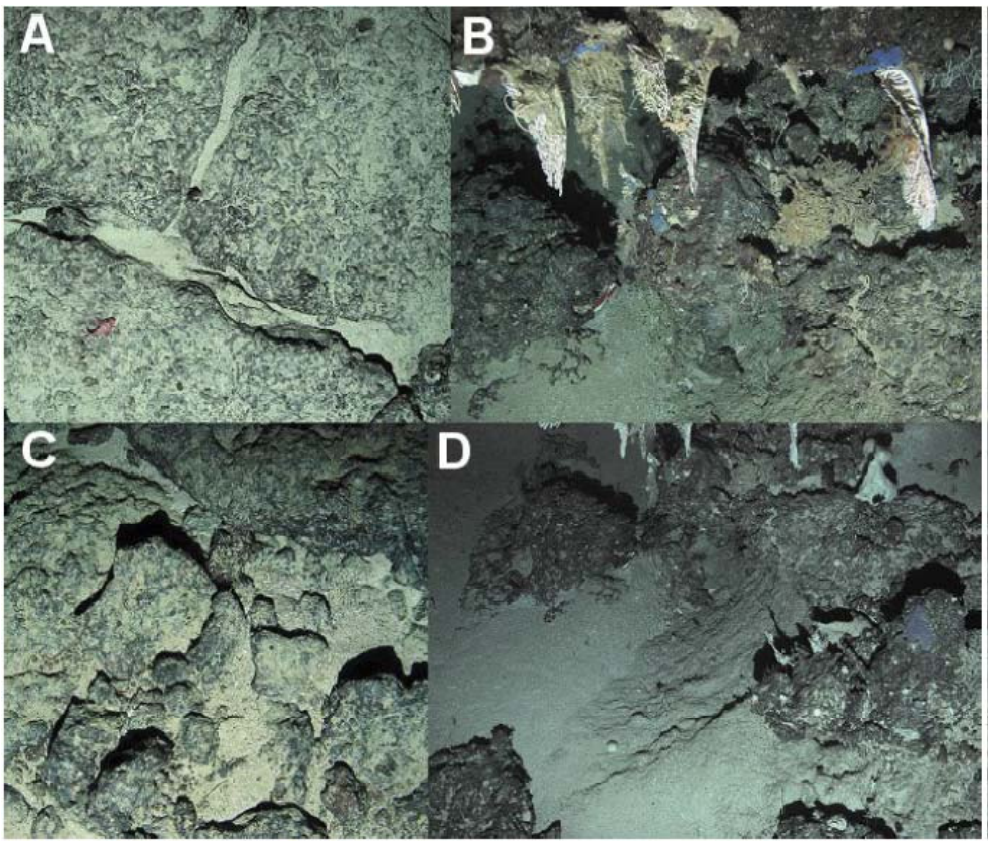

Figure 16: "A. Low-relief jointed pavement on escarpment between high-relief ledges. B. Side of high-relief ledge with projecting lace corals (Stylasteridae). C. Moderate-relief outcrops and boulders. D. Steep sediment and boulder-strewn slope just below figure 16B (projecting lace corals visible at top)" (Messing et al., 2006.b).

If mooring in the northward flowing Florida Current is assumed to experience uni-directional anchor loading, all anchor types function well where their respective bottom type requirements exist (Figure 9) except for the case of a taut mooring with large uplift angle where drag embedment anchors do not function (Table 2). Drag embedment anchors will also not work for limestone or stratified bottom types as they can have erratic behavior and "tend to skid on the top of the hard stratum" (Gerwick, 2007).

Two sessions of manned submersible benthic surveys, aboard HBOI's Johnson Sea-Link Submersible, took place within the area of interest near SNMREC's data

collection along 26°05’ N in joint efforts between SNMREC and HBOI. The first set of submersible dives was conducted in two proposed areas (Sept. 22, 2008) to investigate possible deployment sites for a turbine prototype system and small scale device test berth (SNMREC, 2010). The entirety of the initial set of SNMREC sponsored, sub dive video takes place on top of the Miami Terrace over limestone bottom overlaid by varying amounts of sediment. The second session of dives took place September 15, 2009 while performing demonstration submersible dives. During these dives, HBOI took video and photographs of gravity anchors used to moor ADCP buoys deployed by FAU. At the buoy site located 2nd closest to shore in 260 m of water, the bottom type is characterized by rubble covered by a thin sand layer, and no benthic life was found nearby (SNMREC, 2010). Moving eastward, surveying the buoy in 340 m, photographs show sand with sparse sponge growth, but no significant coral habitat was discovered (SNMREC, 2010). Finally the buoy site located furthest offshore in 660 m shows a bottom characterized by sand with no active benthic habitat (SNMREC, 2010).

These previously conducted benthic surveys provide a regional understanding of the bottom types that may be encountered. Detailed site specific surveys are required for final anchor system design. Depths of sediment overlay, which is very important to anchor selection and design, can be determined through sub-bottom profiling and core samples. Soil properties can also be determined through core and specimen sampling.

3. ANCHOR LOADING EXTRACTION

To accurately estimate the anchor loading from MRE devices, environmental conditions characteristic of the region must be determined for use in numerical simulations. For this reason, a methodology for quantifying metocean conditions is first established from a combination of offshore engineering standards and local data measurements (Section 3.1). Local current data is combined with knowledge of the bathymetry along 26°5’ N to develop a comprehensive range of anchor loading scenarios that may occur for future commercial MHK devices in this region. These anchor loading scenarios are simulated using Orcaflex software (Section 3.2) and the anchor loading is extracted (Section 3.3). Finally, past studies of anchor loading estimates for OTEC systems in the Gulf Stream are discussed (Section 3.4).

3.1 Metocean Conditions

Wind, wave, and current conditions are provided in this section for the future simulation of MRE devices with a surface presence such as floating OTEC plants. For the simulation of subsurface MHK devices presented in this work, only current conditions are applied. Suggested designs for subsurface MHK devices (Figure 4 through 6) acknowledge that control of the device operating depth is desired so that diving to deeper depths to avoid the surface effects of storm events is possible. It is also acknowledged that the operating depth should not create a navigational hazard.

Preliminary design standards and recommended practices for the design and analysis of moored offshore structures in extreme weather, such as 50 or 100 year storms, do not exist specifically for the region offshore southeast Florida that contains the area of interest. It is likely that these standards will not exist until Florida's coasts are opened to offshore oil drilling or there is an increase in MRE activity. Until survivability standards are set for offshore MRE systems, it has been advised by offshore industry professionals to use the conditions for storms with 100 year return periods in the Gulf of Mexico that are provided by the American Petroleum Institute (API) and Det Norske Veritas (DNV). These standards and recommended practices are only a basis for guidance and do not provide as definitively accurate results as site-specific studies (API, 2007).

API's metocean conditions only address hurricane conditions for the Gulf of Mexico and do not address "phenomena such as winter storms, the Loop Current, and other deepwater currents, or the joint occurrence of hurricane and Loop/deepwater current phenomena" (API, 2007). Multiple phenomena may occur simultaneously offshore Southeast Florida a might be the case of a category 5 hurricane, which has a return period of 52 years, traveling over the Florida Current (NDBC, 2010). DNV recommends that in locations where multiple phenomena occur, such as hurricane events where deep water currents exist, "the combination of environmental loads that leads to the largest line tensions should be selected, at this environmental return period" (2008).

API explains that "to combine all extremes at the same return period together when constructing a wind, wave, current and surge load case is very conservative, as the different variables will seldom peak at the same time during a given storm, and the n-year

values of different parameters may not even occur in the same storm event" (2007). Without site specific data, it is recommended by DNV (2008) to apply the most conservative method which API recommends is combining all extremes at the same time (2007). For this reason, hurricane conditions from several sources (Table 3) were compared to find the maximum wave, wind and current conditions to be applied to simulations of MRE devices with a surface presence to ensure the most conservative method is used.

Table 3: Metocean Conditions

Maximum Conditions for Storm with 100 Year Return Period

			Waves			
Agency	Location	Depth (m)	Hs (m)	Hmax (m)	Peak Spectral Period (s)	Period of Maximum Wave (s)
API Bullentin 2INT-MET (2007)	Gulf West Region	700	13	23	15.1	13.6
API Bullentin 2INT-MET (2007)	Gulf Central Region	700	15.75	approx. 23	15.4	13.9
DNV-OS-E301 (2008)	Gulf of Mexico	not specified	15.8	-	-	13.9 -16.9
			Wind (10 m elevation)			
			1-hour Mean Wind Speed (m/s)	10-min Mean Wind Speed (m/s)	1-min Mean Wind Speed (m/s)	3-sec Gust (m/s)
API Bullentin 2INT-MET (2007)	Gulf West Region	All	39.9	44.7	50.8	58.8
API Bullentin 2INT-MET (2007)	Gulf Central Region	All	48	54.5	62.8	73.7
DNV-OS-E301 (2008)	Gulf of Mexico	not specified	48	-	-	-

Maximum Recorded Conditions for Past Hurricanes Passing Near Test Site

Hurricane Floyd (Sept. 1999)			Waves	Wind (5 m elevation)	
Agency	Location	Depth (m)	Max H (m)	Max Speed (m/s)	Max Gust (m/s)
NOAA National Data Buoy Center	Station 41009	44.2	11	27.12	36
NOAA National Data Buoy Center	Station 41010	872.6	15.6	36.78	47.32
				Wind (9.8 m elevation)	
				Max Speed (m/s)	Max Gust (m/s)
NOAA National Data Buoy Center	Station SPGF1	N/A	N/A	28.94	30

Hurricane Wilma (Oct. 2005)			Waves	Wind (5 m elevation)	
Agency	Location	Depth (m)	Max sig. H (m)	Max 8 min Speed (m/s)	Max Gust (m/s)
NOAA National Data Buoy Center	Station 41009	44.2	6	26.8	34.9
NOAA National Data Buoy Center	Station 41010	872.6	10.2	31.6	42.3
				Wind (9.8 m elevation)	
				Max 10 min Speed (m/s)	Max 5-s Gust (m/s)
NOAA National Data Buoy Center	Station SPGF1	N/A	N/A	28.94	52.8

3.1.1 Waves

The wave data required as a basis for the design of a position mooring is the "combinations of significant wave heights and peak periods along the 100-year contour line for a specified location" (DNV, 2008). Maximum wave heights for storms with a 100 year return period in the Gulf of Mexico, provided by API and DNV, were compared to the peak wave heights, measured by data buoys, which occurred during past hurricane events with paths near the area of interest. The closest buoy to the area of interest to collect wave data during past hurricanes is the National Data Buoy Center's (NDBC) station 41009 located 20 nm east of Cape Canaveral (NDBC, 2010). The second closest NDBC buoy to record wave data on the east coast of Florida is station 41010 located 120 nm east of Cape Canaveral. Although the hurricanes that were measured passed near South Florida's coastline, the recorded values may not be characteristic of the area of interest because of the difference in depths, bathymetric features and lack of Bahamian Island influence where the buoys are located. Hurricane Floyd and Wilma varied from category 2 to 3 hurricanes when passing near the buoys (NDBC, 2010), and the recorded wave heights from these storms are presented in Table 3. An additional source for hurricane conditions was the deployment of nine floats used to measure intensity of Hurricane Frances in 2004 which made landfall near Stuart Florida (Black et al., 2007). The wave heights recorded from these floats are presented in Figure 17.

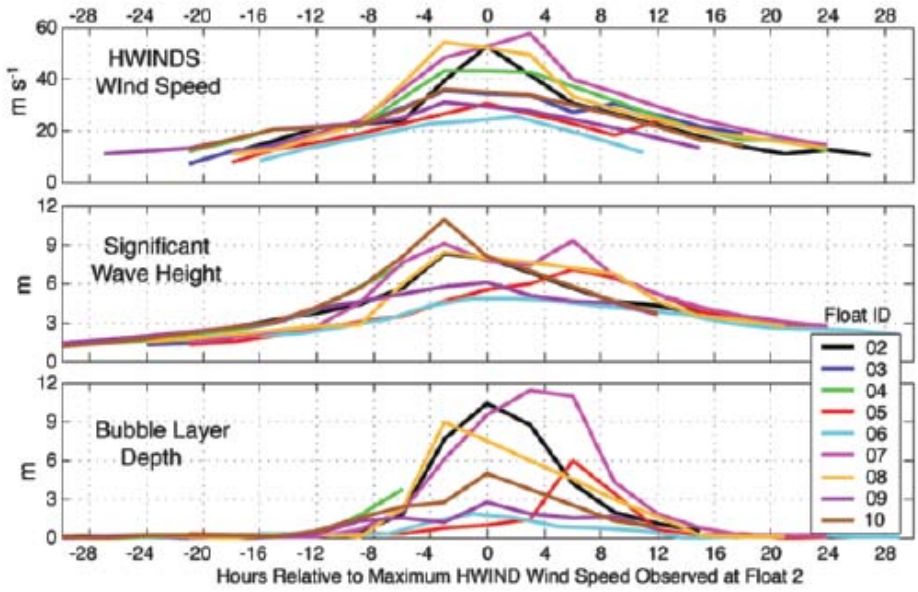

Figure 17: Wind speed, wave height, and bubble layer depth measurements of Hurricane Frances (Black et al., 2007).

Wave heights provided by DNV for the Gulf of Mexico are the largest of the evaluated sources with a significant wave height (H_s) of 15.8 m. The associated period of the maximum wave heights presented by DNV is 13.9 to 16.9 seconds (DNV, 2008). A JONSWAP spectrum is recommended by API and DNV to represent hurricane driven seas. Therefore, a JONSWAP with a significant wave height of 15.8 m is suggested for evaluating MRE devices for Southeast Florida. A peak spectral period of 15.4 s from the API Gulf Central region can be input as the partially specified spectral parameters in Orcaflex. This is suggested to more clearly define the environmental parameters of the simulation and can be justified because values for the peak wave heights and period of maximum waves are similar for the two sources. For large floating structures like OTEC plants, the period of waves should be varied because large structures are dominated by low frequency motions (API, 2005). Therefore, the greatest mooring loads may not be

created by 100 year storm conditions but by the combination of lower wave heights and periods that could yield larger low frequency motions (API, 2005).

3.1.2 Wind

The wind data required as a basis for the design of a position mooring is the "1 hour mean wind speed with a return period of 100 years" (DNV, 2008). The only data for 1-hour mean wind speeds comes from DNV and API for the Gulf of Mexico. This value is included in the independent extreme values for hurricane winds in the Central Gulf of Mexico displayed in Table 4. The available API wind spectrum in Orcaflex can be used with a 1-hour mean wind speed of 48 m/s for simulations where wind loads play an effect. For further characterization of the wind parameters, maximum wind speeds experienced during past hurricanes can be found in Table 3 for Hurricane Floyd and Wilma and in Figure 17 for Hurricane Frances, but values for the 1-hour mean wind speed for these storm events were not found.

Table 4: Independent Extreme Values for Hurricane Winds in The Central Gulf of Mexico (89.5°W To 86.5°W) (API, 2007).

Wind (10 m Elevation) for 100 Year Return Period	Speed (m/s)
1-hour Mean Wind Speed (m/s)	48.0
10-min Mean Wind Speed (m/s)	54.5
1-min Mean Wind Speed (m/s)	62.8
3-sec Gust (m/s)	73.7

3.1.3 Current

In order to create a comprehensive range of anchor loading scenarios, the available current profile data closest to 26° 05'N was chosen for two different depths. The core of

the Florida Current straddles a seafloor feature called the Terrace Escarpment where anchoring may want to be avoided due to steep slopes and high relief. The anchoring scenarios created are characteristic of locations both east and west of this feature. To the west of the Terrace Escarpment is the Miami Terrace with depths of 200 m to 400 m, and moving East beyond the Terrace Escarpment are depths of 600 m to near 800 m (Figure 19). A map of the bathymetry transect along 26° 05'N including locations of ADCP buoys from which current data for simulations on top of the Miami Terrace was used, is displayed in Figure 18.

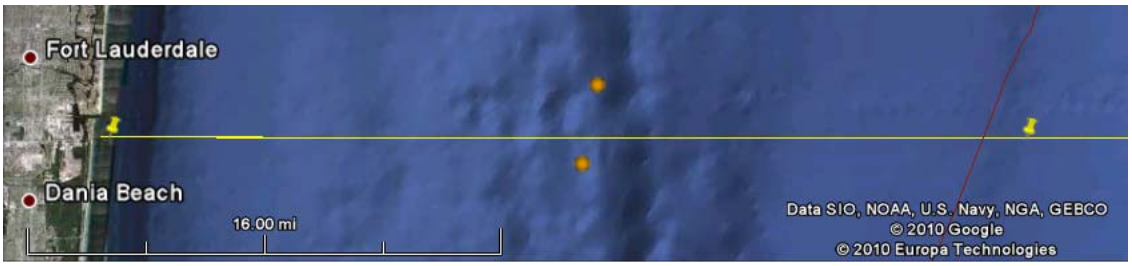

Figure 18: Map of bathymetry transect along 26° 05' N represented by yellow line. Yellow pushpins denote 80.1° W and 79.6° W corresponding to Figure 19. Orange circles denote location of ADCP buoy deployed for 18 months (top circle) in 330 m and SNMREC's buoy deployed for 13 months (bottom circle) in 340 m.

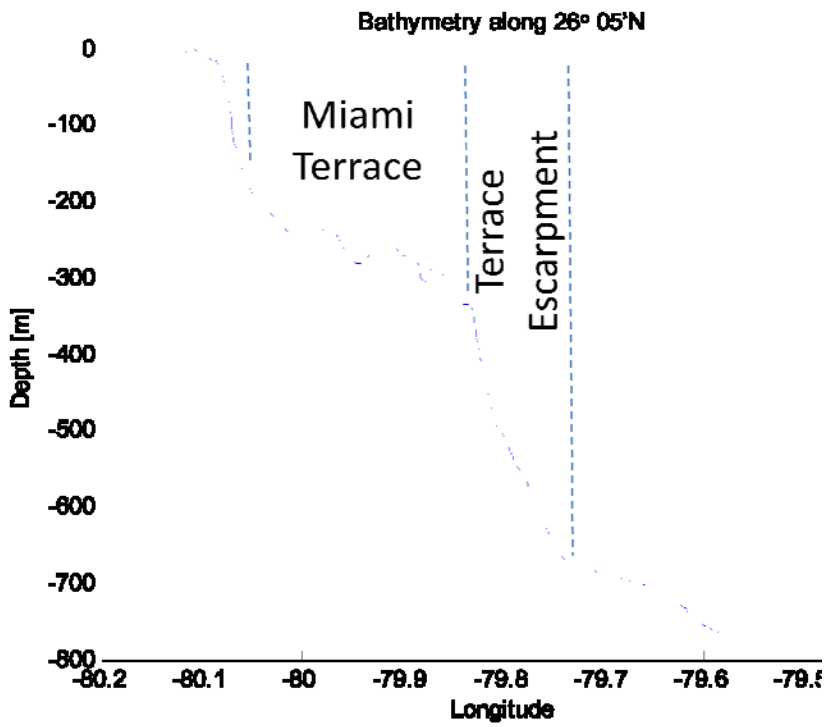

Figure 19: Bathymetry along 26° 05'N (Leland, 2009). Estimated position of Miami Terrace and Terrace Escarpment at this latitude.

Although DNV recommends that a surface current speed with a 10-year return period should be used, maximum current data obtained from ADCP buoys deployed by FAU will be used, because the surface current value with a 10-year return period is not known for this region (DNV, 2008). An ADCP buoy was deployed three miles west of the mean axis of the Florida Current at 26° 6.6'N, 79° 30.0'W for an 18 month period in approximately 330 m of water (Figure 18) (Raye, 2002) and an additional ADCP buoy was placed upstream of this location by SNMREC (Figure 18). Combining the data from the two sets of deployments creates almost a full three year long data set for current measurements within the Florida Current. The ADCP buoy deployed for 18 months measured a maximum surface current of 2.5 m/s (Raye, 2002). The additional ADCP buoy data set, combining to create the nearly three year long data set, also measured a

maximum surface current of 2.5 m/s (VanZwieten et al., 2011). These maximum values are higher than the maximum surface current provided by API of 2.4 m/s for the Gulf Central region which has the highest values of all API defined Gulf Regions (API, 2007). Continued measurements within the region may reveal the 10 year return period current to be slightly higher than the measured 2.5 m/s surface current. The maximum current profile used for simulating an anchor loading scenario on the Miami Terrace was created by interpolating between maximum currents specified at depths between the surface and seafloor with 50 m increments. The resulting maximum current profile for a 325 meter depth is displayed in Figure 20.

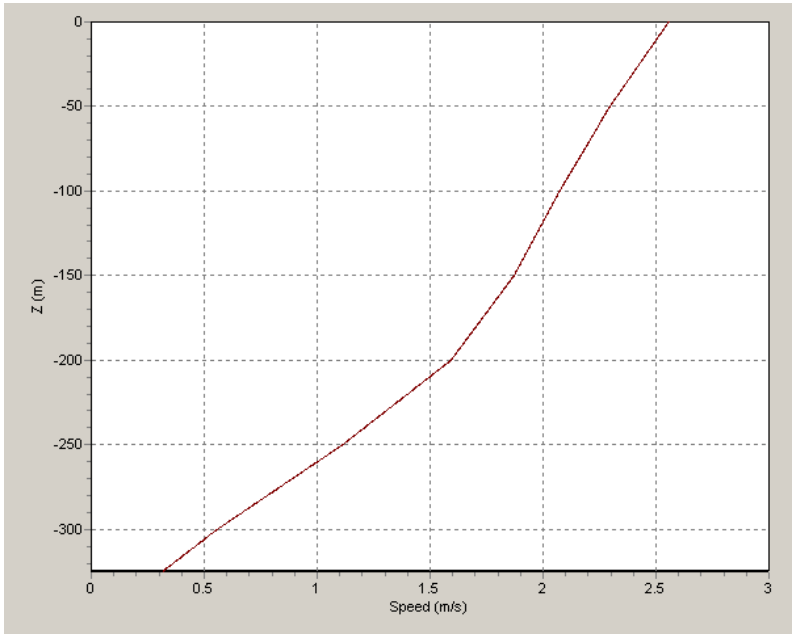

Figure 20: Maximum Current Profile for 325 m depth (FAU ADCP data).

ADCP data was not available for the portion of the area of interest east of the Terrace Escarpment. Therefore, a 700 m depth was selected to represent anchor loading scenarios beyond the Terrace Escarpment and numeric model data is used to predict the

maximum flow speeds. The current profile for the 700 m depth was developed from the Hybrid Coordinate Ocean Model (HYCOM) which is a data assimilative hybrid isopycnal-sigma-pressure (generalized) coordinate ocean model that can simulate oceanographic values including north and east velocity variables at a given location (Duerr et al., 2010). The data used to create the current profile was the maximum velocity magnitude at each depth bin for two months of daily snapshots of the Florida Current at 27° 00' N, 79° 36' W taken in November and December 2008. This location is north of the area of interest but is characteristic of the Florida Straits and is at the moment the best available estimation for the 700 m current profile. The resulting current profile for the 700 meter depth is displayed in Figure 21.

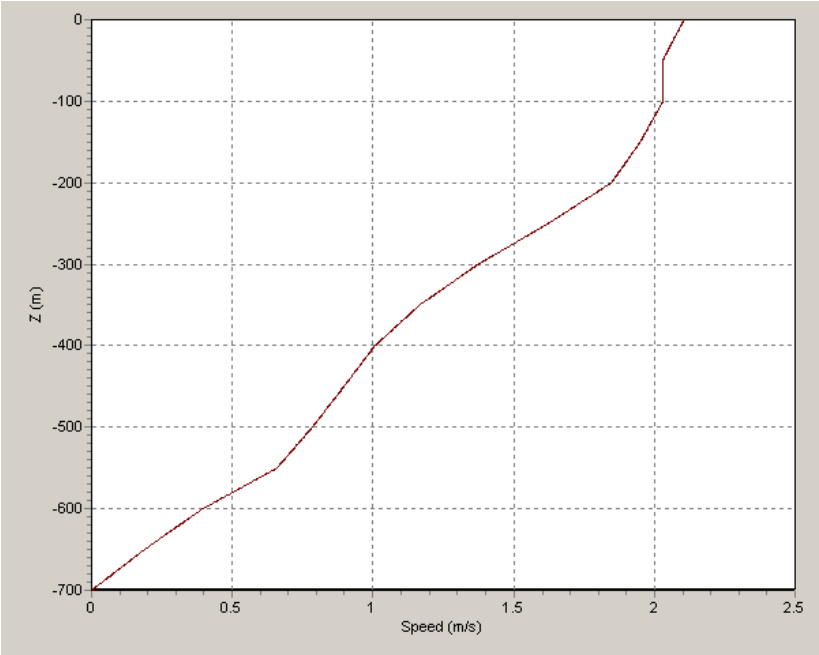

Figure 21: Maximum current Profile for 700 m depth (HYCOM data).

3.1.4 Recommendations for Floating OTEC System Analysis

Subsurface marine hydrokinetic devices may not be greatly affected by conditions of the air sea interface (dependent on the depth of operation) whereas floating systems are affected by the environmental loading of waves, wind, and current. For floating position moorings, waves, wind and current should be applied in both a collinear and non-collinear environment for areas where site specific environmental directionality data is not available (DNV, 2008). The collinear environment applies the waves, wind and current in the same direction 15˚ relative to the devices bow (DNV, 2008). The non-collinear environment applies the waves towards the devices bow at 0˚, the wind 30˚ relative to the waves and the current 45 ˚relative to the waves (DNV, 2008).

The selected maximum wave conditions that should be applied to the MRE device dynamic simulations are a significant wave height (H_s) of 15.8 m with a peak spectral period of 15.4 s using a JONSWAP spectrum. As stated in Section 3.1.1, for large floating structures like OTEC plants, the period and height waves should be varied to find the maximum loading conditions. The selected maximum wind conditions are a 1-hour mean wind speed of 48 m/s using an API spectrum. The wave and wind conditions should be applied in combination with the maximum current profiles displayed in Figures 20 and 21. To reiterate, it is seldom that maximum environmental conditions will all occur at the same time or even all occur during the same storm event but until site specific surveys have been completed it is recommended that the combined maximum environmental conditions are used for conservative analysis. Future site specific surveys could reveal different metocean conditions, but until they are created the most conservative conditions developed for the most similar regions are being used. Future

design standards for MRE devices may be less stringent than those for the offshore oil industry, but since they have not yet been defined, standards for the offshore oil industry can be used as basis for the simulation of future MRE systems.

3.2 Marine Hydrokinetic Turbine Anchor Loading

In order to investigate anchoring options for in-stream hydrokinetic turbines, single point moored hydrokinetic turbines are modeled in Orcaflex as subsurface 3D buoys to predict a range of anchor loadings that is a function of rotor diameter. Drag characteristics of the buoys are set to match the estimated drag characteristics for a turbine with the desired rotor diameter. Drag of an ocean current turbine is calculated using the equation:

$$D = \frac{1}{2} C_d \rho U^2 A, \tag{1}$$

where D is the drag force, C_d is the drag coefficient, ρ is the density of seawater, U is the current speed and A is rotor swept area calculated by $A = \pi r^2$. It is noted that the drag force and drag coefficient may be referenced as the thrust force and thrust coefficient in the design of marine hydrokinetic turbines. A drag coefficient was found by using results of a numerical simulation created for predicting the performance of FAU's first generation experimental ocean current turbine. The version of the experimental prototype for which the mathematically model was created is seen in Figure 22. Drag forces on the streamlined body members of the prototype, including the nacelle (generator housing) and two buoyancy compensation modules, were calculated using the strip theory for a cross flow (Vanrietvelde, 2009). This numerical model uses unsteady

blade element momentum theory to calculate drag and other hydrodynamic forces of the rotor. The maximum drag of FAU's system in a 2.5 m/s current, including the drag created by the generator housing and buoyancy modules, for a three meter diameter blade operating with a tip speed ratio of 3.9 is 20.25 kN. The tip speed ratio of 3.9 is where maximum power output is generated and is close to where the maximum drag is produced. The rotor drag accounted for 81% of the total drag of FAU's system and the remaining 19% was created by the generator housing and buoyancy modules. As seen in this case, and similarly expected in future commercial systems, the majority of drag force will be due to the rotor because remaining components are expected to be streamlined. A drag of 20.25 kN with the associated current speed of 2.5 m/s, sea density of 1,026 kg/m^3, and a swept area of 7.07 m^2 (for the 3 m diameter blade) were used in a variation of Equation 1:

$$C_d = \frac{D}{\frac{1}{2}\rho U^2 A}, \tag{2}$$

to get a drag coefficient of 0.89 for the entire turbine. The calculated drag coefficient is similar to the 8/9 that Betz identifies as the drag coefficient when a turbine operates at its maximum power coefficient (Clarke et al, 2009). The drag coefficient for FAU's rotor is less than the calculated 0.89 drag coefficient for the entire turbine (including buoyancy modules and generator housing) with a value of 0.72. The drag coefficient of the rotor is less than the Betz coefficient because real systems operate at an efficiency below the Betz limit. This drag coefficient is input as the x-direction (perpendicular to the face of the rotor) drag coefficient in Orcaflex, and because a 3D buoy always has the same heading,

this direction is always perpendicular to the flow. The drag area is the swept area of the rotor and is applied in the x-direction for each simulation.

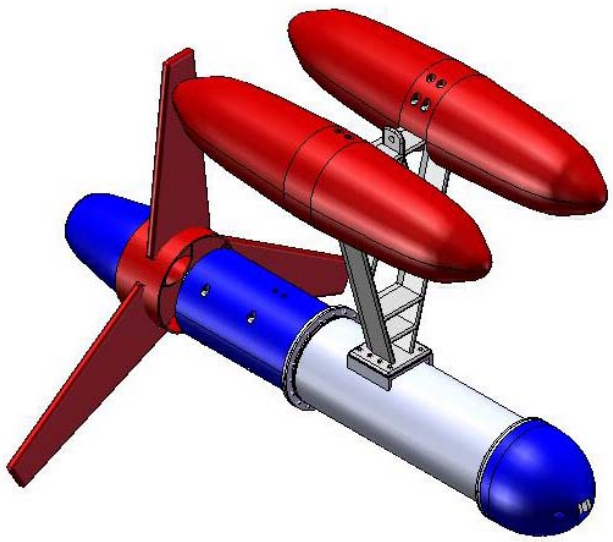

Figure 22: CAD Drawing of FAU's First Generation Experimental Hydrokinetic Turbine.

For each simulation iteration, the mass of the turbine was set to a constant value and buoyancy of the turbine was changed until it reached a steady state position within one meter of the target operational depth of 50 meters in the maximum current profile at the 325 m and 700 m depth locations. The current profiles were applied in the x-direction of the mooring system. Once enough buoyancy was added to operate at the target depth in the maximum current profile, the 6 x 19 wire strand with wire core diameter of the taut mooring was increased in increments of 0.005 m until minimum breaking loads were greater than the effective tension of the mooring line under the evaluated conditions with an applied safety factor of 2.04. As previously stated, offshore standards do not exist specifically for these applications, and therefore a safety factor of

2.04 was calculated following the DNV's *Offshore Standards for Position Moorings* (DNV, 2008). The simulated moored turbine system was placed in a class 1 consequence class which includes position moorings "where mooring system failure is unlikely to lead to unacceptable consequences such as loss of life, collision with an adjacent platform, uncontrolled outflow of oil or gas, capsize or sinking" which first yields a partial safety factor of 1.70 for a quasi-static analysis (DNV, 2008). The partial safety factor which is applicable to chain, steel wire ropes and synthetic fibre ropes must then be multiplied by a factor of 1.2 to be acceptable, to compensate for the lack of redundancy of a single point mooring, yielding the safety factor of 2.04 (DNV, 2008). As the size of mooring line diameter increased, the process was repeated to change the buoyancy of the turbine until it remained within one meter of the 50 meter depth in maximum currents.

Ideally, a commercial turbine system would employ adjustable buoyancy systems or lifting surfaces in order to dive to a safer depth prior to the arrival of a hurricane or major environmental surface forcing. For this reason, wave and wind conditions for a 100 year storm were not applied to the simulations. The dynamic analysis was performed until the turbine reached a steady state z and x position. At this point, the net buoyancy used for each rotor size to remain at 50 meters could be determined (Figure 29 and 30). Mooring scope, the ratio of mooring line to water depth, was selected so the wire remained taut as buoyancy was optimized to force each turbine to remain at the 50 meter depth. A scope of 1.25, 1.5, and 2 were examined for the 325 meter depth. Scopes of 1.25 and 1.5 were examined for the 700 meter depth. Scopes of 1.25 and 1.5 for both simulations created an approximate range of anchor loading angles with the seafloor from 30° to 45° which is the loading angle range typical of taut moorings (Tension Tech,

2010). A scope of 2 was applied to the 325 meter depth to provide insight into the affects of larger scopes. It is noted that larger scopes required more time to reach steady state. This may be evidence that "variations in operating depth with current velocity would then be significantly reduced" with higher uplift angles and therefore more necessary buoyancy for shorter scopes (Clarke et al., 2009). It can also be noted that for commercially deployed systems, it may be desirable to use a mooring scope large enough such that the system can surface in normal operating currents with its available buoyancy for maintenance purposes as shorter scopes require greater buoyancy to operate at a 50 m depth.

This process was repeated for eight rotor diameters, ranging from 3 meters to 50 meters, with current conditions characteristic of two different locations within the area of interest in order to identify the range of anchors that could be used.

3.3 Marine Hydrokinetic Turbine Simulation Results

Forty unique mooring scenarios were created to encompass a range of anchor loading scenarios that may occur with variations in rotor size, mooring design, and location. The simulation results from these 40 scenarios include anchor loadings, the primary focus of these simulations (Section 3.3.1). These results also include the upward force required to hold the turbines at the desired location in the water column (Section 3.3.2), as these will help device developers size either the lifting surfaces or required buoyancy to maintain systems at the designed operating depth. An SI to English unit conversion scale is provided as Figure 23 for easy conversion of values presented in

anchor loading and sizing plots in Chapters 3 and 4 respectively. Finally, the associated power output, which can be used to refine the cable sizes and thus cable drag and anchor loading estimates in a later study, are presented in Section 3.3.3.

3.3.1 Anchor Loads

The results from these simulations indicate that overall anchor loading increases with decreasing scopes (Figure 24 and 27), the majority of which is seen in the vertical anchor loading component (Figure 25 and 28) due to the increased buoyancy necessary for the device to remain at the same (50 m) operating depth with a shorter mooring line. For a 20 m diameter rotor (Figure 25), the vertical loading increases from 318.5 kN, with a scope of 2.00, to 666.4 kN with a scope of 1.25. This is a 109% increase in vertical loading between the two scopes. Horizontal loads on the anchor connection point (Figure 26 and 29) remain near the same values as scopes are changed, differing by less than 5% for each rotor diameter. The same trends can be observed for both the 325 m and 700 m depth locations, but the overall anchor loading of the 700 m depth is less than the 325 m depth, because the available current profile for 700 m has smaller maximums than the 325 m depth. A 20 m diameter rotor with a scope of 1.25 at the 325 m depth creates a tension in the line of 1016.6 kN at the anchor connection point (Figure 24), whereas at the 700 m depth with the same scope of 1.25, it creates a tension of 864.9 kN (Figure 27). The benefits of extracting anchor loading are described in Chapter 4, particularly in regards to the size of anchor necessary to hold a certain size device in place.

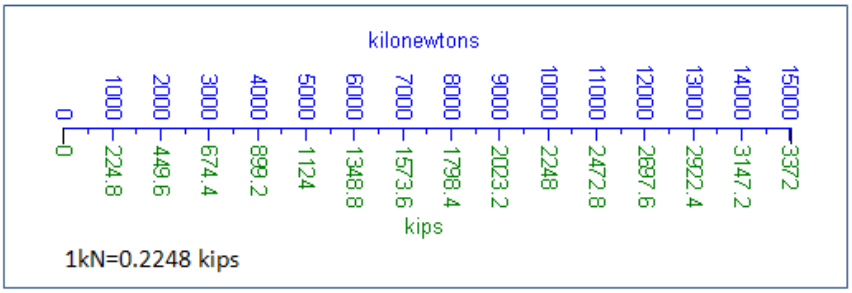

Figure 23: SI to English unit conversion scale.

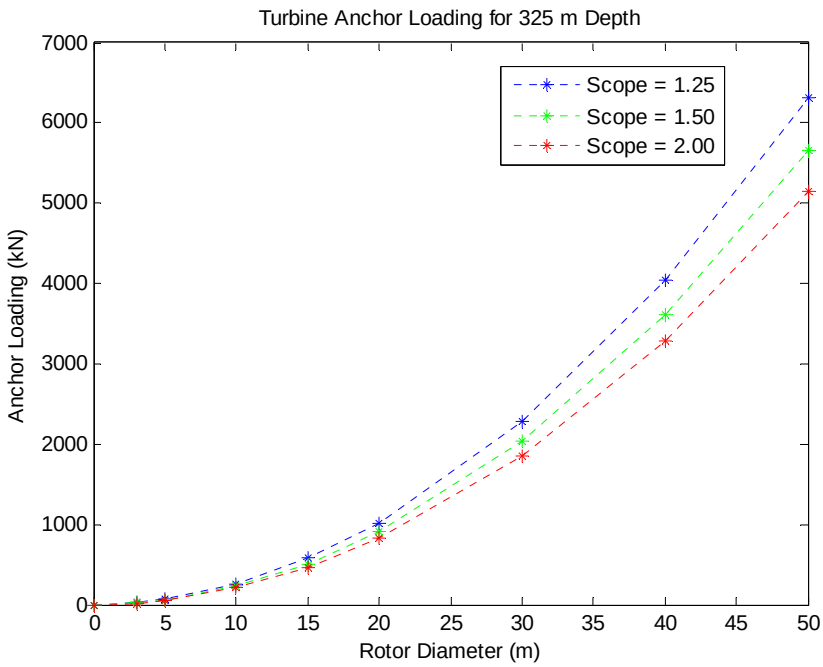

Figure 24: Turbine anchor loading for 325 m depth.

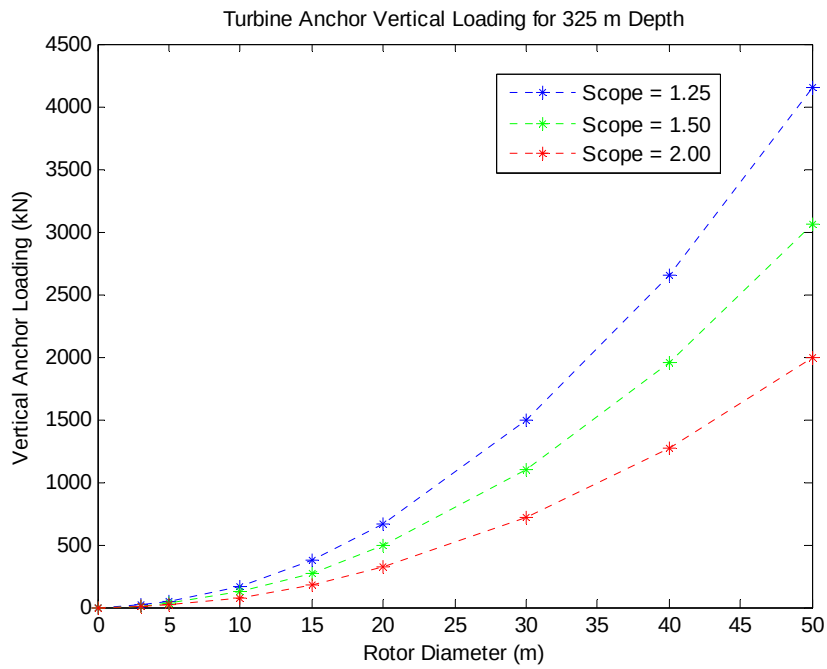

Figure 25: Turbine anchor vertical loading for 325 m depth.

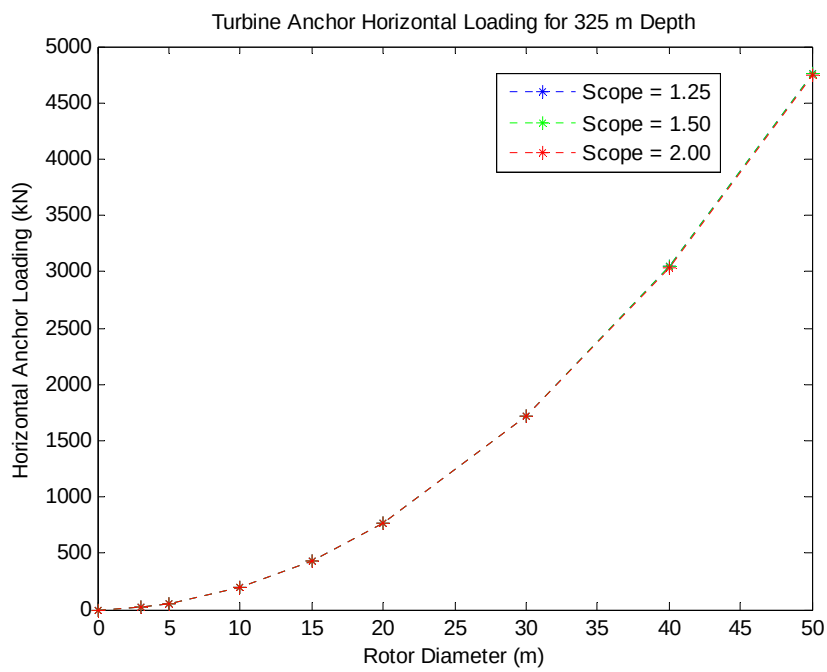

Figure 26: Turbine anchor horizontal loading for 325 m depth.

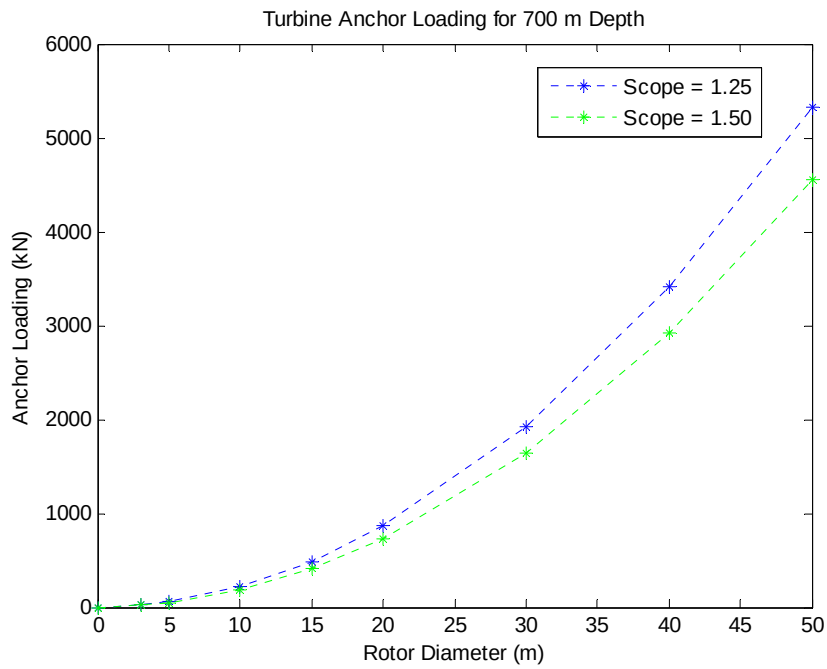

Figure 27: Turbine anchor loading for 700 m depth.

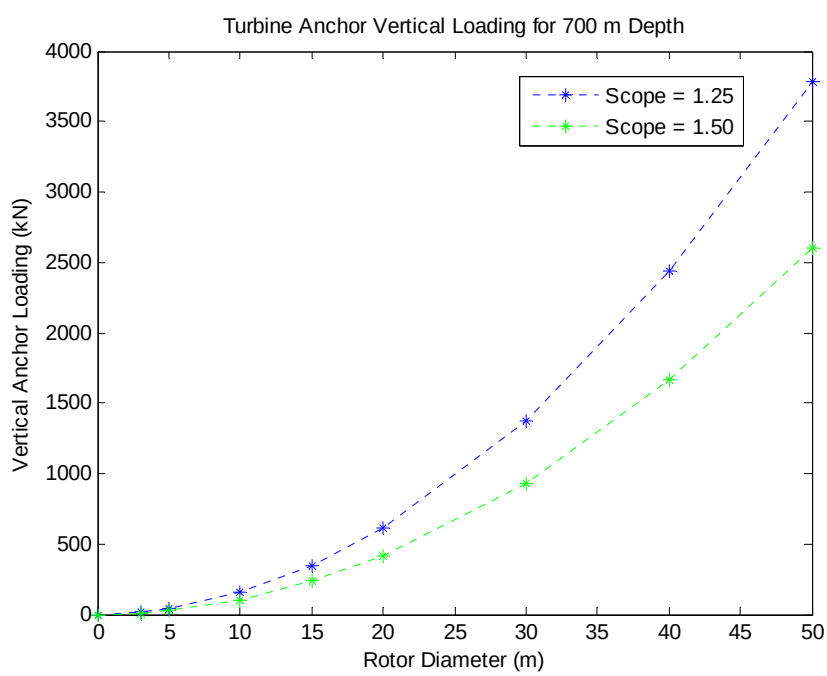

Figure 28: Turbine anchor vertical loading for 700 m depth.

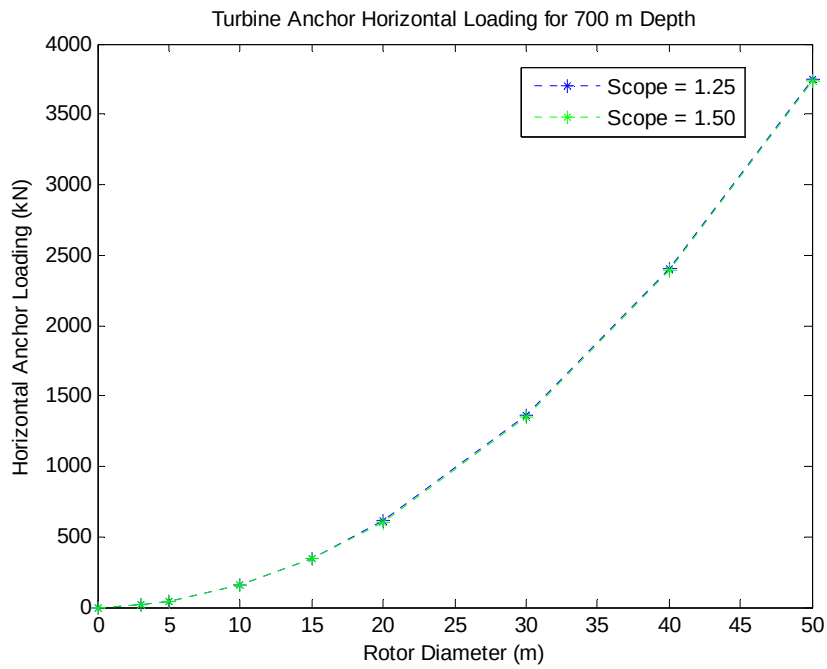

Figure 29: Turbine anchor horizontal loading for 700 m depth.

3.3.2 Required Lift Force

The results of necessary lift force calculation to hold the simulated turbine at a depth of 50 meters will be useful to device developers when designing variable buoyancy devices. The results are also equivalently useful to determine the lifting force required for neutrally buoyant designs employing lifting surfaces. The increase in necessary buoyancy to account for the shorter mooring line while the turbine operates at the same 50 m operating depth in 325 m of water is displayed in Figure 30. For a 20 m rotor diameter the necessary buoyancy increases from 393.0 kN for a scope of 2.00 to 727.3 kN for a scope of 1.25. These positive buoyancies are equivalent to displacing 39.1 m^3 and 72.3 m^3 respectively, with the smaller scope requiring an 85% increase in necessary buoyancy. Assuming a lift coefficient of 1.0 and no 3D hydrodynamic effects, a lifting area of 145 m^3 will be required for a scope of 2.0 at this location.

The necessary buoyant force needed to remain at the 50 m depth (Figure 30 and 31) was determined by subtracting the 3D buoy's, representing the hydrokinetic turbine, weight from the 3D buoy's buoyant force which is determined by multiplying the submerged volume by the specific weight of the seawater. It should be noted that to increase the buoyancy of the 3D buoy, the volume of the unit was increased. The increase in volume did not directly increase the drag because Orcaflex uses only the input drag area of the turbine with the determined drag coefficient to calculate the drag in the applied current. The type and shape of the buoyancy device used (floatation or lifting surface) will affect the lateral drag, but a specific buoyancy device is not being examined in this analysis. Instead, only the necessary buoyant force required for the input drag area and drag coefficient is identified.

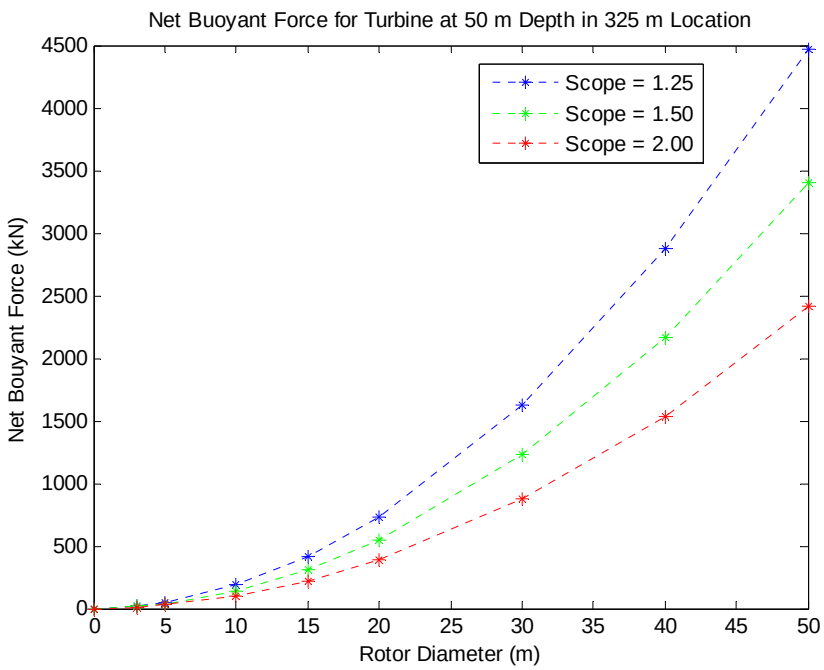

Figure 30: Net buoyant force for turbine at 50 m depth in 325 m location.

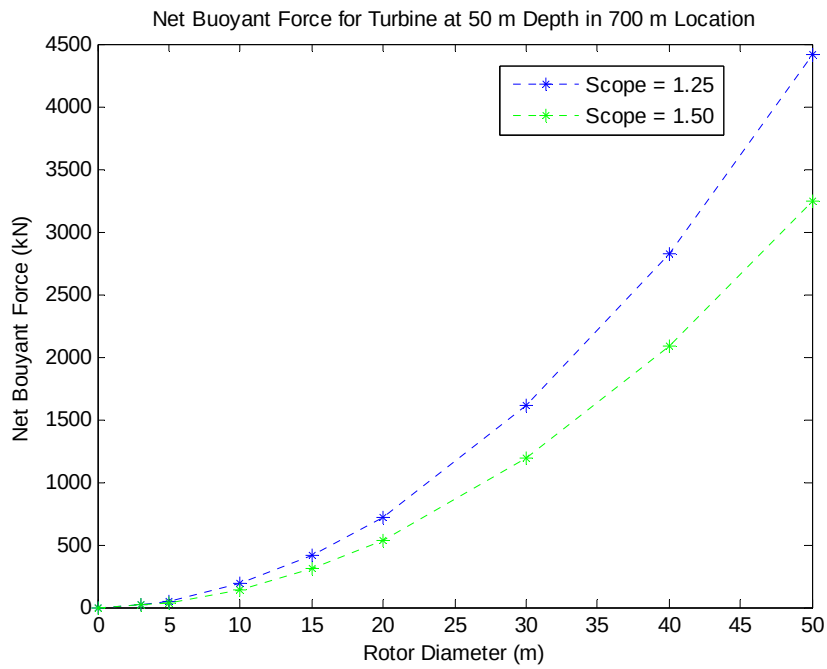

Figure 31: Net buoyant force for turbine at 50 m depth in 700 m location.

3.3.3 Estimated Power Outputs

The simulations do not take in to account the increased diameters of electromechanical mooring lines required for power transmission to the seafloor. Anchor loading predictions will increase as drag increases with future simulations that take this into account. The design power for most systems will be less than those created by maximum or extreme conditions, and therefore might limit the power production of extreme conditions by either diving, using stall regulated rotor blades, or feathering the rotor blades. The estimated power output of the simulated MHK devices is also an important factor for future feasibility assessments in comparing size and cost of anchor systems to the power production of a device.

The theoretical maximum power output before power losses from transmission to shore is:

$$P = \frac{1}{2}\rho U^3 A\eta \,, \tag{3}$$

where η is the Betz maximum efficiency of 0.593. Table 5 displays the maximum power output predicted using the Betz efficiency for both the 325 m location, where the maximum velocity at the 50 meter operational depth is 2.3 m/s and for the 700 meter location where the velocity at 50 meter operational depth is 2.03 m/s (HYCOM data) for the eight rotor diameters that were simulated. A more comprehensive plot of predicted power output with the Betz efficiency for several different current speeds and rotor diameters is displayed in Figures 32 and 33.

Table 5: Estimated Power Outputs for 325m and 700m depths at Maximum Current Velocity

Rotor Diameter [m]	325 m Location Estimated Power Output at 50 m (2.3 m/s) with Betz eff. = 0.593 [kW]	700 m Location Estimated Power Output at 50 m (2.03 m/s) with Betz eff. = 0.593 [kW]
3	26.16	17.99
5	72.68	49.97
10	290.70	199.87
15	654.08	449.71
20	1162.80	799.48
30	2616.30	1798.84
40	4651.20	3197.94
50	7267.50	4996.77

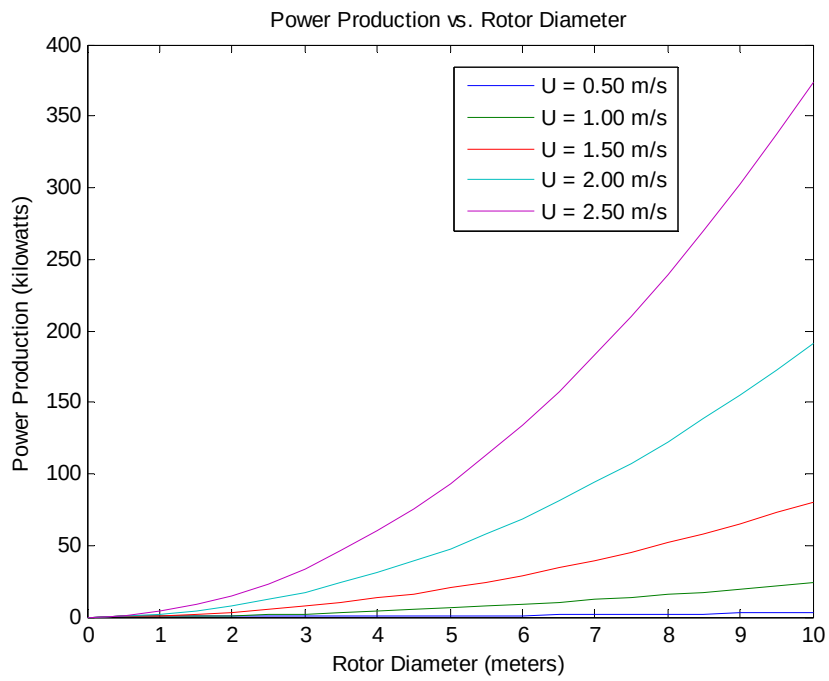

Figure 32: Maximum theoretical power production vs. rotor diameter for 0 to 10 m diameters.

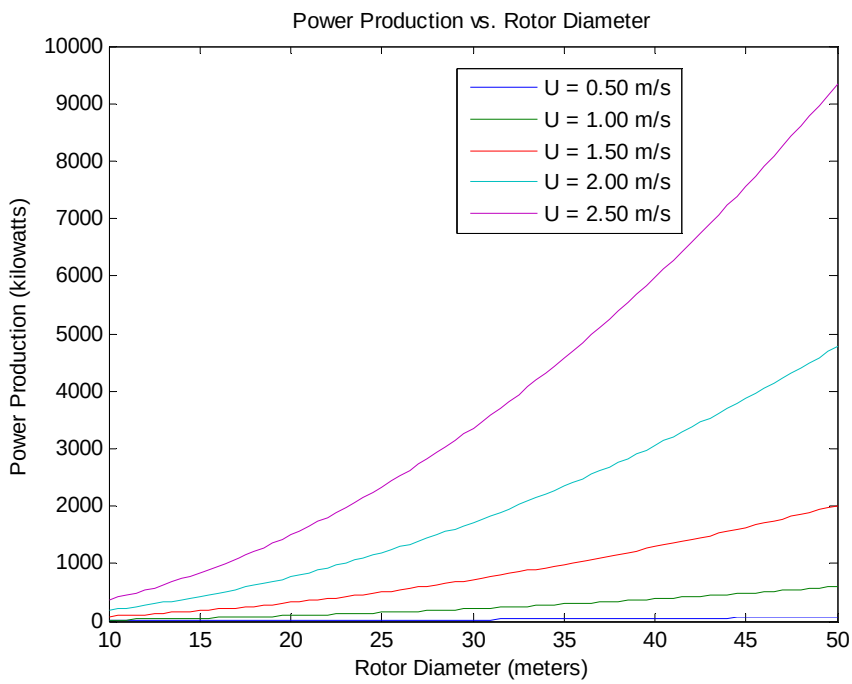

Figure 33: Maximum theoretical power production vs. rotor diameter for 10 to 50 m diameters.

3.4 Floating OTEC System Anchor Loading

As stated in the introduction, the three types of platforms deemed most feasible for housing OTEC plants are semi-submersible, spar, and ship shape (monohull) (Coastal Response Research Center, 2010), while past floating OTEC plants and prototypes have been housed on barges or tankers. Most recently, the Navy initiative to deploy a 10 MW pilot plant to enable OTEC commercialization has resulted in a design which incorporates a semi-submersible platform with a multipoint mooring (Cable et al., 2010). Both single and multipoint moorings have been addressed for use with floating OTEC plants dependent on location and platform type. A study done in the 1990s, determined cost competitive OTEC systems in the U.S. were required to be larger than 50 MW (Vega, 2010). The layout of a closed cycle 50 MW plant with modern available OTEC components requires a 198 m length between perpendiculars (L.B.P) vessel if a ship shape were to be chosen as a platform (Vega, 2010). A vessel, comparable in size, that could be easily fabricated or converted for this use, is a typical double hull tanker with a L.B.P. of about 180 m (Vega, 2010).

The diversity in plant designs, specifically platform type and mooring configuration, makes it difficult to generalize anchor loading estimates. In addition to platform type, other major features of the plant which contribute to anchor loading are the dimensions and configurations of the cold water intake pipe and warm water discharge pipes. Accuracy of anchor loading predictions for OTEC systems in the region being analyzed is difficult to achieve, because a specific system has not been proposed for deployment. However, anchor loading estimates and preliminary anchor sizing for OTEC plants in the Gulf Stream was addressed in the 1970s (Valent et al., 1979).

Although details of the two systems compared for the anchor studies were not discussed, an order of magnitude of anchor loading can be taken from the work for discussion of proposed anchoring solutions for a system of such size.

To include all possible OTEC system configurations, the "required horizontal holding capacity was set at about twice the capacities required" for plant concepts of that time. The upper bound of horizontal load capacity for deployment in the Gulf Stream was set at 180 MN, about twice the estimated horizontal loading at the anchor of 67 MN to 71 MN for two concepts (Valent et al., 1979). The initial anchor selection for OTEC systems in the Gulf Stream environment resulted in the following conclusions, mindful that advancements in mooring system deployment and OTEC system design are likely to have been achieved since this report was prepared:

1. "On unconsolidated seafloors (sand and stiff clay) the deadweight anchor system offers an effective and economical OTEC anchor system" (Atturio et al., 1979).
2. "On unconsolidated seafloors, pile anchor systems are competitive with deadweight systems in the Gulf Stream environment. The efficiencies of pile anchors, expressed in terms of weight of anchor material, are considerably better than those of deadweight anchors, somewhat offsetting the higher cost of constructing the pile anchor on the seafloor" (Atturio et al., 1979).
3. "On rock seafloors, the pile anchor system offers considerable savings in material over the deadweight anchor (provided that a suitable installation system can be developed)" (Atturio et al., 1979).

Preliminary anchor sizing for deadweight anchors that can resist a 180 MN lateral anchor loading revealed the necessary base size of a single concrete deadweight anchor with cutting edges to be 57m by 57m for a sand bottom, and 60m by 60m for a clayey silt bottom both with a height to base length ratio of 0.1. (Valent et al., 1979). The offshore oil industry has improved pile anchor abilities and has advanced deployment methods since the referenced work was written. There have been far fewer advancements in gravity anchors due to the simplicity of the position holding concept. The immense size necessary for a single gravity anchor to hold position reinforces the use of pile anchors if much smaller seafloor footprints are desired and larger anchor holding capacities are necessary. Drag embedment anchors were examined, but were deemed unfeasible because "eight to ten 64 Mg drag embedment anchors, bridled together so as to equally distribute the load, would be required" (Valent et al., 1979). Difficulties in proper installation of multiple drag embedment anchors rendered it unsuitable for the Gulf Stream environment and plate anchors were also deemed unsuitable because of the necessary anchor holding capacities (Valent et al., 1979). It is clear from past studies of preliminary anchor sizing for OTEC systems in the Gulf Stream and also by modern studies for solving anchoring design problems for the multipoint mooring system of the Navy's OTEC prototype plant that preliminary anchor sizing for these systems requires the examination of a specific system to be deployed and site specific studies of greater detail are required.

4. PRELIMINARY ANCHOR SIZING FOR SINGLE POINT MOORED MHK DEVICES

Mooring system development can sometimes become an afterthought to the design of MRE devices to be deployed in ocean current applications. However, the relationship between anchor and mooring system cost and the potential power output of a specific device over its life time will affect the size and economic potential of commercial devices. Conceptualizing the deployment of such devices provides developers with preliminary anchor sizes and anchoring options which may impact the design of the device. Examined in this chapter are the anchor sizing methods for deadweight anchors with and without shear keys, plate anchors, and drag embedment anchors. Estimates are made to the maximum rotor diameter applicable to each type of pile anchor. Anchor sizing methods for both cohesionless soil (sand or gravel) and cohesive soil (mud, silt and clay) are addressed for each anchor type. Preliminary anchor sizing is preformed for MHK devices, but the presented anchor sizing approach can be applied to any moored system.

4.1 Deadweight (Gravity) Anchor Sizing

Deadweight anchors can be used on each of the presented bottom types within the area of interest (Section 2.2) and require the least geotechnical data for design, making it a versatile and inexpensive mode of station keeping. At the same time, they are the least

efficient of the anchor types because their holding capacity to weight ratio is the lowest of the evaluated anchor types. Deadweight (gravity) anchors may be selected from a commonly used design such as the Navy's Pearl Harbor Anchor design (Seelig et al., 2001), or designed on a customized basis dependent on the requirements of the project. Deadweight anchor design procedures from Navy design guides and OWET's advanced anchoring and mooring study for ocean wave energy conversion are followed in this section to show example anchor design procedures and provide plots for an anchor sizing reference. Deadweight anchor sizes are plotted for areas consisting of either cohesionless or cohesive soil.

All anchor sizing scenarios in this thesis were assumed to be on a flat seabed. Additional considerations exist for designing deadweight anchors for use on slopes and are included in references such as the *Handbook for Marine Geotechnical Engineering* (NCEL, 1985). While a seafloor sloping towards an anchored object reduces anchor capacity of a gravity anchor, the upslope anchor capacity can be substantially increased by an increased slope angle (Sound and Sea Technology, 2009). The effects of anchoring on the eastward sloping seabed of the Florida coast for a moored object in the northward flowing Florida Current on deadweight anchor loading capacity would have to be further examined for specific cases.

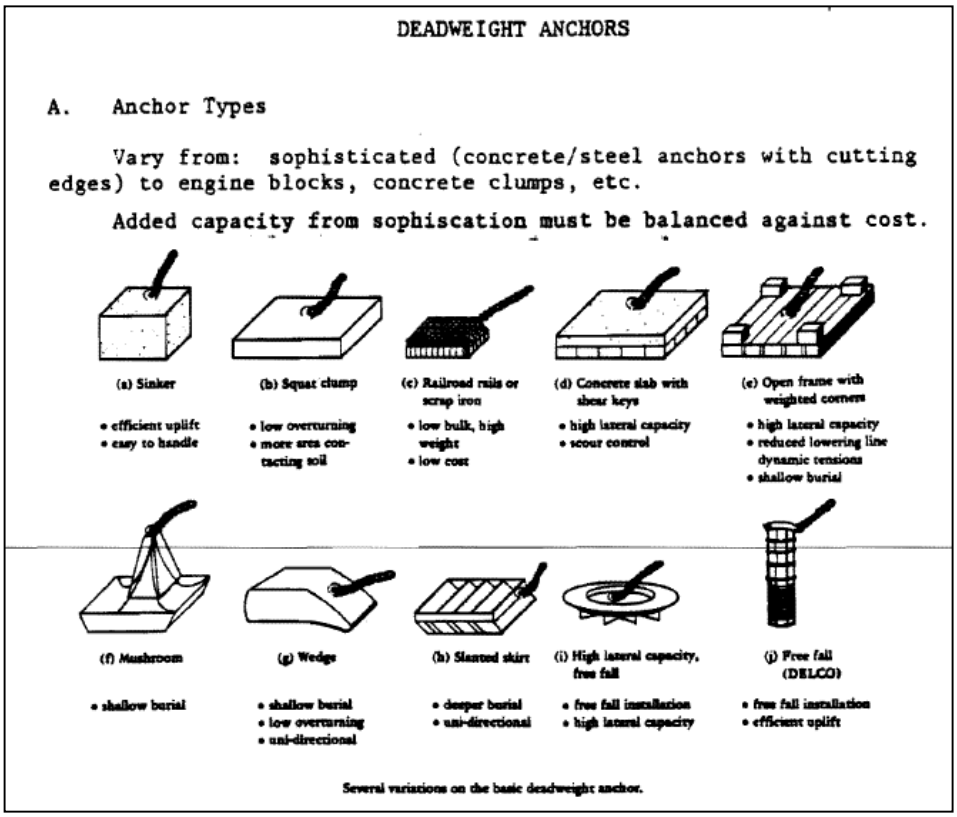

Figure 34: Deadweight anchor types (Taylor, 1982).

4.1.1 Deadweight Anchor with no Shear Keys on Cohesionless Soil

The first anchor to be examined is a simple concrete sinker or squat clump style anchor with no shear keys (Figure 34). The anchor loading results (Section 3.3.1) are used to calculate the weight (in water) required to resist sliding on cohesionless soils,

$$W = \frac{F_h}{\tan(\phi - 5°)} + F_v, \tag{4}$$

where F_h equals the horizontal anchor loading (Figure 26 and 29), ϕ is the angle of internal friction of the sediment, and F_v is the vertical anchor loading (Figure 25 and 28) (Taylor, 1982). The tangent of internal friction in Equation 4 is the coefficient of sliding friction. The five degree reduction in sliding friction is the result of empirical tests where

flat anchor bottoms did not cause the soil to fail by mobilizing the complete internal friction of soil and the average of the data suggested the five degree reduction (Taylor, 2010).

The angle of internal friction needed for determining anchor weight on cohesionless soil can be estimated based on soil description or estimated from on-site values. Soil descriptions are classified by their grain size (Table 6) and angles of internal friction for different types of sand are displayed in Table 8 (Vryhof Anchors, 2005). Undrained shear strength values (S_u) derived from unconfined unconsolidated test (UU) are displayed in Table 7. On site values can be estimated from the results of a Standard Penetration Test (SPT) or Cone Penetrometer Test (CPT) (Vryhof Anchors, 2005) and an approximate relation between shear strength and the test values are shown in Table 7. Table 8 can then be referenced to estimate the angle of internal friction from the results of the site values.

Table 6: Soil type classified by grain size distribution (Vryhof Anchors, 2005).

Grain size	Soil description
< - 2 µm	Clay
2 - 6 µm	Fine Silt
6 - 20 µm	Medium Silt
20 - 60 µm	Coarse Silt
60 - 200 µm	Fine Sand
200 - 600 µm	Medium Sand
0.6 - 2 mm	Coarse Sand
2 - 6 mm	Fine Gravel
6 - 20 mm	Medium Gravel
20 - 60 mm	Coarse Gravel
60 - 200 mm	Cobbles
> - 200 mm	Boulders

Table 7: Relation between shear strength and test values (Vryhof Anchors, 2005).

S_u kPa	UU kPa	SPT N	CPT MPa
0 - 13	0 - 25	0 - 2	0.0 - 0.2
13 - 25	25 - 50	2 - 4	0.2 - 0.4
25 - 50	50 - 100	4 - 8	0.4 - 0.7
50 - 100	100 - 200	6 - 15	0.7 - 1.5
100 - 200	200 - 400	15 - 30	1.5 - 3.0
> 200	> 400	>-30	>3.0

table C

Table 8: "Approximate correlation between the angle of internal friction φ and the relative density of fine to medium sand" (Vryhof Anchors, 2005).

Descriptive term	Relative Density	Angle φ	SPT N	CPT MPa
Very loose	< 0.15	< 30	0- 4	0 - 5
Loose	0.15 - 0.35	30 - 32	4 - 10	5 - 10
Medium dense	0.35 - 0.65	32 - 35	10 - 30	10 - 15
Dense	0.65 - 0.85	35 - 38	30 - 50	15 - 20
Very dense	≥ 0.85	≥ 38	> 50	≥ 20

table D

Equation 4 can also be used with values in Table 9 which lists the tangent of the friction angle equivalent to the sliding coefficient between the bottom surface of the anchor and the underlying soil, $\tan\phi$ (Sound and Sea Technology, 2009). The term $\tan(\phi - 5°)$ in Equation 4 is replaced with empirical values of Table 9.

Table 9: "Friction Coefficients for Anchor Materials on Granular Soils (tan φ)" (Sound and Sea Technology, 2009).

	For Soil On:				
Soil	Smooth Steel	Rough Steel	Smooth Concrete	Rough Concrete	Trapped Soil
Quartz Sand	0.27	0.60	0.60	0.69	0.67
Coralline Sand	0.20	0.63	0.63	0.66	0.67
Oolitic Sand	0.23	0.56	0.58	0.74	0.79
Foram Sand-Silt	0.40	0.66	0.67	—	0.64

After the weight (in water) required to resist sliding is determined, the minimum anchor width (B) without shear keys can be determined from:

$$B = \left[\frac{6WF_h}{\gamma_s (W - F_v)} \right]^{\frac{1}{3}}, \tag{5}$$

where W is the required weight in water, and γ_s is the submerged density of the anchor material (Taylor, 1982). The value of γ_s for concrete is 13.51 kN/m^3 (86 lbs/ft^3) (Taylor, 1982). The maximum height (H) of the mooring line connection point above the base of the anchor with or without shear keys as determined by Taylor is:

$$H = \frac{B(W - F_v)}{6F_h}. \tag{6}$$

Lastly, the length (L) of the anchor necessary to achieve the required weight in water can be determined by:

$$L = \frac{W}{gHB(\rho_c - \rho_{sw})}, \tag{7}$$

where g is acceleration of gravity equal to 9.81 m/s^2, ρ_c is the density of concrete equal to 2400 kg/m^3, and ρ_{sw} is the density of sea water equal to 1026 kg/m^3.

This method was followed to create Figures 35 through 39. Loose sand with angle of internal friction of 30° was initially used for example sizing. Examining the results for a 20 m rotor diameter at the 325 m depth (Figure 35), the dimensions of the necessary concrete gravity anchor are a base, width and height of 7.8 m x 7.8 m x 2.8 m and a weight of 2,312.8 kN. For a 20 m diameter rotor, this is the maximum presented anchor weight for this section of all the locations and scopes simulated. The minimum anchor size for a 20 m rotor in this section is at the 700 m location and 1.50 scope with dimensions 7.1 m x 7.1 m x 2.53 m, and a weight of 1,712.7 kN. The maximum and

minimum anchor sizes correspond to the maximum and minimum loading conditions of Section 3.3. Different angles of internal frictions or friction coefficients of Table 8 and 9 can be applied to the given sizing equations for different sediments and anchor materials. The anchor size necessary to achieve the required weight in water can be reduced by using a material with a higher density than concrete, such as steel. It is observed in Figures 35 through 39 that the width and length of the base of the anchors nearly overlap each other on each plot showing a near square bottom for each case. It should be noted that no safety factors other than those applied to mooring line sizing during simulation were applied to the anchor sizing charts.

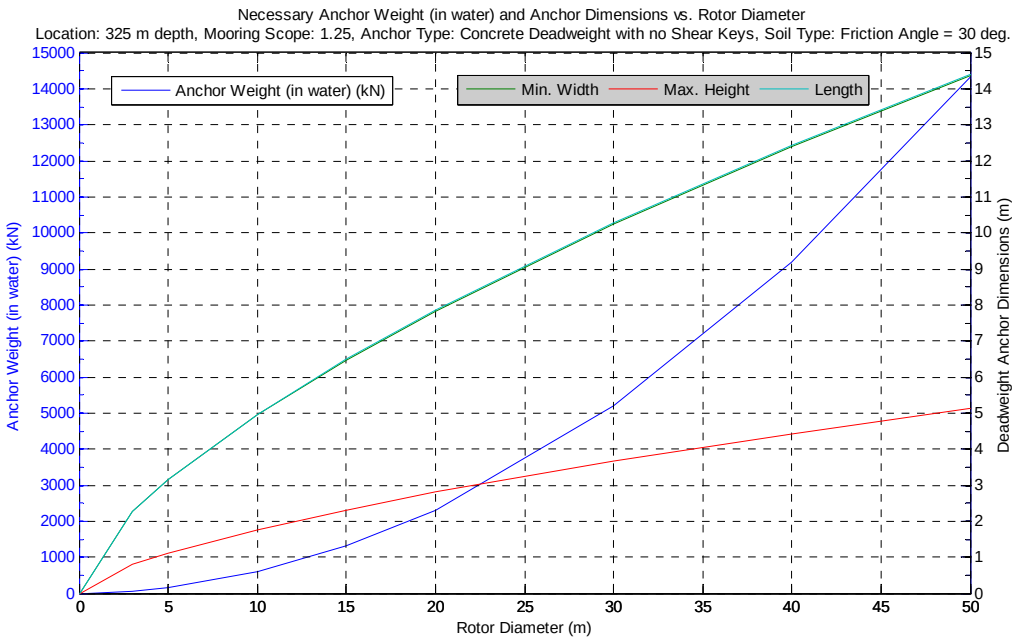

Figure 35: Anchor dimensions for concrete deadweight anchor with no shear keys at 325 m depth location and 1.25 mooring scope for loose sand.

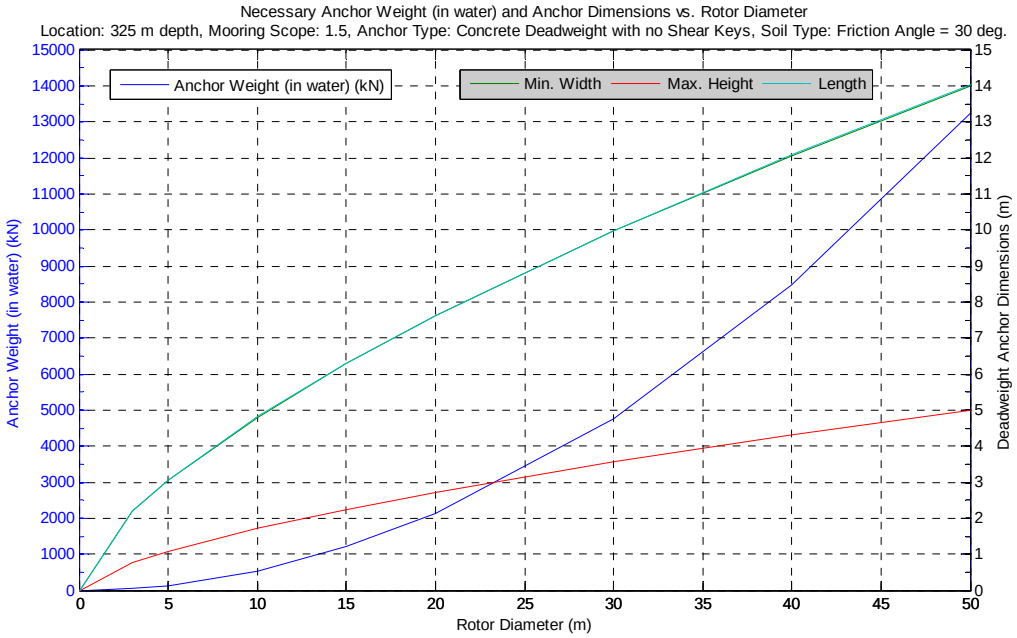

Figure 36: Anchor dimensions for concrete deadweight anchor with no shear keys at 325 m depth location and 1.50 mooring scope for loose sand.

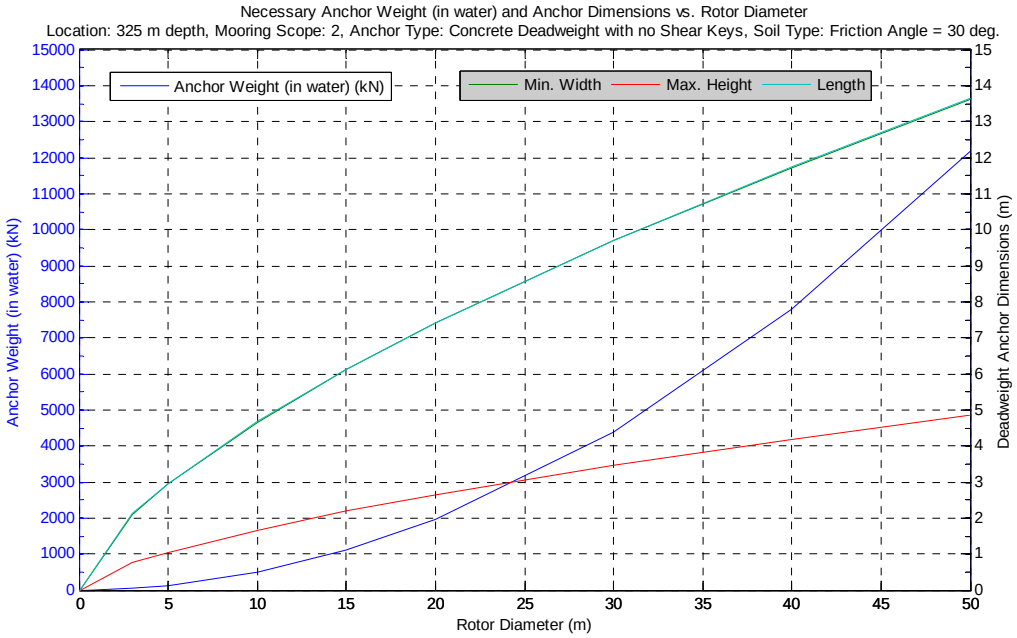

Figure 37: Anchor dimensions for concrete deadweight anchor with no shear keys at 325 m depth location and 2.00 mooring scope for loose sand.

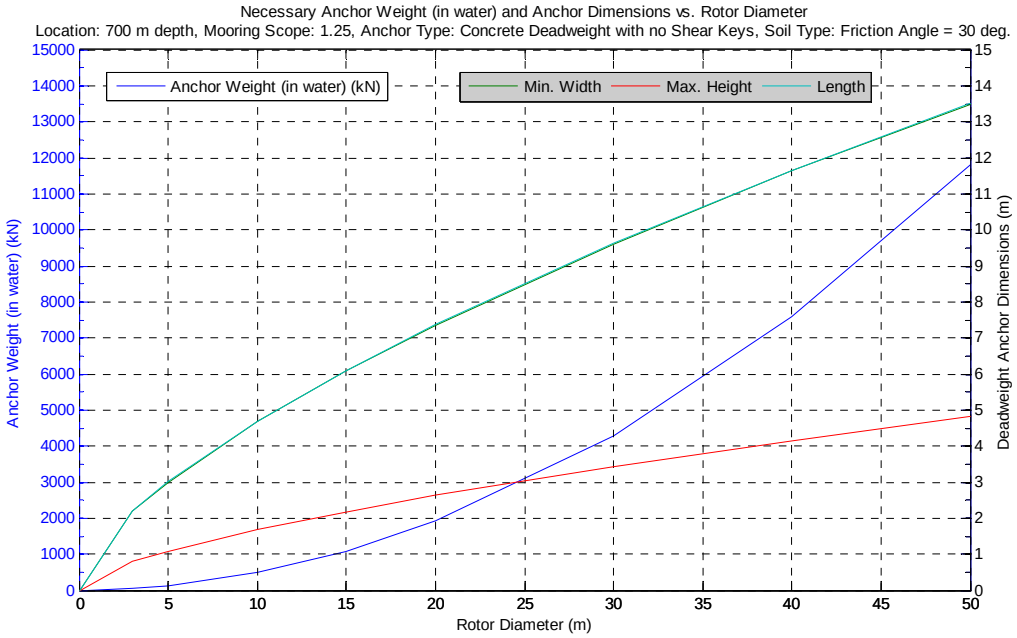

Figure 38: Anchor dimensions for concrete deadweight anchor with no shear keys at 700 m depth location and 1.25 mooring scope for loose sand.

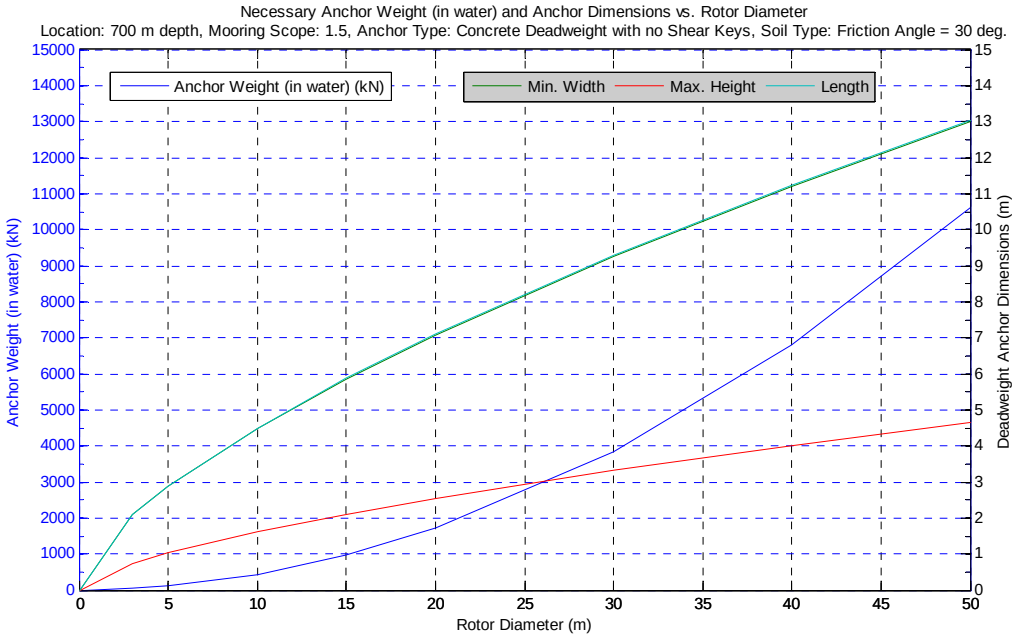

Figure 39: Anchor dimensions for concrete deadweight anchor with no shear keys at 700 m depth location and 1.50 mooring scope for loose sand.

4.1.2 Deadweight Anchor with no Shear Keys on Cohesive Soil

Areas of sediment observed during past surveys may be cohesive depending on the soil's grain size distribution and its index properties such as water content (NCEL, 1985). The holding capacity of a simple deadweight anchor in cohesive soil such as clay, silt, or mud is given by:

$$F_h = S_{uz}(A) + (2S_{ua}z + \frac{1}{2}\gamma_b z^2)B, \tag{8}$$

where S_{uz} is the undrained shear strength at the bottom of the anchor, A is the plan area, S_{ua} is the average undrained shear strength from the seabed surface to depth z, z is the depth from the surface of the seabed to the bottom of the anchor, γ_b is the buoyant unit weight of soil, and B is the anchor width (Sound and Sea Technology, 2009). Shear strengths can be measured at the deployment location or can be estimated for preliminary sizing using:

$$\mathrm{S}_{\mathrm{uz}} = \frac{W}{N_c A}, \tag{9}$$

where "N_c is the bearing capacity factor, conservatively approximated at 5.7" (Sound and Sea Technology, 2009). The consistency of clay is classified by its undrained shear strength in Table 10. The average shear strength, if assumed to increase linearly from zero at the surface, is (Sound and Sea Technology, 2009):

$$S_{ua} = 0.5S_{uz} \tag{10}$$

and the depth is:

$$z = \frac{S_{uz}}{G_{su}}, \tag{11}$$

where G_{su} is the rate of increase of shear strength with depth, approximated at 1.89 kN/m^3 (12 psf/ft) (Sound and Sea Technology, 2009). If the given estimations for cohesive soil are used, horizontal loads (F_h) are obtained from simulation, and the buoyant weight of soil is set to 4.4 kN/m^3 (28 pcf) for clay (Taylor, 1982), then the equation for holding capacity becomes a function of two unknowns:

$$F_h = \frac{W}{N_c} + \left[\frac{\sqrt{A} W^2 (2G_{su} + \gamma_b)}{2A^2 N_c^2 G_{su}^2} \right]. \tag{12}$$

Both weight and plan area are unknown, therefore one dimension has to be assumed to size the other dimension or vice versa. The plan area is assumed to be square so the width (B) given in Equation 8 was replaced by the square root of the area (A).

To calculate two possible design solutions to this anchor sizing problem, both the anchor plan area and anchor weights calculated in Section 4.1.1 are individually used. First the anchor plan areas from Section 4.1.1 were input into Equation 12 to determine the necessary anchor weights presented in Figures 40 through 44. Next, the anchor weights from Section 4.1.1 were input into Equation 12 to determine the corresponding plan areas presented in Figures 45 through 49. For both solutions, the heights of the anchors were determined from the volume of concrete necessary to create the anchor weight in water. The results for determining necessary anchor weight from the already determined areas of Section 4.1.1 (Figures 40 through 44) were similar to results when determining anchor plan area from anchor weights determined in Section 4.1.1 (Figures 45 through 49). For a 20 m diameter rotor at the 325 m location (Figures 40 and 45) there was a 2.77% increase in weight, 5.6% increase in plan area, and a 2.8% decrease in height when the second method of determining anchor dimensions from already

determined anchor weights was used instead of the first method of determining anchor weights from already determined plan areas.

Table 10: American (ASTM) and British (BS) standards for consistency of clays (Vryhof Anchors, 2005).

Undrained Shear Strength (kPa)		
Consistency of Clay	ASTM D-2488	BS CP-2004
Very soft	0 - 13	0 - 20
Soft	13 - 25	20 - 40
Firm	25 - 50	40 - 75
Stiff	50 - 100	75 - 150
Very stiff	100 - 200	150 - 300
Hard	200 - 400	300 - 600
Very hard	> 400	> 600

table B

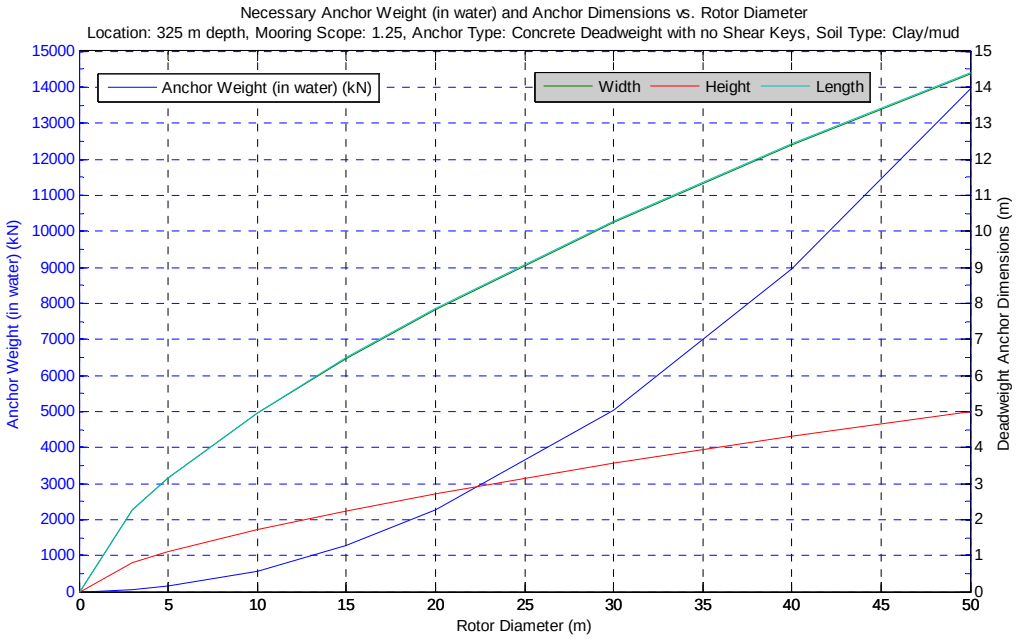

Figure 40: Anchor dimensions for concrete deadweight anchor with no shear keys at 325 m depth location and 1.25 mooring scope for cohesive soil solved for using plan area from Figure 35.

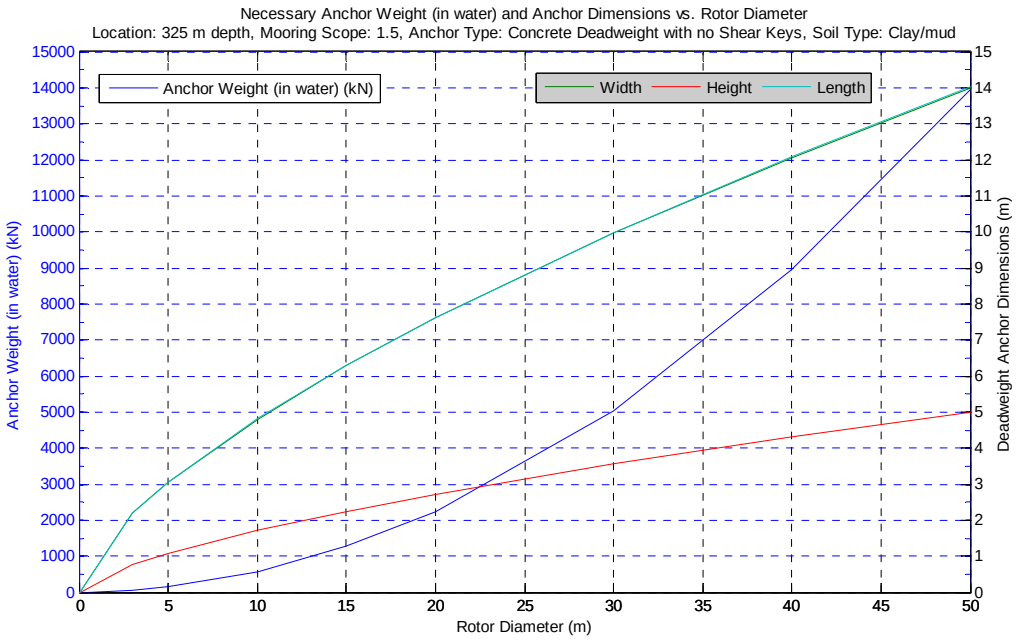

Figure 41: Anchor dimensions for concrete deadweight anchor with no shear keys at 325 m depth location and 1.50 mooring scope for cohesive soil solved for using plan area from Figure 36.

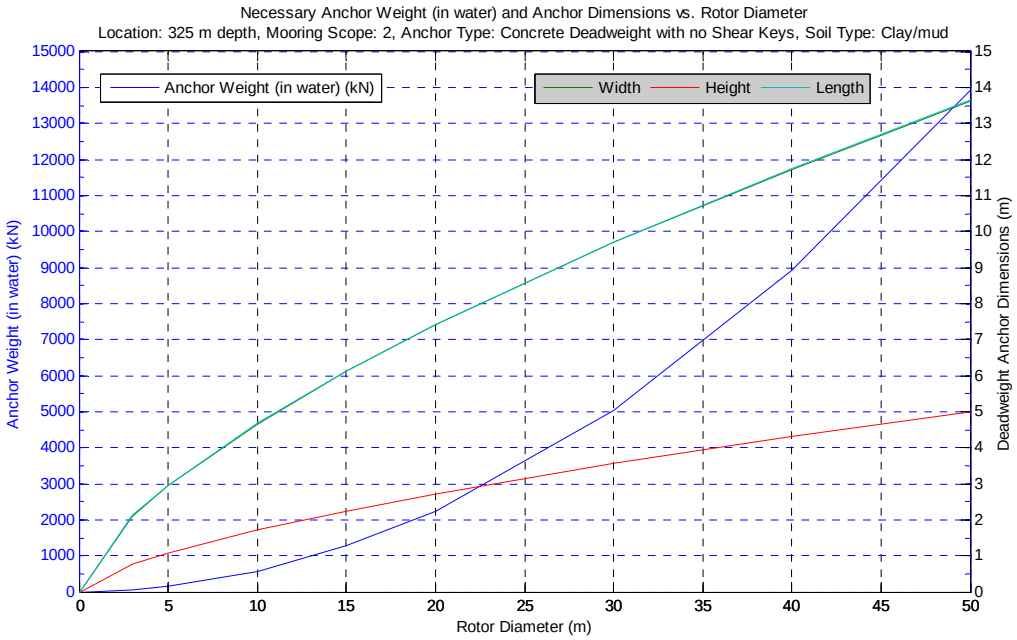

Figure 42: Anchor dimensions for concrete deadweight anchor with no shear keys at 325 m depth location and 2.00 mooring scope for cohesive soil solved for using plan area from Figure 37.

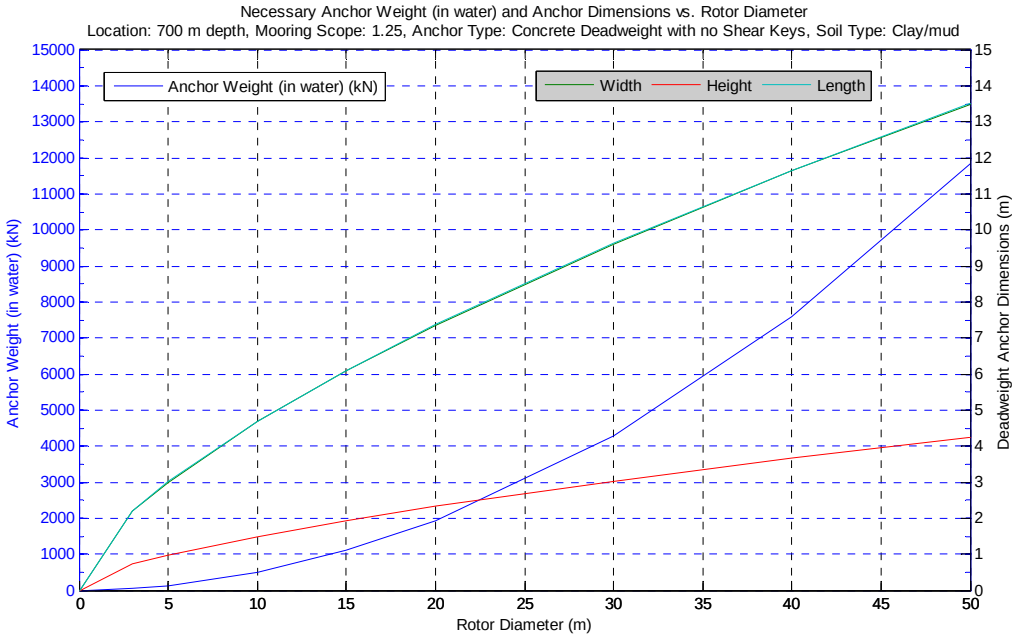

Figure 43: Anchor dimensions for concrete deadweight anchor with no shear keys at 700 m depth location and 1.25 mooring scope for cohesive soil solved for using plan area from Figure 38.

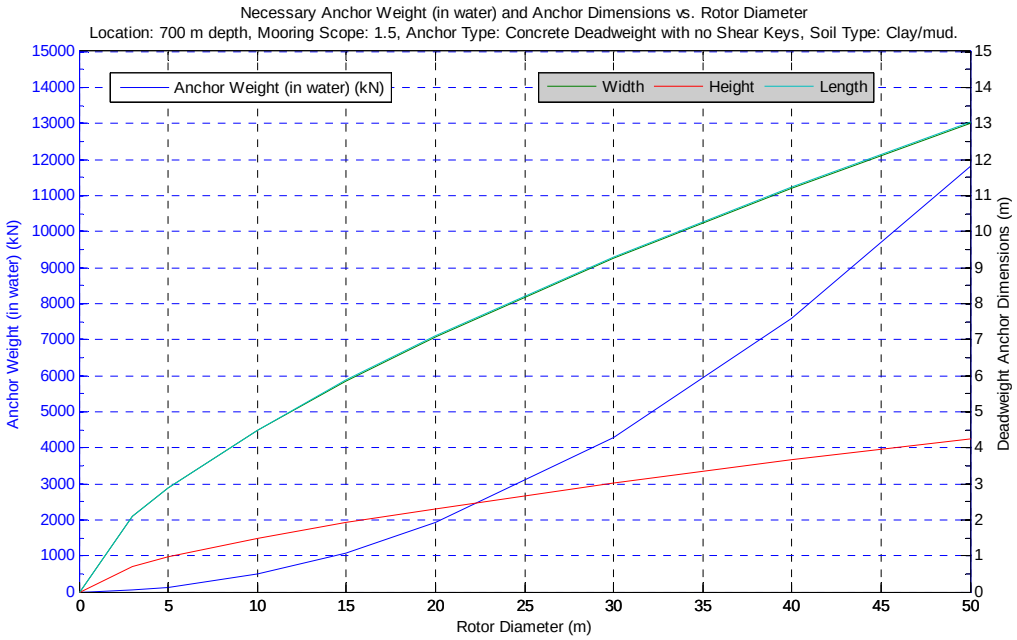

Figure 44: Anchor dimensions for concrete deadweight anchor with no shear keys at 700 m depth location and 1.50 mooring scope for cohesive soil solved for using plan area from Figure 39.

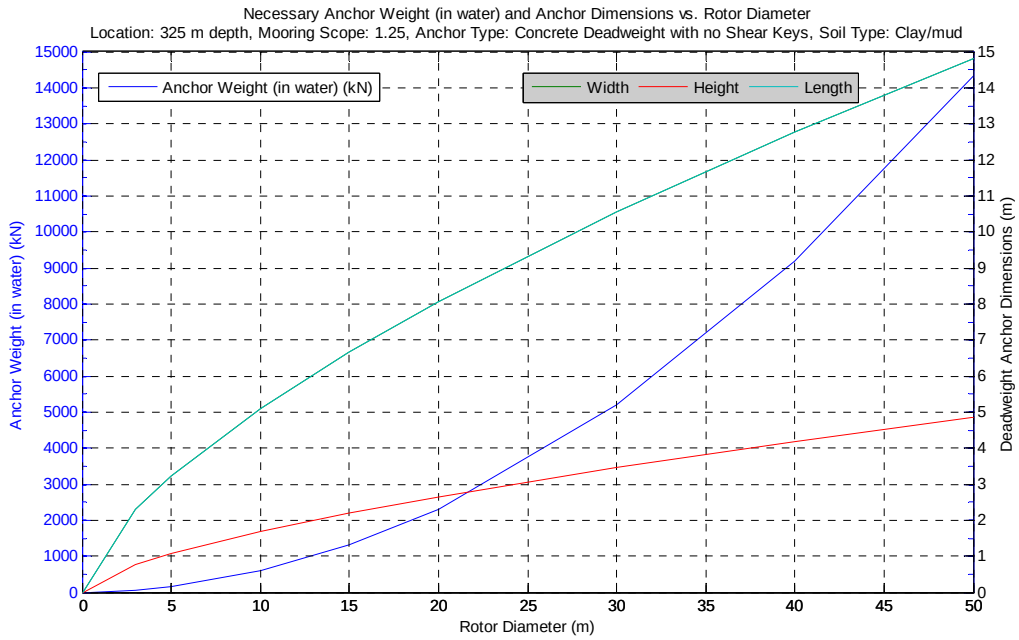

Figure 45: Anchor dimensions for concrete deadweight anchor with no shear keys at 325 m depth location and 1.25 mooring scope for cohesive soil solved for using weight from Figure 35.

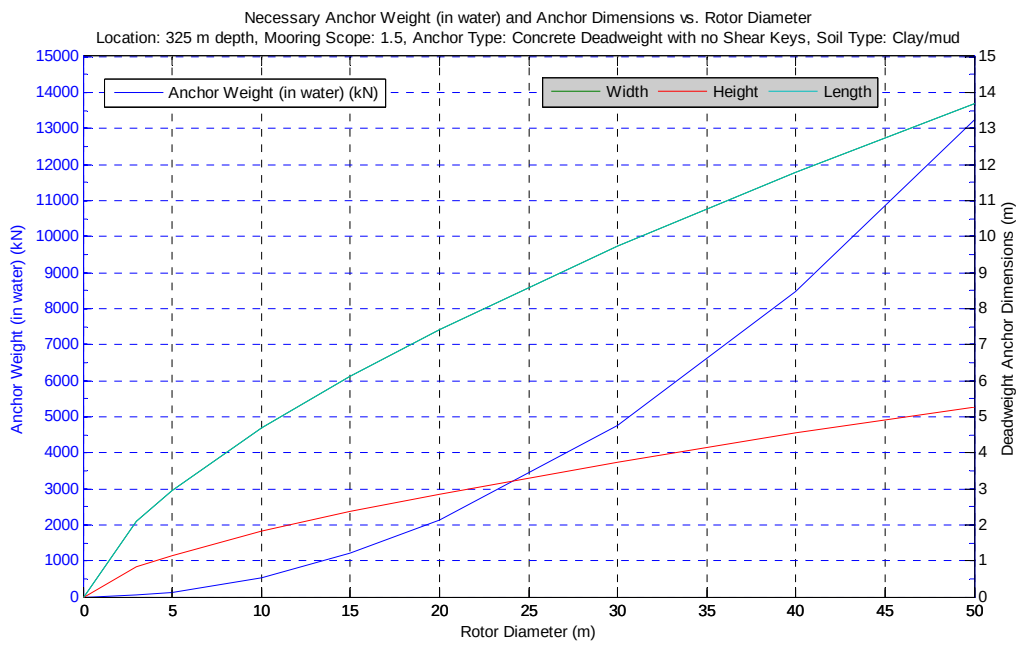

Figure 46: Anchor dimensions for concrete deadweight anchor with no shear keys at 325 m depth location and 1.50 mooring scope for cohesive soil solved for using weight from Figure 36.

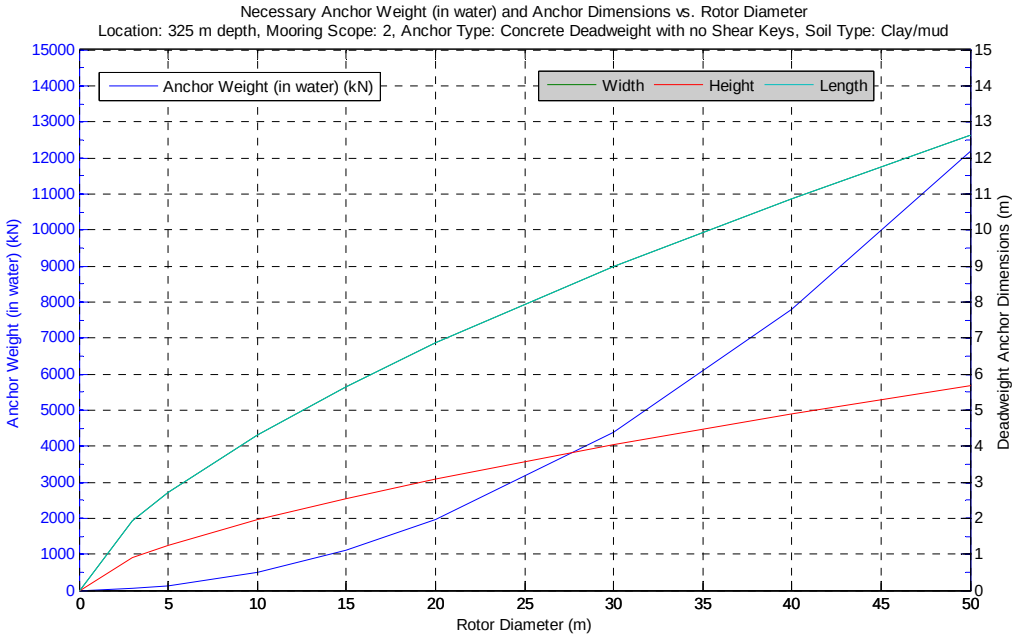

Figure 47: Anchor dimensions for concrete deadweight anchor with no shear keys at 325 m depth location and 2.00 mooring scope for cohesive soil solved for using weight from Figure 37.

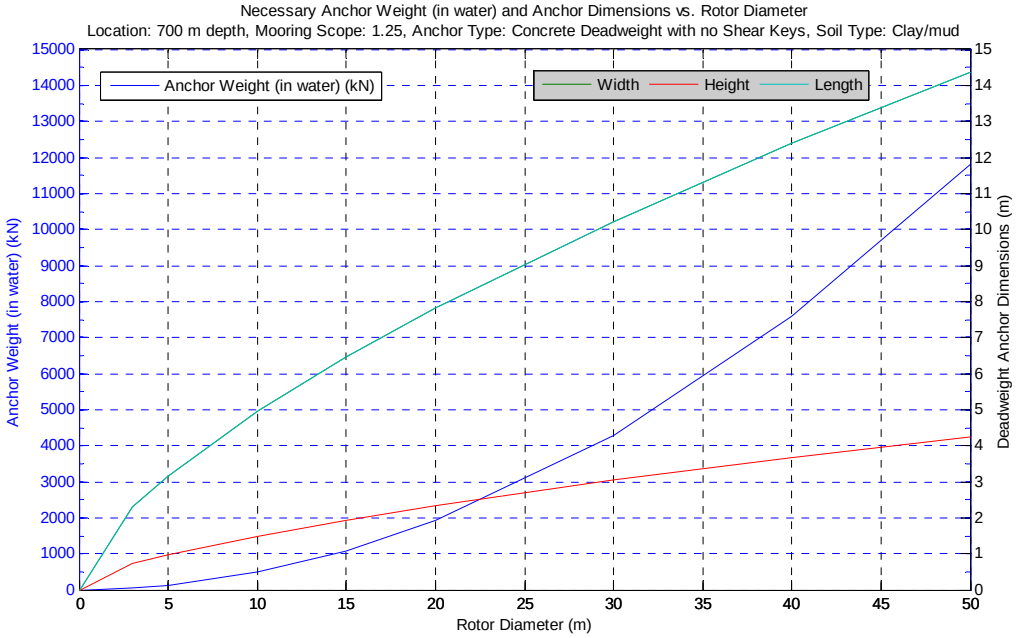

Figure 48: Anchor dimensions for concrete deadweight anchor with no shear keys at 700 m depth location and 1.25 mooring scope for cohesive soil solved for using weight from Figure 38.

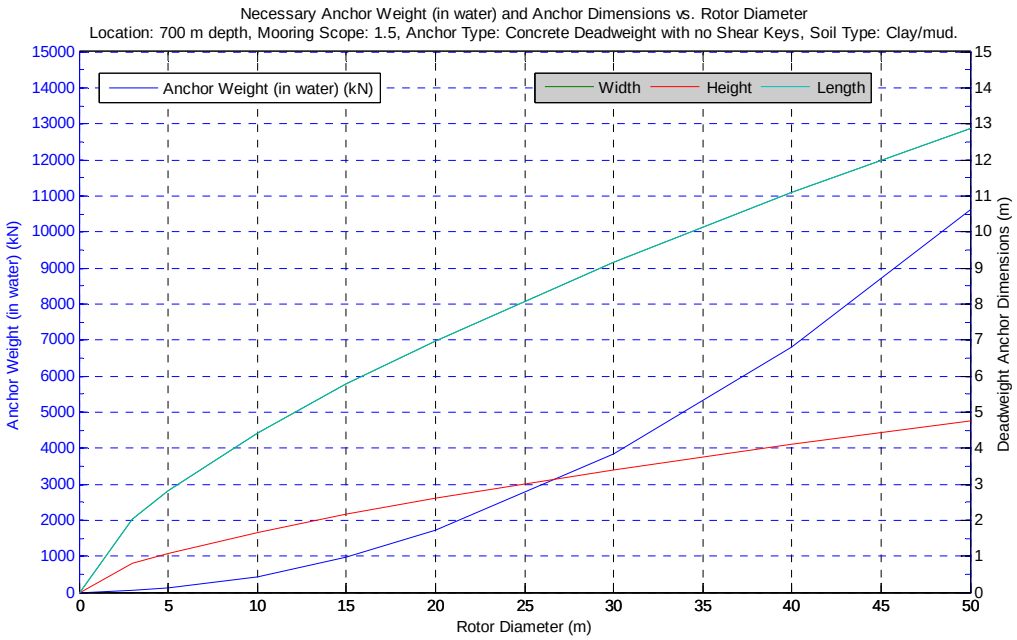

Figure 49: Anchor dimensions for concrete deadweight anchor with no shear keys at 700 m depth location and 1.50 mooring scope for cohesive soil solved for using weight from Figure 39.

4.1.3 Deadweight Anchor with Shear Keys on Cohesionless Soil

The addition of shear keys will increase anchor lateral holding capacity by causing failure to occur in the soil and not at the anchor soil interface (Taylor, 2010). Precise deadweight anchor sizing and shear key design can be completed through an iterative process by determining the weight necessary to resist sliding along with anchor width. A grid of shear keys can then be designed, but it must be ensured that the weight of the anchor will fully embed the shear keys. If this is not accomplished, the anchor weight must be increased or shear keys redesigned. Although an iterative process is demonstrated in the *Interaction of Anchors with Soil and Design* to design and size shear keys, a single formula can be used to determine preliminary anchor weight of a deadweight anchor with full-base keying skirts if values are assumed for soil properties.

The lateral capacity of a deadweight anchor with full-base keying skirts in cohesionless soil is:

$$F_h = (W - F_v)(\tan\phi) + K_p \gamma_b \frac{1}{2} z_s^2 B, \tag{13}$$

where W is the anchor weight in water, F_v is the vertical component of line pull, $\tan\phi$ is the tangent of the friction angle at depth z_s (at the bottom surface of the soil trapped within the peripheral skirts), provided in Table 9, K_p is the passive earth pressure coefficient equal to:

$$K_p = \tan^2(45 + \phi/2), \tag{14}$$

where ϕ is the soil friction angle, z_s is depth to the bottom of the skirts and B is width of the anchor (Sound and Sea Technology, 2009). The tangent of friction angle at depth z_s for the trapped soil is set to 0.67 (Table 9). The buoyant weight of soil γ_b for sand with an angle of internal friction of 30° is approximately 8.63 kN/m^3 (55 pcf) (Taylor, 1982). A shear key penetration depth of $0.05B$ is assumed as a minimum (Taylor, 1982).

Both the anchor weight and width are variables that need to be solved for in Equation 13. To accomplish this, the anchor widths determined in Section 4.1.1 are input to Equation 13 to observe the change in necessary anchor weight with the addition of shear keys. Figure 50 shows the necessary anchor weight for increasing rotor diameters at each location. For an anchor with the same base dimensions as solved for in the case of a deadweight anchor on sand with no shear keys, the addition of full keying skirts reduced the necessary anchor weight in water. For a 20 m diameter rotor blade at the 325

meter location the necessary submerged anchor weight was reduced from 2,312.8 kN without shear keys to 1,720.0 kN with shear keys which is a 25.6% reduction in weight.

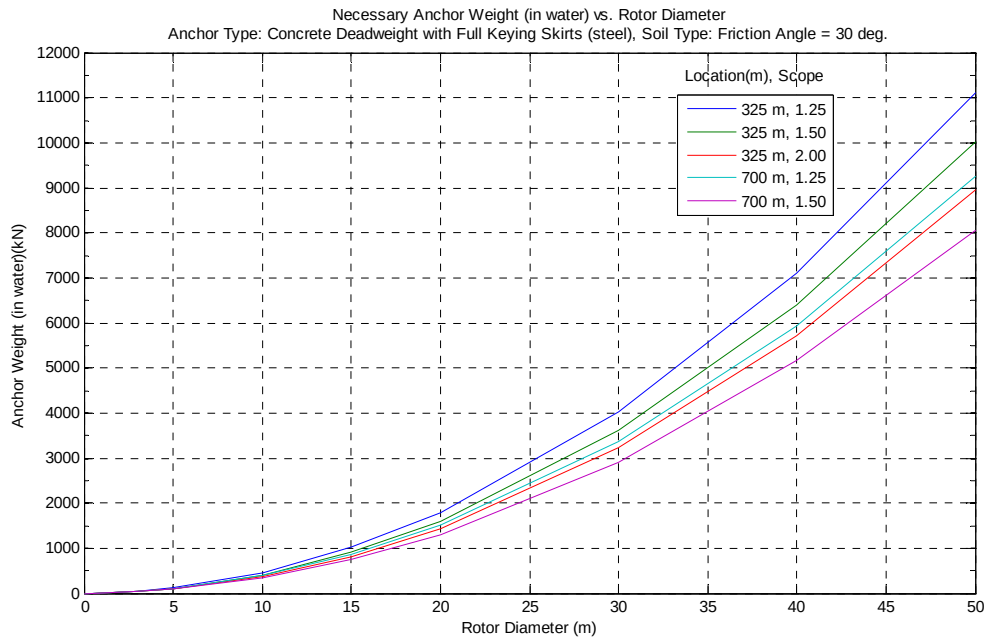

Figure 50: Necessary anchor weight of concrete deadweight with full keying skirts on cohesionless soil at each location.

4.1.4 Deadweight Anchor with Shear Keys on Cohesive Soil

Solving for the necessary submerged weight of a deadweight anchor with shear keys on cohesive soil has been addressed with set dimension ratios, and Equation 15 was developed to find the submerged weight such that it will resist overturning with these dimension ratios (Taylor, 1982). The necessary submerged weight to resist overturning a deadweight anchor with shear keys on cohesive soil, for an anchor height of $H = 0.2B$ and a shear key penetration of $z_s = 0.1B$, is calculated by:

$$W=1.2Fh+Fv, \tag{15}$$

where F_h is the horizontal anchor loading and F_v is the vertical anchor loading (Taylor, 1982). The anchor loading presented in Section 3.3.1 was used in Equation 15 and the results for necessary submerged anchor weight are displayed in Figure 51. When designing the anchor, it must be assured that the submerged weight solved for using Equation 15 is larger than the weight required to embed the shear keys. If it is not, a larger weight must be selected or shear keys must be redesigned to assure penetration.

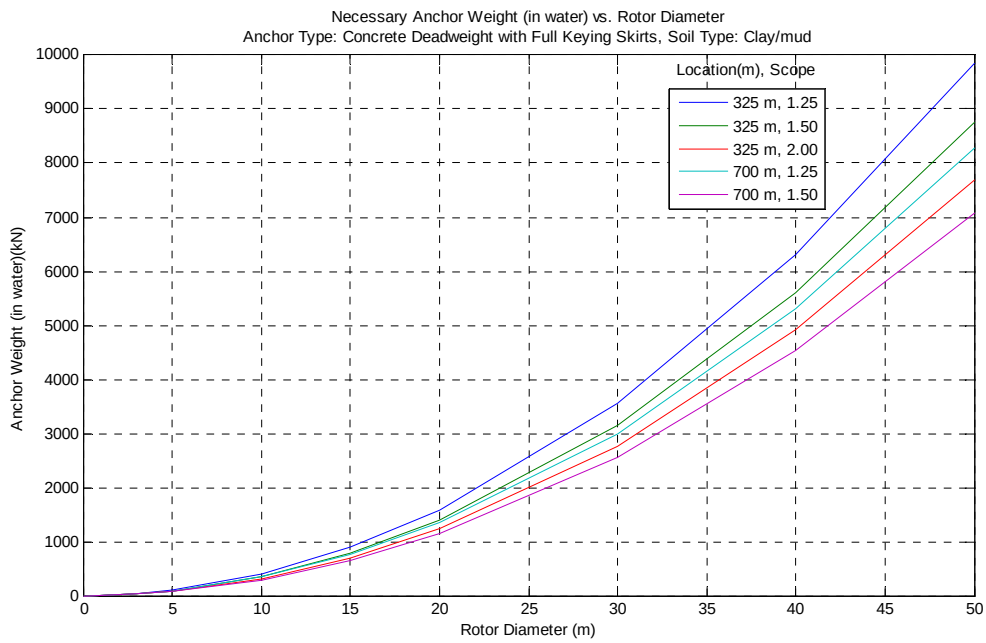

Figure 51: Necessary weight of deadweight anchor with shear keys to resist overturning in cohesive soil.

Similar to the results of Section 4.1.3, for cohesive soil, the addition of full keying skirts reduced the necessary anchor weight in water. For a 20 m diameter rotor blade at the 325 meter location the necessary anchor weight was reduced from either 2,250.5 kN (Figure 40) or 2,312.8 kN (Figure 45) depending on dimensions without shear keys to

1,588.0 kN with shear keys. These results correspond to either a 29.4% or 31.3% reduction in submerged anchor weight.

Decreases in necessary submerged anchor weight from dead weight anchors with shear keys on cohesionless soil presented in Section 4.1.3 versus dead weight anchors with shear keys on cohesive soil presented in this section can be attributed to the increase in skirt length to anchor width ratio recommended for cohesive soil. Shear key lengths for cohesionless soil were set to $0.05B$, B being the width of the anchor, where shear key lengths for cohesive soil are recommended to have an optimum length of $0.1B$ to reach deeper, stronger soil (Taylor, 1982). Detailed shear key design methods can be completed for each case using methods presented in *Interaction of Anchors with Soil and Anchor Design* (Taylor, 1982).

4.2 Driven Plate Anchors

Pile driven plate anchors function by being driven in to the seafloor by a pile-driving hammer to what is referred to as the driven depth (Forrest et al., 1995). The follower, which is a structural component attached to the plate while being driven by the hammer, is retrieved and the anchor is pull tested to rotate or key the anchor into its operating position, called the keyed depth (Forrest et al., 1995).

4.2.1 Driven Plate Anchors in Cohesionless Soil

The holding strength of driven plate anchors is directly related to the keyed depth of the anchor. It is also dependent on the size of the plate and the strength of the soil

(Forrest et al., 1995). The necessary keyed depth of driven plate anchors in cohesionless soil was found using:

$$D = \frac{F_u}{A g_b N_q}, \tag{16}$$

where F_u is the ultimate anchor holding capacity, A is the area of the plate, g_b is the effective (buoyant) weight of the soil, D is the embedded depth of the (keyed) anchor, and N_q is the holding capacity factor for cohesionless soils (Forrest et al., 1995). The ultimate anchor holding capacity was set equal to the vertical anchor loading (Figure 25 and 28). For primarily horizontal anchor loading the ultimate anchor capacity can be increased by a factor of 1.25 in cohesionless soils to account for the embedded chain (Forrest et al., 1995). No safety factors were applied to the anchor sizing, although it is recommended to use a safety factor of 2 for most applications (Forrest et al., 1995). Areas of the driven plates, A, were given a range from one to four square meters in increments of 0.5 m. The effective (buoyant) weight for sand (g_b) with a friction angle of 30° is approximately 7.85 kN/m^3 (50 pcf) (Forrest et al., 1995). This value for the buoyant weight of sand with a friction angle of 30˚ differs from the value for the same sand presented in Section 4.1.3. Buoyant weight values from the two manuals from which the formulas are used differ by 0.78 kN/m^3. So the value corresponding to the manual from which each formula was taken is being used for calculation.

The holding capacity factor (N_q) was selected from Figure 52. For a friction angle of 30°, the line shows asymptotic behavior above a holding capacity of 10 for an embedment depth to anchor width ratio greater than 6. A holding capacity of 10 was conservatively chosen, although "in both normally consolidated soils or over-

consolidated clay, if the keyed depth to width ratio (D/B) is 6 or greater, long term load capacity factors in excess of 15 are noted" (Forrest et al., 1995).

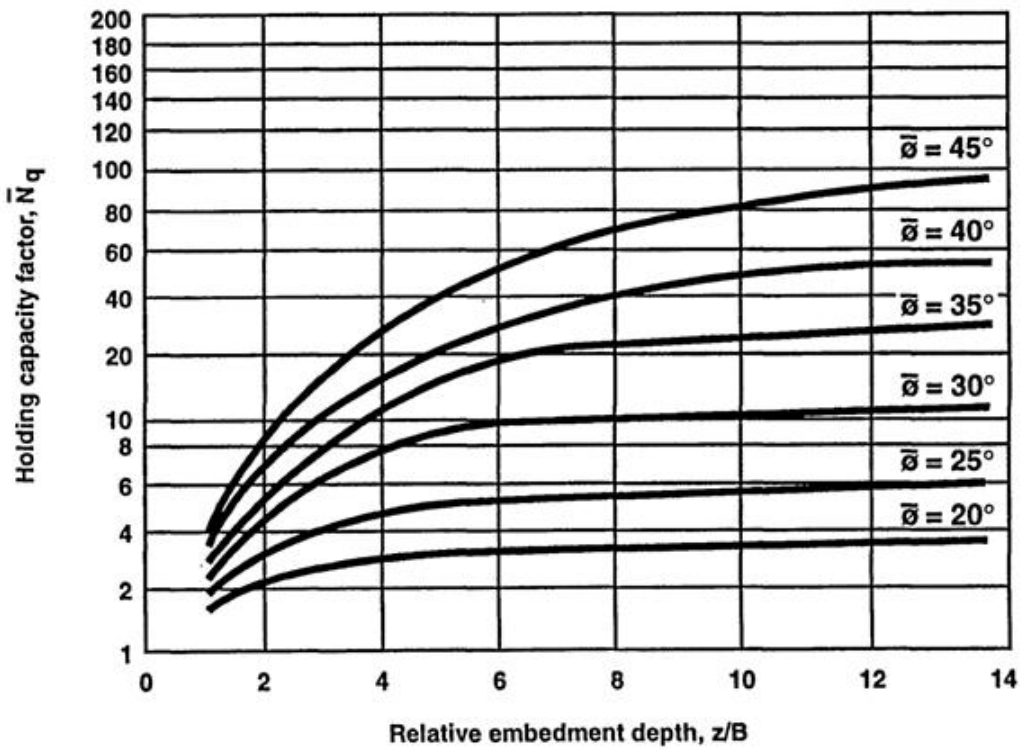

Figure 52: "Holding capacity factors for cohesionless soils" (Forrest et al., 1995).

The necessary keyed depths for plate areas ranging from one to four square meters with increasing rotor diameters are displayed in Figures 53 through 57 for sand with an angle of internal friction equal to 30°. An anchor driven depth can be determined with methods presented in *Design Guide for Pile Driven Plate Anchors* for cohesionless and cohesive soils to ensure the final anchor position is at the necessary keyed depth.

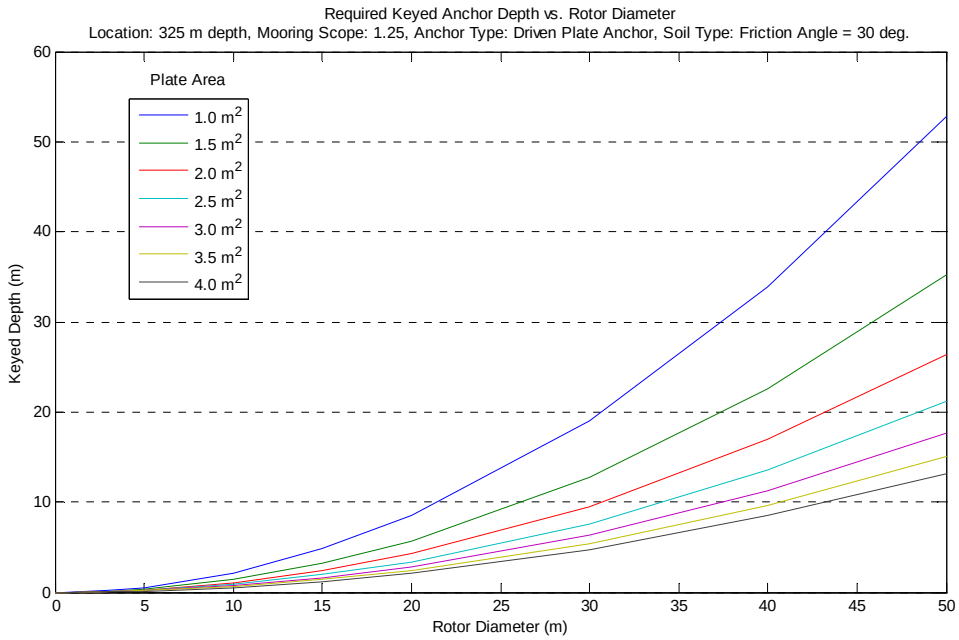

Figure 53: Necessary keyed depth for seven plate areas presented as a function of rotor diameter at 325 m depth location and 1.25 mooring scope for loose sand.

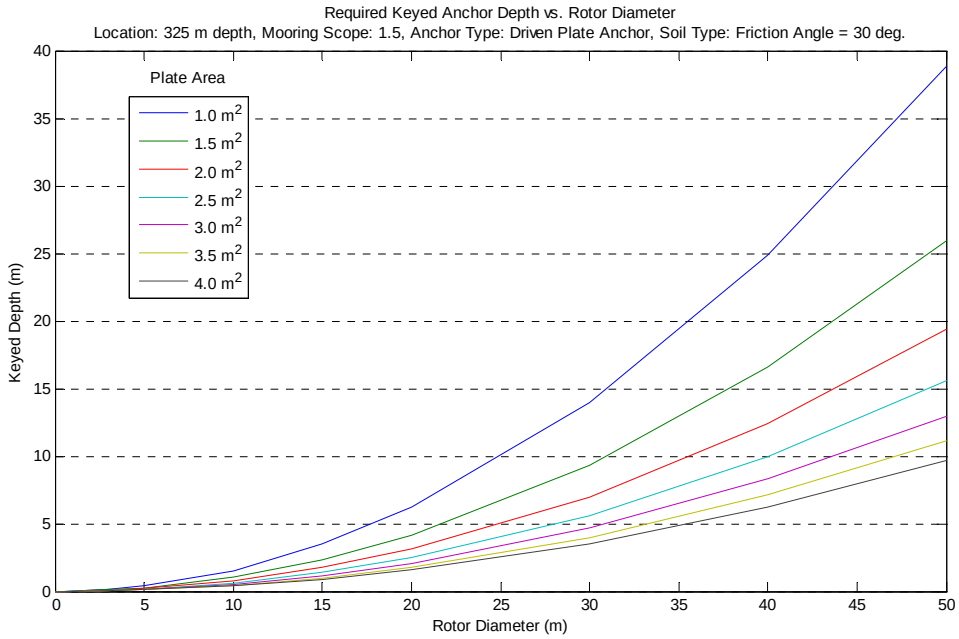

Figure 54: Necessary keyed depth for seven plate areas presented as a function of rotor diameter at 325 m depth location and 1.50 mooring scope for loose sand.

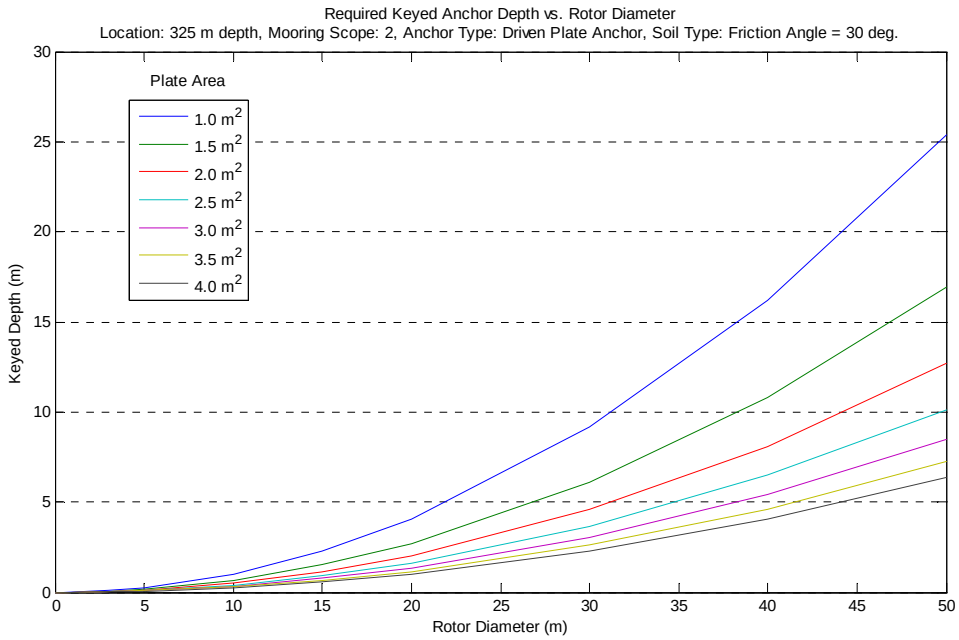

Figure 55: Necessary keyed depth for seven plate areas presented as a function of rotor diameter at 325 m depth location and 2.00 mooring scope for loose sand.

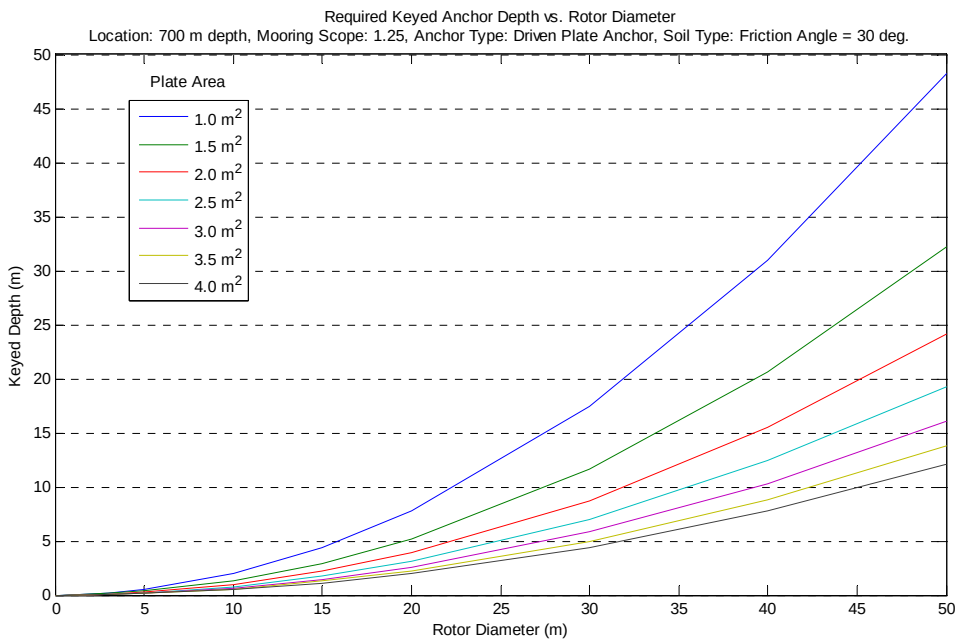

Figure 56: Necessary keyed depth for seven plate areas presented as a function of rotor diameter at 700 m depth location and 1.25 mooring scope for loose sand.

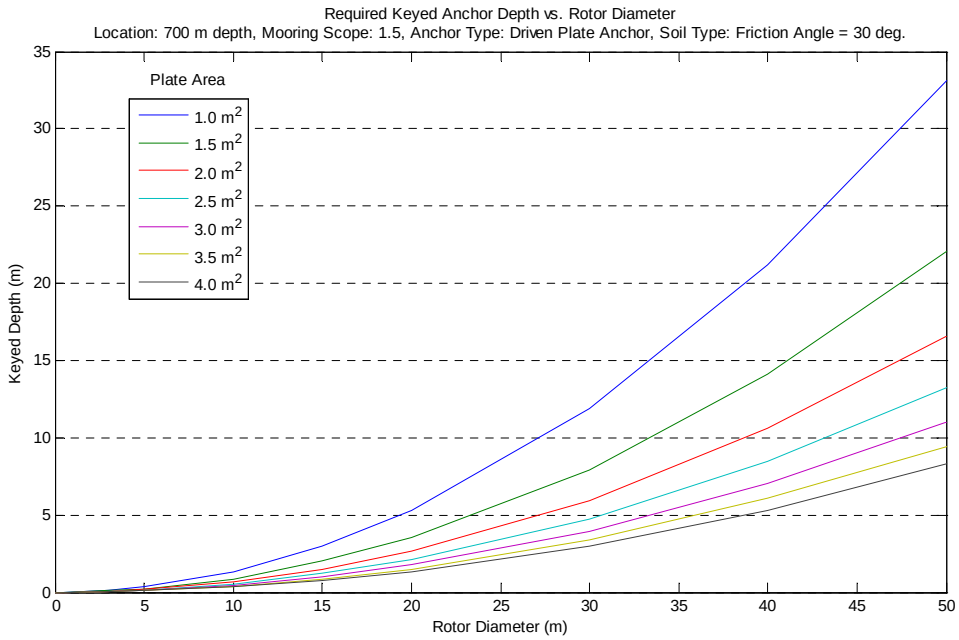

Figure 57: Necessary keyed depth for seven plate areas presented as a function of rotor diameter at 700 m depth location and 1.50 mooring scope for loose sand.

4.2.2 Driven Plate Anchors in Cohesive Soil

Similarly to driven plates in cohesionless soil, plate anchor holding capacity in cohesive soil is directly related to plate size and soil strength. The plate is sized for the soil strength at the designed depth (Forrest et al., 1995). The necessary plate area (A) for varying cohesive soil shear strengths (c) was determined using:

$$A = \frac{F_u}{cN_c}, \tag{17}$$

where F_u is the ultimate anchor holding capacity, N_c is the bearing capacity factor for cohesive soils (Forrest et al., 1995). A maximum bearing capacity factor, or holding capacity factor (N_c), of 12 was recommended for all marine (saturated) situations as seen in Figure 58. An example of the relationship between required plate area and soil shear strength, calculated using Equation 17, is displayed in Figure 59 using a

logarithmic scale. These plate anchors have a keyed depth to width ratio greater than five for a bearing capacity equal to 12.

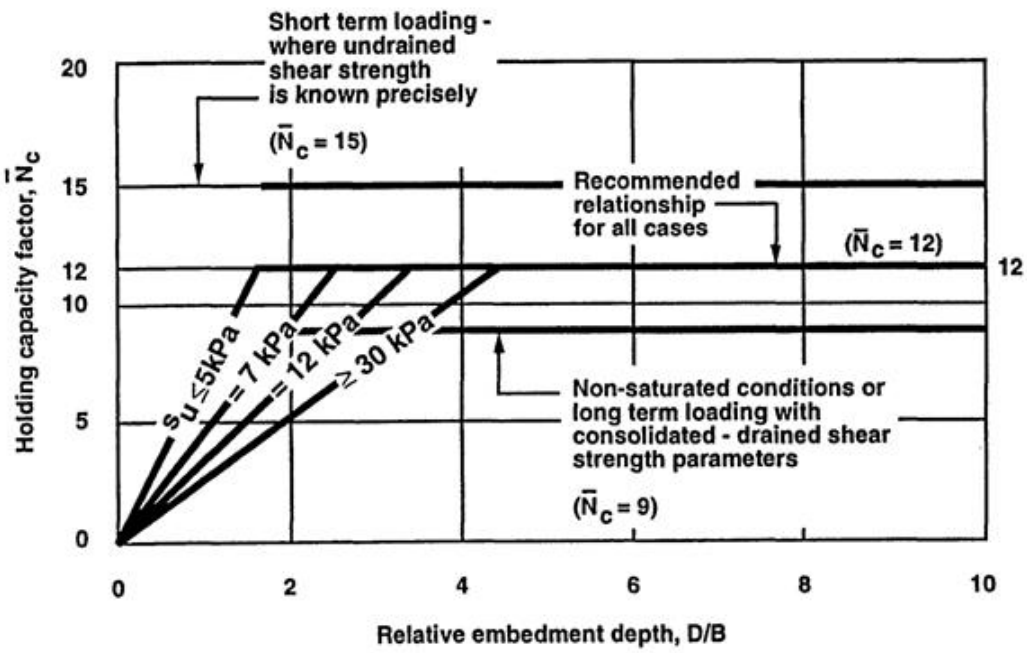

Figure 58: "Holding capacity factors for cohesive soils" (Forrest et al., 1995).

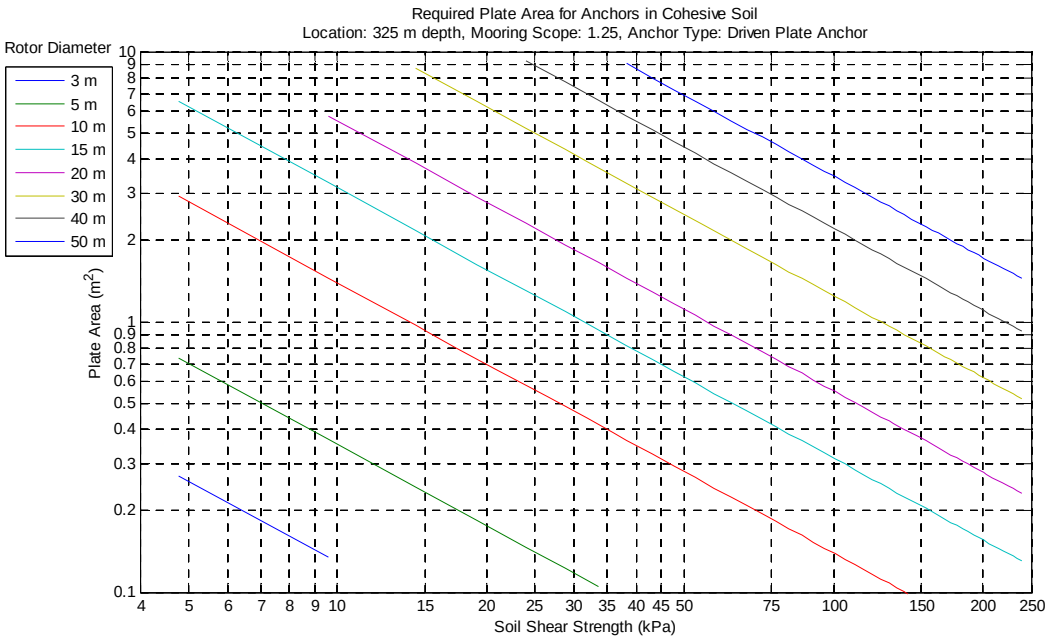

Figure 59: Necessary plate area with increasing soil shear strength for eight rotor diameters at 325 m depth location and 1.25 mooring scope in cohesive soil.

4.3 Traditional Drag Embedment Anchors

Traditional drag embedment anchors are not applicable for the determined anchor loading requirements because of the high uplift angles of the evaluated taut moorings. Drag embedment anchors are typically used in catenary moorings and may be useful for MRE systems which require or benefit from catenary mooring configurations, and are therefore discussed within this work. It is difficult to predict the holding capacity of a drag embedment anchor, therefore estimates are normally obtained through empirical approaches and exact holding power can only be determined after deployment (API, 2005). Estimates for horizontal anchor holding capacity based off Navy Techdata Sheets, industry anchor tests, and field experience can be found in Figure 60 for sand and Figure 61 for soft clay or mud (API, 2005). Anchor guidelines for predicting holding capacity in hard clay, calcareous sand, coral, rock seafloor or layered floors are not available at the time API RP2SK was written (API, 2005).

Catenary moorings usually consist of lengths of chain on the seafloor to transfer vertical loads to lateral loads, but mooring scopes can be reduced with the addition of a clump weight to the mooring configuration to negate vertical loading on the drag embedment anchor. Additional holding capacity from chain and wire rope on the seafloor can be predicted with methods found in API RP2SK. The corresponding drag distance to fluke length ratio with respect to the percent of maximum capacity for drag embedment anchors in clay is displayed in Figure 62. For sand bottoms “the maximum capacity is achieved in less than about 10 fluke lengths of drag” (NCEL, 1985). The

necessary fluke tip penetration is displayed in Figure 63. The necessary penetration depth along with the necessary drag distance for a particular anchor is important when seeking an area during regional site surveys with sufficient sediment area and depth for deployment.

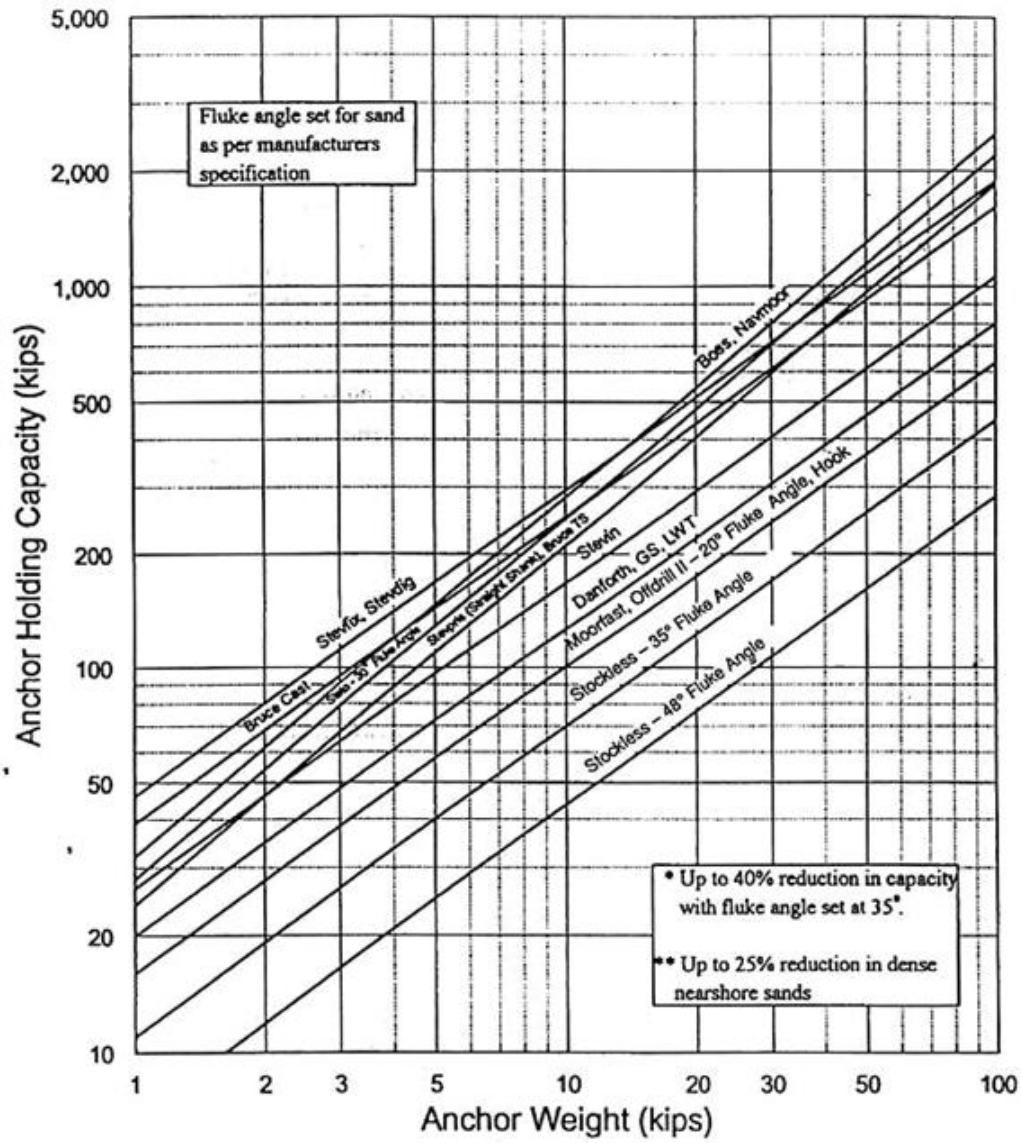

Figure 60: Anchor holding capacity in sand (API, 2005).

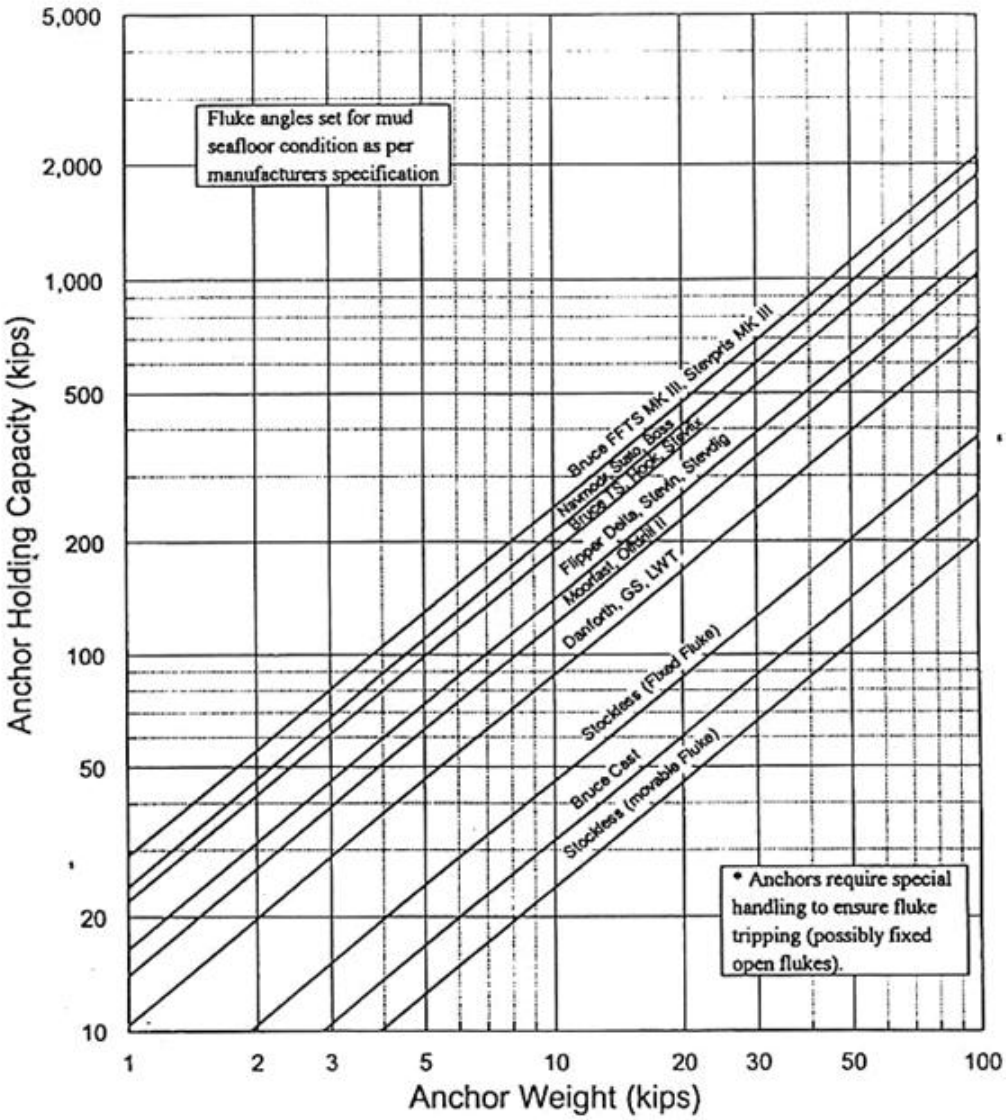

Figure 61: Anchor holding capacity in soft clay or mud (API, 2005).

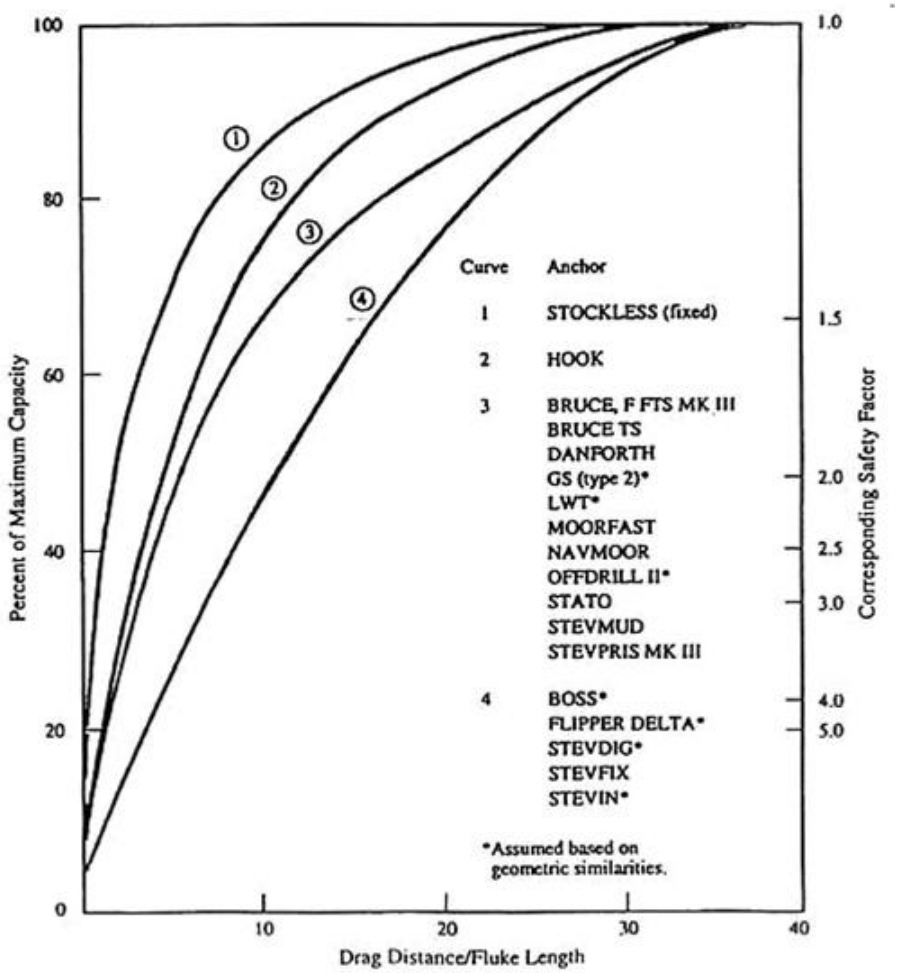

Figure 62: Percent holding capacity versus drag distance in soft clay (API, 2005).

Anchor Type	Normalized Fluke Tip Penetration (Fluke Lengths)` Sands/Stiff Clays	Mud (e.g., Soft Silts and Clays)
Stockless	1	3*
Moorfast Offdrill II	1	4
Boss Danforth Flipper Delta GS (Type 2) LWT Stato Stevfix	1	4 ½
Stevpris MK III Bruce FFTS MK III Bruce TS Hook Stevmud	1	5

*Fixed fluke stockless

Figure 63: Estimated maximum fluke tip penetration (API, 2005).

The horizontal anchor loading results presented in Figures 26 and 29 do not have significant variation between mooring scopes for their respective locations because the majority of lateral anchor loading is due to the horizontal drag of the rotor and not the increase in line length. An estimate to the size and type of traditional embedment anchor that could resist the horizontal loading created by 50 m diameter rotor can be made assuming that the horizontal anchor loading is near the same values regardless of the scope and the chosen scope has near 0° uplift angle. The maximum horizontal anchor loading for a 50 m diameter rotor is 4760 kN (1070 kips) at the 325 m depth location. This is the maximum horizontal load of all the simulations and would require an anchor

size between a 177.9 kN (40 kips) Boss, Navmoor anchor and a 444. 8 kN (100 kips) Stevin anchor in sand. The same rotor diameter and location would require between a 213.5 kN (48 kips) Bruce FFTS MK III or Stevpris MK III and a 444.8 kN (100 kips) Moorfast or Offdrill II anchor in soft clay or mud. These estimates do not take into account the decrease in horizontal anchor loading due to friction of chain on the seafloor and safety factors have not been applied. It should also be noted that drag embedment anchors can be sized and used as deadweight anchors where their load capacity is determined by their submerged weight with the additional benefit of embedment. This may be a desirable option if a stock drag embedment anchor is readily available or if full penetration is not obtainable.

While traditional drag embedment anchors are not applicable to taut moorings, there is a type of drag embedment anchor designed for use with taut moorings. Vertical loaded anchors (VLA), such as the Vryhof Stevmanta VLA, are suitable for use in soft clay soil conditions and are embedded into the seabed like a conventional drag embedment anchor (Ruinen, n.d.). Upon adjusting the anchor into normal mode with either the use of two mooring lines or a shear pin it can resist high uplift angles (Ruinen, n.d.). This anchor method is an option for MRE devices where high uplift capacity can be obtained by deep penetration into soft soil (Ruinen, n.d.).

4.4 Pile Anchors

Pile anchors are typically used as a last resort when less costly anchors described previously are not sufficient. Drilled and grouted piles might also be a desirable anchoring method in rock seafloors if a footprint smaller than those created by large

gravity anchors are desired. Increased costs are associated with significant floating assets required for transportation, installation support, and obtaining geophysical and geotechnical data required for penetration depths reaching tens of meters (Sound and Sea Technology, 2009). However, as stated in OWET studies "piles may afford an economical mooring solution for large scale commercial WEC system installations" (Sound and Sea Technology, 2009). This option may also be an economical mooring solution for large scale commercial MHK and OTEC devices as well. Performing generalized preliminary sizing of piles without specific site conditions is difficult because designing piles requires the most geotechnical data of all anchor types (Sound and Sea Technology, 2009). Also, variations in pile design (as seen in Figure 64) make it difficult to present generalized preliminary sizing for pile anchor types.

Characteristics	Pipe and H-Piles	Umbrella Piles[a]	Chain-in-Hole[a]	Rock Bolts[a]
Applications	Foundations and Anchors	Anchors	Anchors	Anchors
Approximate Maximum Capacity	Axial: 20,000 kips Lateral: 1,500 kips	300 kips in sand 100 kips in mud	550 kips	30 kips
Installation Methods	driven or drilled and grouted	driven	drilled and grouted	drilled and grouted, or mechanically wedged
Applicable Soil Type	soil and rock	soils without boulders and other obstructions	rock, with overlying soil strata	rock
Advantages	easy to splice; high capacity; can penetrate through light obstructions	high capacity in uplift	high capacity	very low cost, no heavy mechanical equipment necessary
Disadvantages	high cost; vulnerable to corrosion	maximum depth limited by hammer; soils must be homogeneous; inspection of connection not possible	inspection of connection not possible	rock must be competent, non-fractured (shallow water only), low capacity
Remarks	pipe piles resist bending in any direction	resistance developed similar to plate-embedment anchor (Chapter 6)		diver hand-installed, much smaller size than normal piles
Illustration	(anchor pile shown) 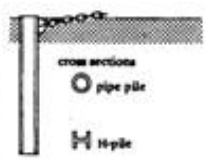	(in-service position)	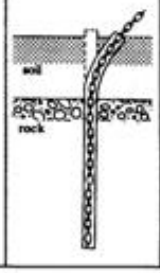	(wedged bolt shown) 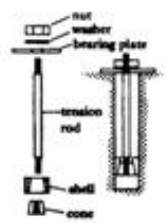

[a]Special anchor pile.

Figure 64: Pile Anchor Types (Sound and Sea Technology, 2009).

If approximate maximum capacities presented in Figure 64 are used for anchor capacity estimates, an estimate to the maximum rotor diameter applicable to each type of pile anchor can be determined using anchor loading data from Section 3.3.1. For pile and H-pipe anchors, approximated maximum capacities for both axial and lateral loading are greater than the estimated vertical and horizontal loading of all MHK mooring scenarios presented in Section 3.3.1, the maximum of which is the 325 m location with a scope of 1.25. Here the axial or vertical load is 4,150.5 kN and the lateral load is 4,756.2 kN, less than the approximate maximum axial capacity of 88,968.0 kN (20,000 kips) and

approximate maximum lateral capacity of 6672.6 kN (1,500 kips). This shows pipe or H-pile anchors may have the capability of mooring devices with rotor diameters in excess of 50 m. The anchor loading presented in Section 3.3.1 was fit with 2nd degree polynomials and the capacities of umbrella piles and chain in hole piles are plotted over the anchor loading for both the 325 m depth and the 700 m depth in Figures 65 and 66. Rock bolt anchors were not displayed on Figures 65 and 66 because they are typically hand installed by divers in shallow waters as described in Figure 64. More detailed anchor design may reveal pile anchors with larger capacity as lateral capacity can be changed by methods such as "lowering the mooring line attachment point, burying the pile below grade, attaching fins to the upper end of the pile, and using an upper-end shear collar and lower-end anchor to effect a combination of increased soil bearing and confinement with uplift resistance" (Sound and Sea Technology, 2009). The method of combining multiple piles into cluster piles is also an option where increased loading capacity is required.

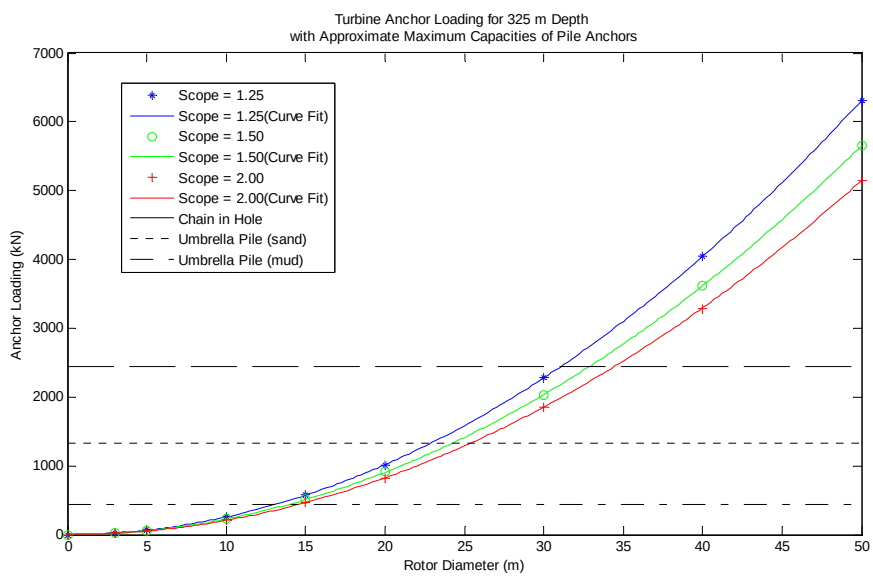

Figure 65: Turbine Anchor Loading for 325 m Depth with Approximate Maximum Capacities of Pile Anchors.

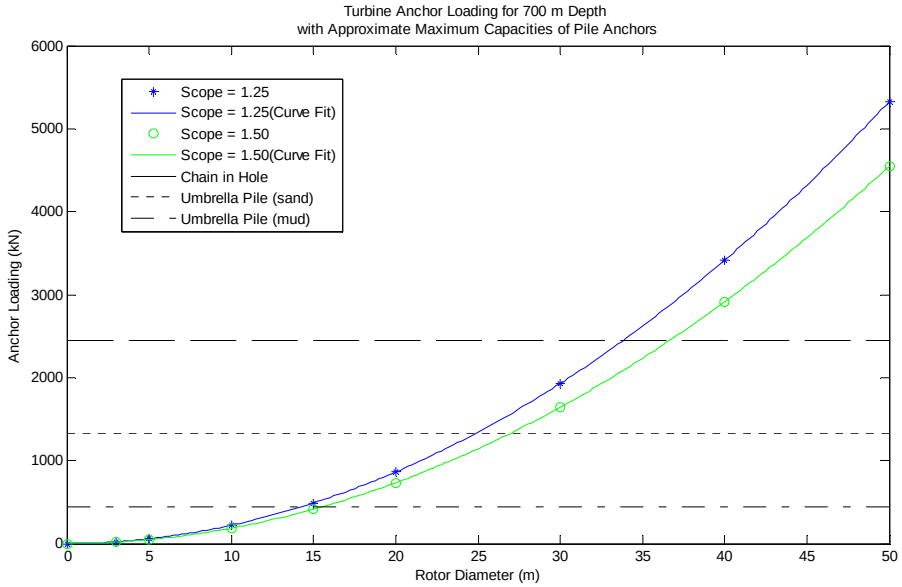

Figure 66: Turbine Anchor Loading for 700 m Depth with Approximate Maximum Capacities of Pile Anchors.

5. CONCLUDING REMARKS

5.1 Summary and Conclusions

An anchor study was completed for an area off the coast of Southeast Florida that is being considered for commercial energy extraction with marine renewable energy devices. Applicable MRE devices (MHK and OTEC) capable of harnessing the local ocean current and ocean thermal resources were discussed, and a detailed examination of the potential anchoring systems that could be used to hold these systems in place with local environmental conditions was performed. Simulating the deployment of single point moored MHK devices off South Florida's coast led to the preliminary sizing of potential anchors to provide insight to device developers of future commercial MHK devices.

A regional study of bottom types was performed using existing benthic survey data. The benthic surveys revealed that both west of the Miami Terrace Escarpment in approximately 200 to 400 m water depth and east of the Miami Terrace Escarpment in approximately 600 to 800 m water depth are areas with the least slope and lower relief. Although anchoring may be possible with increased costs and possibly uncertain performance on the areas of the Miami Terrace Escarpment that combine steep slopes and high relief, it may be desirable to avoid these areas if more efficient and reliable anchoring can be achieved in locations to the west and east, while ensuring sufficient available energy resources.

Hard limestone bottoms, gravel or rubble bottoms, and hard bottoms overlaid by sand (stratified seafloors) observed on the Miami Terrace limit anchor types to either deadweight anchors or more costly pile anchors that may require being drilled and grouted. Plate anchors have been driven into hardbottoms and have minimal footprint but are not normally the desired choice and may not penetrate hard monolithic slabs of limestone. However, areas of sediment have been observed on top of the Miami Terrace, west of the escarpment, but the subbottom profiling has not been completed to determine the depth of this sediment. If adequate sediment depths exist in these locations then all anchor types can be used on top the Miami Terrace. If drag embedment anchors are to be used where the required sediment depth exists, then it must also be assured that there is adequate surface area of the sediment to drag the anchor the necessary distance to embed it to the required depth to achieve the required holding capacity.

In areas where only a thin layer of sediment is believed to overlay hard limestone, deadweight anchor design can be optimized with shear keys and wedge shapes to partially embed the anchor, mobilizing deeper sediments and achieving a higher lateral load capacity. In areas east of the Miami Terrace Escarpment, where a mostly sediment bottom was observed, all four anchor types will function if required sediment depths exist for the specific type of anchor. In addition to sediment depth, each anchor type requires further geotechnical data for design. Coring and sub-bottom profiling can determine the sub-bottom makeup and samples taken can reveal soil properties needed for detailed anchor design. Methods and procedures for first performing a more general benthic survey for site selection and necessary data collection and procedures for a site specific

survey can be found from the *Handbook for Marine Geotechnical Engineering* to collect the necessary information for selection and design (NCEL, 1985).

Anchor loading predictions, necessary to size the anchors, were extracted from numerical simulations of moored ocean current turbines with environmental conditions characteristic of the region of proposed deployment. A comprehensive range of anchor loading was developed by examining two potential deployment locations, multiple mooring scopes, and by increasing turbine rotor diameters to represent advancements in technology. Areas on top of the Miami Terrace, west of the Terrace Escarpment, were generalized with a 325 m depth, scopes of 1.25, 1.5 and 2.00, the available maximum current profile at that depth, and turbine rotors up to 50 m in diameter. Maximum anchor loading occurred with a mooring scope of 1.25. Example values for vertical anchor loading at this location with a scope of 1.25 are 15.5 kN for a 3 m diameter rotor, 167.5 kN for a 10 m diameter rotor, and 666.4 kN for a 20 m diameter rotor. Corresponding values for lateral anchor loading for this scenario are 18.8 kN for a 3 m diameter rotor, 194.4 kN for a 10 m diameter rotor, and 767.7 kN for a 20 m diameter rotor. Areas to the east of the Terrace Escarpment, were generalized with a 700 m depth, scopes of 1.25 and 1.50, the available maximum current profile at that depth, and turbine rotors up to 50 m in diameter. Anchor loading was the greatest at this location for a scope of 1.25, but less than that of the 325 m depth for a scope of 1.25, because the available current profile for the 700 m depth location had lower maximum values.

Past OTEC studies identify deadweight and pile anchors as the best options if mooring in the Gulf Stream. Pile anchors have advantages over deadweight anchors for holding an OTEC plant in place in the Gulf Stream because of their greater efficiency and

smaller seabed footprint than the large gravity anchor that would be required to hold the plant in place.

Results from MHK simulations were used to size anchors applicable to the taut mooring systems, but no safety factors were applied to the anchor sizing in this thesis. Safety factors would have to be selected for the respective anchor type and calculated for the specific device being moored. Deadweight anchors with no shear keys in both cohesionless and cohesive soils as well as deadweight anchors with shear keys in both soil types were sized for increasing rotor diameters. In both cohesionless and cohesive soils, the addition of shear keys to dead weight anchors reduced the necessary anchor weight in water by over 25% for a 20 m diameter rotor blade at the 325 m location with a scope of 1.25. Results were also used to size driven plate anchors in cohesionless and cohesive soils. To use a plate anchor at the 325 m location in sand for a 20 meter diameter rotor, it would require that keyed depth of the plate be as much as 8.5 m for a 1 m^2 plate to 2.1 m for a 4 m^2 plate. It also must be assured that there is enough sediment to drive the anchor beyond these depths so that the final keyed depth after being loaded is equal to these depths.

At the 700 m location where the presence of sediment with adequate depths is more likely, the required keyed depth of a plate anchor for a 20 m diameter rotor and scope of 1.25 is 7.8 m for a 1 m^2 plate and 2.0 m for 4 m^2 plate. Traditional drag embedment anchors, not typically applicable to taut moorings, were not sized using the MHK simulation results, however plots of anchor holding capacities and the required drag distance for the corresponding soil types are presented for use in catenary mooring systems. Estimated maximum capacities of pile anchors were overlaid on the anchor

loading plots to identify the maximum rotor diameters associated with each pile anchor type. The supplied maximum anchor holding capacities of Figure 63 show that pile anchors have potential for use with rotor diameters in excess of 50 m.

As the necessary deadweight anchor size increases with increasing rotor diameter, there may be an optimal point at which a more efficient anchoring method that requires embedment should be used. Economically speaking, this would occur where the increased cost of surveying, design, permitting, and deployment of a more complex anchoring method outweighs the increased cost of deployment of a larger gravity anchor. Quantifying the effects of environmental impact to compare MRE systems and their designs is an issue currently being assessed by the MRE community, and would also be a factor in deciding at what point to move to select a more expensive anchor type that may have a smaller benthic footprint than a large gravity anchor.

5.2 Gaps in Current Knowledge of the Area of Interest and Related Future Work

Information on the benthic environment where marine renewable energy systems could be deployed is limited to video and photographic surveys which only show the surface of the sea bottom, allowing only preliminary predictions of the sub-bottom makeup. These surveys have also only been conducted over a small portion of the area where devices could be deployed. This research shows that it is necessary to perform sub-bottom profiling in the future to determine sediment and rock layer depths for appropriate anchor design and selection.

In addition, site specific surveys for metocean conditions as well as continuation of FAU's current data collection will better predict the conditions for storms with 50 and

100 year return periods that would better define environmental inputs and constraints for numerical simulations of offshore MRE systems. Although future standards for MRE systems in the U.S. could be less stringent than those expected of the offshore oil industry, it is necessary to gather data sets for longer periods of time to predict maximum metocean conditions local to South Florida and quantify conditions that occur during extreme events like hurricanes. Wave conditions occurring during past hurricanes on the East Coast of Florida are available, but are not necessarily characteristic of the area of interest. The survivability of future MRE anchor and mooring systems to be deployed off the coast of Southeast Florida would greatly benefit from an increase in the available knowledge of extreme metocean conditions that might occur in the area being considered for future commercial deployments.

REFERENCES

American Petroleum Institute (API). (2007). Interim Guidance on Hurricane Conditions in the Gulf of Mexico. Bulletin 2INT-MET.

American Petroleum Institute (API). (2005). Design and Analysis of Stationkeeping Systems for Floating Structures, Third Edition. API RP 2SK.

Atturio, J.M., Valent, P.J. and Taylor, R.J. (1979). Preliminary Selection of Anchor Systems for Ocean Thermal Energy Conversion. *Ocean Engineering, 6(1-2),* 139-167.

Ballard, R.and Uchupi, E. (1971). Geological observations of the Miami Terrace from the submersible Ben Franklin. *Marine Tech. Soc. J., 5,* 43-48.

Black, P. G., D'Asaro, E. A., Drennan, W.M., French, J.R., Niller, P.P., Sanford, T.B., Terrill, E.J., Walsh, E.J., Zhang, J.A. (2007). Air-sea Exchange in Hurricanes, Synthesis of Observations from the Coupled Boundary Layer Air-Sea Transfer Experiment. Bullletin of the American Meteorological Society, March 2007.

Cable, B., Tayler, W., Tindal, C., Varley, R., and Brissey, L. (2010). The Navy's Ocean Thermal Energy Conversion Program. *Oceans 2010 MTS/IEEE Seattle Conference and Exhibition, Proceedings,* September 20-23, Seattle, WA.

Clarke, J.A., Connor, G., Grant, A.D., Johnstone, C., and Ordonez-Sanches, S. (2008). Contra-rotating marine current turbines: Performance in field trials and power train developments. *10th World Renewable Energy Congress, Proceedings,* July 19-25, Glasgow.

Clarke, J., Grant, A., Connor, G., and Johnstone, C. (2009). Development and In-sea Performance Testing of a Single Point Mooring Supported Contra-Rotating Tidal Turbine. *International Conference on Ocean, Offshore, and Arctic Engineering, Proceedings,* OMAE 2009, May 31 – June 5, Honolulu, HI.

Coastal Response Research Center. (2010). Technical Readiness of Ocean Thermal Energy Conversion (OTEC). University of New Hampshire, Durham, NH.

Davis, B.V., Farrell, J.R., Swan, D. H., and Jeffers, K. A. (1986). Generation of Electric Power From the Florida Current. *18th annual Offshore Technology Conference, Proceedings,* OTC-5120, May 5-8, Houston, TX.

Driscoll, F.R., Skemp, S.H., Alsenas, G. M., Coley, C. J., and Leland, A. (2008). Florida's Center for Ocean Energy Technology. *MTS/IEEE Oceans Conference, Proceedings,* September 15-18, Quebec City, Canada.

Duerr, A.E.S. and Dhanak, M.R. (2010). Hydrokinetic Power Resource Assessment of the Florida Current. *Oceans 2010 MTS/IEEE Seattle Conference and Exhibition, Proceedings,* September 20-23, Seattle, WA.

Forrest, J., Taylor, R., and Bowman, L. (1995). Design Guide For Pile Driven Plate Anchors. Technical Report TR-2039-OCN, Naval Facilities Engineering Service Center, Port Hueneme, CA.

Gerwick, Ben C. (2007). Construction of Marine and Offshore Structures. Third ed. Taylor & Francis, Inc., 2007. Googlebooks. Web.

India OTEC Pipeline. Deep Pipelines for Ocean Thermal Energy Conversion. Makai Ocean Engineering. Accessed April 25, 2010, from http://www.makai.com/p-otec.htm

NDBC – Hurricane Data and Plots. National Data Buoy Center. NOAA. Accessed July, 9, 2010, from http://www.ndbc.noaa.gov/hurricanes.shtml

National Civil Engineering Laboratory (NCEL). (1987). Drag Embedment Anchors for Navy Moorings. Techdata Sheet 83-08R. Port Hueneme, CA.

National Civil Engineering Laboratory (NCEL). (1985). Handbook for Marine Geotechnical Engineering. Port Hueneme, CA.

Neumann, A.C. and Ball, M.M. (1970). Submersible observations in the Straits of Florida: geology and bottom currents. *Geol. Soc. Amer. Bull., 81*, 2861-2874.

Leland, A. (2009). A Resource Assessment of Southeast Florida as Related to Ocean Thermal Energy. MS thesis Florida Atlantic University, Boca Raton, FL.

Malloy, R.J. and Hurley, R.J. (1970). Geomorphology and Geologic Structure: Straits of Florida. Environmental Science Services Administration, Atlantic Oceanographic and Meteorological Laboratories, Miami, FL.

Messing, C.G., Walker, B.K., Dodge, R.E., Reed, J., and Brooke, S.D. (2006.a). Calypso LNG Deepwater Port Project, Florida Marine Benthic Video Survey. Submitted to Ecology and Environment, Inc. & SUEZ Energy North America, Inc.

Messing, C.G., Walker, B.K., Dodge, R.E., and Reed, J. (2006.b). Calypso U.S. Pipeline, LLC, Mile Post (MP) 31- MP 0 Deep-water Marine Benthic Video Survey. Submitted to Calypso U.S. Pipeline, LLC.

NDBC - Moored Buoy Program. National Data Buoy Center. NOAA. Accessed April 25, 2010, from http://www.ndbc.noaa.gov/mooredbuoy.shtml

Ravindran, M. (2000). The Indian 1 MW Floating OTEC Plant, An Overview. Accessed April 25, 2010, from http://www.clubdesargonautes.org/otec/vol/vol11-2-1.htm

Raye, R.E. (2002). Characterization Study of the Florida Current at 26.11 North Latitude, 79.50 West Longitude for Ocean Current Power Generation. MS thesis Florida Atlantic University, Boca Raton, FL.

Ruinen, R. (n.d.). Use of Drag Embedment Anchor for Floating Wind Turbines. Powerpoint presentation by Vryhof Anchors BV.

Seelig, W.N., Taylor, R., and Bang, S. (2001). Improved Pearl Harbor and Kings Bay Anchor Designs. Technical Report TR-6073-OCN, Naval Facilities Engineering Service Center, Port Hueneme, CA.

SNMREC. (2010). NOEL Phase 1a – Temporary Ocean Current Observing and Monitoring System. Dania Beach, FL. Unpublished.

Sound and Sea Technology. (2009). Advance Anchoring and Mooring Study. Prepared for Oregon Wave Energy Trust.

Taylor, R.J. (1982). Interaction of Anchors with Soil and Anchor Design. Naval Civil Engineering Laboratory. Port Hueneme, CA.

Taylor, R.J. (2010). Email October 19, 2010.

Deep Water Moorings. Accessed November 27, 2010, from http://www.tensiontech.com/services/mooring.html

Valent, P.J., Taylor, R.J., Atturio, J.M., and Beard, R.M. (1979). Single Anchor Holding Capacities for Ocean Thermal Energy Conversion (OTEC) in Typical Deep Sea Sediments. *Ocean Engineering*, *6*, 169-245.

Vanrietvelde, N. (2009). Numerical Performance Prediction for FAU's First Generation Ocean Current Turbine. MS thesis Florida Atlantic University, Boca Raton, FL.

VanZwieten, J., Driscoll, F.R., Leonessa, A., and Deane, G. (2006). Design of a prototype ocean current turbine—Part I: mathematical modeling and dynamics simulation. Ocean Engineering, vol. 33, pp. 1485-1521

VanZweiten, J.H., Oster, and C.M., Duerr, A.E.S. (2011). Design and Analysis of a Rotor Blade Optimized for Extracting Energy From the Florida Current. Accepted to the ASME 2011 International Conference on Ocean, Offshore, and Arctic Engineering, Rotterdam, Netherlands, June 19-24. No. OMAE2011-49827.

Vryhof Anchors. (2005). Anchor Manual 2005. Krimpen a/d yssel, Netherlands.